

# Strange Quark Matter In Astrophysics

Thesis submitted for the degree of  
Doctor of Philosophy (Science)

in

Physics

by

*Sayan Biswas*

Department of Physics

University of Calcutta

2017

## DECLARATION

I hereby declare that the work presented in this thesis is based on my ideas and original research work. I have adequately cited the references of the original sources. I also declare that I have stood by to all principles of academic integrity and honesty and neither this thesis nor any part of it has been submitted for any degree/diploma or any academic award anywhere before.

Sayan Biswas  
Kolkata, India

# To My Parents

## Acknowledgements

*I would like to use this space to convey my sincere gratitude to all the individuals who have helped me in the completion of this work along with my heartiest appreciation for all the assistance and support that I have received in the course of this research work.*

*Institute Research Fellowship of Bose Institute was the primary source of support during the period of my research. I am thankful to the Director, Bose Institute, Kolkata, India for providing me the fellowship and the facilities during the tenure of my work.*

*I am indebted to my research supervisor, Prof. Sibaji Raha, who acts as a guide in a true sense in the course of this work. He has given me complete freedom in choosing what, when and how to go about work, but frequently rescued from the complicated situations which appeared as a consequence of such freedom. I have learned a lot by discussing physics with him which helped me to strengthen my basic concepts of physics.*

*I am also indebted to Dr. Parthasarathi Joarder, who, apart from being my joint supervisor continues to act as a friend and philosopher. He often rescued me from the heat and frustration generated as a natural consequence of the enhanced degrees of freedom that he has provided me. I will always cherish the physics discussions which I had with him over a cup of tea or coffee which helped me to develop an ability of thinking for resolving any problem and made my fundamentals of physics more strong.*

*I am equally grateful to my (senior) collaborators – Dr. J.N. De, Dr. Debapriyo Syam, and Dr. Arunava Bhadra. I learned many tricks of the trade, about the community, various mathematical tools useful for complicated calculations and about making sense out of a list of numbers from them. Indeed, they were my virtual mentors and family throughout this period. I would also like to thank Prof. Paolo Lipari as his lectures on high energy astrophysics and clear illustrations in the conferences, and school sessions of Winter School on Astro-Particle Physics (WAPP) helped me to develop the concepts of high energy astrophysics especially the fundamentals of cosmic rays.*

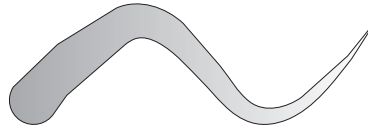
---

*I earnestly thank the office staffs of Department of Physics, Main Campus and the Centre for Astroparticle Physics and Space Science (CAPSS), Salt Lake Campus as well as the staffs of the Canteen of CAPSS, who have been very supportive during the period. Along with, I would also like to thank the hostel warden of Bose Institute Research Scholars' Hostel and the staffs of the Hostel Canteen for providing the hostel facilities and a research-friendly environment at the hostel.*

*I would also like to thank my friends and colleagues at Bose Institute - Ramaprasad, Subhashis, Shibali, Sadhan, Sujoy, Shyam, Soumitra, Prosenjit, Shubhrangshu, Atanu, Sarbani, Anirban, Soumendra, Sumana (senior), Kaushik, Subhasish (senior), Tamal, Alok, and Ritam with whom I shared this part of my life. The thanks extend to my other friends - Debamita, Rajkumar, Jyotirmoy, Biplab (senior), and Pratyusha. They were always there to share the moments of joy and lift my spirits when I was down.*

*At last, I would like to express my sincere gratitude and appreciation to my parents for their constant support, patience and endurance shown during the period. I am also grateful to them as they have instilled in me both love and respect for knowledge from an early age.*

Sayan Biswas



## List of publications

1. **Sayan Biswas**, Arunava Bhadra, J.N. De, Partha S. Joarder, Sibaji Raha, and Debapriyo Syam, “*A production scenario of the galactic strangelets and an estimation of their possible flux in the solar neighborhood*”, *Proceedings of Science ICRC 2015*, 504 (2016).
2. **Sayan Biswas**, J.N. De, Partha S. Joarder, Sibaji Raha, and Debapriyo Syam, “*Multifragmentation model for the production of astrophysical strangelets*”, arXiv: 1409.8366v5 [nucl-th](2015).
3. **Sayan Biswas**, J.N. De, Partha S. Joarder, Sibaji Raha, and Debapriyo Syam, “*Disassembly model for the production of astrophysical strangelets*”, *Proceedings of the Indian National Science Academy* **81** No. 1, 277 (2015).
4. **Sayan Biswas**, J.N. De, Partha S. Joarder, Sibaji Raha, and Debapriyo Syam, “*Quantum statistical multifragmentation model for the production of astrophysical strangelets*”, *Proceedings of the 33rd International Cosmic Rays Conference* (2013) [ISBN: 978-85-89064-29-3].
5. **Sayan Biswas**, J.N. De, Partha S. Joarder, Sibaji Raha, and Debapriyo Syam, “*Multifragmentation model for astrophysical strangelets*”, *Physics Letters B* **715**, 30 (2012).

# Abstract

According to strange matter hypothesis (SMH), strange quark matter (SQM) may be the true ground state of strongly interacting matter. Such hypothesis opens up new possibilities as stable SQM would have several implications in astrophysics. One of such possibilities is related to the existence of strange stars (SSs). SQM plays an important role in the context of SSs and cosmic rays (CR). Several exotic events with the unusual charge to mass (or, baryon number) ratio have been reported in CR experiments which can't be explained by our knowledge of known nuclei. But such events can be explained with strangelets, small lumps of SQM. Recent numerical simulations of SS merger in a compact binary stellar system show that some SQM material will be ejected from the tip of tidal arms formed during the merging process, and such ejected material can fragment into strangelets and mix with CR to provide the strangelet abundance in CR. Space-borne detectors such as PAMELA, AMS-02 are now engaged in searching for strangelets in galactic cosmic rays (GCR). Hence, in the present context, it is quite important to estimate the possible flux of strangelets in the solar neighborhood and that is the key motivation behind this work. In this work, we have provided a possible production scenario of the galactic strangelets and determine the plausible baryon number (or, mass) distribution of such strangelets by invoking the statistical multifragmentation model (SMM) often used in nuclear systems. The strangelets originated in binary SS mergers are then likely to be accelerated by the shock waves generated in such mergers and they attain a power-law spectrum with a spectral index close to -2. We then apply the standard diffusive propagation model to describe the propagation of the strangelets through the randomly oriented magnetic field of the interstellar medium (ISM) and finally estimate the flux of the strangelets near the vicinity of the Sun. We have also compared our theoretical estimates with the upper limits of fluxes of strangelets reported by PAMELA. We have seen that our theoretical estimates are consistent with the observation of PAMELA, and such estimates are also useful for AMS-02 and other future experiments to vindicate the SMH.

# Strange Quark Matter In Astrophysics

## Abstract

According to strange matter hypothesis (SMH), strange quark matter (SQM) may be the true ground state of strongly interacting matter. Such hypothesis opens up new possibilities as stable SQM would have several implications in astrophysics. One of such possibilities is related to the existence of strange stars (SSs). SQM plays an important role in the context of SSs and cosmic rays (CR). Several exotic events with the unusual charge to mass (or, baryon number) ratio have been reported in CR experiments which can't be explained by our knowledge of known nuclei. But such events can be explained with strangelets, small lumps of SQM. Recent numerical simulations of SS merger in a compact binary stellar system show that some SQM material will be ejected from the tip of tidal arms formed during the merging process, and such ejected material can fragment into strangelets and mix with CR to provide the strangelet abundance in CR. Space-borne detectors such as PAMELA, AMS-02 are now engaged in searching for strangelets in galactic cosmic rays (GCR). Hence, in the present context, it is quite important to estimate the possible flux of strangelets in the solar neighborhood and that is the key motivation behind this work. In this work, we have provided a possible production scenario of the galactic strangelets and determine the plausible baryon number (or, mass) distribution of such strangelets by invoking the statistical multifragmentation model (SMM) often used in nuclear systems. The strangelets originated in binary SS mergers are then likely to be accelerated by the shock waves generated in such mergers and they attain a power-law spectrum with a spectral index close to -2. We then apply the standard diffusive propagation model to describe the propagation of the strangelets through the randomly oriented magnetic field of the interstellar medium (ISM) and finally estimate the flux of the strangelets near the vicinity of the Sun. We have also compared our theoretical estimates with the upper limits of fluxes of strangelets reported by PAMELA. We have seen that our theoretical estimates are consistent with the observation of PAMELA, and such estimates are also useful for AMS-02 and other future experiments to vindicate the SMH.

Jayan Biswas

<b>List of Figures</b>	<b>viii</b>
<b>List of Tables</b>	<b>ix</b>
<b>1. Introduction and overview</b>	<b>1</b>
1.1. Prelude . . . . .	1
1.2. Compact stars . . . . .	6
1.3. Connection between cosmic rays (CR) and strangelets . . . . .	8
1.4. Quantum Chromodynamics (QCD) & the MIT bag model of SQM . . . . .	12
1.5. Strange quark matter (SQM) . . . . .	15
1.6. Properties of Strange Quark Matter (SQM) . . . . .	18
1.6.1. Bulk SQM . . . . .	18
1.6.2. Strangelets . . . . .	20
1.6.3. Color Flavor Locked (CFL) SQM and the corresponding strangelets	21
1.7. Experimental searches for strangelets and a few possible evidences of their existence . . . . .	24
1.7.1. Experimental searches . . . . .	24
1.7.2. Existing reports of exotic events . . . . .	29
1.8. A possible scenario for the production of astrophysical strangelets . . . . .	33
1.9. Statistical multifragmentation model (SMM) . . . . .	35

1.10. The outline of the thesis . . . . .	38
Bibliography . . . . .	41
<b>2. A preliminary calculation for fragmentation of astrophysical SQM</b>	<b>51</b>
2.1. Mass-spectrum of strangelets . . . . .	53
2.2. Discussion . . . . .	58
Bibliography . . . . .	62
<b>3. A trend in fragmentation pattern in CFL SQM</b>	<b>64</b>
3.1. Possible production scenario of CFL strangelets . . . . .	66
3.2. Quantum statistical multifragmentation model for CFL strangelets . . . . .	67
3.3. Equilibrium equations for a CFL strangelet . . . . .	69
3.4. Mass spectra of CFL strangelets . . . . .	74
3.5. An approximate estimate for the flux of CFL strangelets in the vicinity of the solar system . . . . .	80
3.6. Discussion . . . . .	82
Bibliography . . . . .	85
<b>4. An improved fragment distribution for unpaired SQM</b>	<b>89</b>
4.1. The multifragmentation model . . . . .	91
4.2. Thermodynamics of a strangelet . . . . .	96
4.3. Mass spectra of strangelets . . . . .	105
4.4. Stability of the produced fragments . . . . .	111
4.5. Discussion . . . . .	113
Bibliography . . . . .	117
<b>5. Estimation of flux of galactic strangelets in the solar neighborhood</b>	<b>122</b>
5.1. Acceleration and propagation of galactic strangelets . . . . .	122
5.2. Estimation of flux of galactic strangelets . . . . .	126
5.3. Discussion . . . . .	130
Bibliography . . . . .	133

<b>6. Summary and future outlook</b>	<b>135</b>
Bibliography . . . . .	141
<b>Appendices</b>	<b>142</b>
<b>Appendix A. Calculations of thermodynamic quantities (<math>m_s = 0</math>)</b>	<b>142</b>
A.1. Standard thermodynamic quantities of strangelets ( $m_s = 0$ ) . . . . .	142
A.2. Analytical approach to estimate the range of $\mu_q$ . . . . .	144
<b>Appendix B. Calculation of Fermi &amp; Bose integrals</b>	<b>146</b>
B.1. Expressions of Fermi and Bose integrals used in the expression of multiplicity	146
B.2. Mathematical expressions of Bose & Fermi integrals . . . . .	148
B.3. MATLAB codes for calculation of Bose & Fermi integrals . . . . .	149
<b>Appendix C. Debye screening and thermodynamic potential</b>	<b>157</b>
C.1. Debye screening in strangelet . . . . .	157
C.2. An approach to calculate thermodynamic potential for $m_s \neq 0$ . . . . .	158
<b>Appendix D. Calculations related to estimation of flux of strangelets</b>	<b>161</b>

	List of Figures
--	-----------------

1.1.	The fundamental particles as well as the quanta of the three fundamental force-fields that act upon those particles according to the Standard model of particle physics. . . . .	3
1.2.	Various combinations of quarks in the hadrons are shown in the figure. Ordinary matter (ie., the nuclear matter) are formed out of the nuclei consisting of the two lightest quarks, namely, the $u$ and the $d$ quarks. The combinations of three quarks (or, their antiquarks) are called the baryons (such as the nucleons) and the combinations of only one quark and an antiquark are called the mesons (such as the $\pi$ -meson). The heavier $s$ quarks (or, their antiquarks $\bar{s}$ ) have, so far, been found only in unstable particles, ie., in heavier mesons and in hyperons, such as the K-mesons and the lambda particles respectively, as shown in the figure. Each of the nucleons retains its individuality in ordinary nuclear matter. On the other hand, individual hadrons lose their identity (ie., the hadrons are so close to each other that their separate boundaries get dissolved and the quark degrees of freedom dominate) in the hypothesized SQM that may exist as a more stable form of matter than the nuclear matter. . . . .	4
1.3.	Observed differential spectrum of CR above the Earth's atmosphere. . . . .	9

1.4. A pictorial representation of the standard MIT bag model showing free quarks inside the bag that can not escape from the bag. The quarks are confined inside the bag due to the pressure exerted on them by the QCD vacuum from outside the bag boundary on the system of quarks inside the bag. . . . .	13
1.5. The presence of an additional Fermi well lowers the energy per baryon of a 3-flavor system in comparison with the 2-flavor system. . . . .	16
1.6. CFL phase is shown in the figure in which the quarks of all the flavors (u, d and s) and colors (red, green and blue) in an SQM together form the condensates with a common Fermi momentum $p_F$ . . . . .	22
1.7. The picture shows the cargo bay of the Discovery space shuttle in which AMS-01 detector was placed at the tail part of the cargo bay. . . . .	25
1.8. The picture shows the AMS-02 detector (shown in the red circle). The detector has been installed at the International Space Station (ISS). . . . .	26
1.9. Three unusual events detected in CR, along with the normal CR nuclei like O, Fe, Pb and U are displayed in the $Z$ vs. $A$ diagram. . . . .	30
1.10. Different possible stages of a binary SS merger are shown in the figure that actually displays the quark matter density contours at different time steps obtained in the simulations of such merger between two model SSs. The formation of the tidal arms are shown at the bottom left panel of the diagram. A fraction of the strange matter located at the tips of those tidal arms becomes gravitationally unbound of the merged stellar remnant to escape freely in the ISM. . . . .	34
1.11. A schematic diagram depicting the process of fragmentation, in which an warm and excited nuclear or strange matter expands in quasi-thermodynamic equilibrium and cools down simultaneously. Fluctuations in the bulk matter produce fractures that develop into lumpy structures (or, the quasi-fragments) with the further expansion of the fragmenting system. At the freeze out, the residual strong interactions between those lumpy structures cease to exist so that the fully developed fragments are produced. . . . .	36

2.1. Variation of $\ln \omega(A)$ with the variation in $A$ for the strangelets at different temperatures for a fixed value of the available volume $\mathcal{V} = 5V_b$ are displayed for (a) the full range of the available baryon numbers and (b) for a limited range of baryon numbers of the strangelets. Here, $A_b = 1 \times 10^{53}$ . . . . .	55
2.2. $\ln \omega$ vs. $A$ for different values of the available volumes $\mathcal{V}$ are shown for (a) the full range of the available baryon numbers and (b) for a limited range of baryon numbers of the strangelet-fragments. Temperature is taken as 10 keV. Here, $A_b = 1 \times 10^{53}$ . . . . .	56
2.3. Energy per baryon ( $E/A$ ) vs. baryon number ( $A$ ) of the strangelets at $T = 1$ MeV but for a fixed value of the available volume $\mathcal{V} = 5V_b$ . The solid horizontal line indicates the $E/A$ of $^{56}\text{Fe}$ (ie., 930 MeV). The strangelets having $E/A \lesssim 930$ MeV are considered to be absolutely stable. . . . .	57
3.1. Variation of $(\ln \omega)$ of CFL strangelets with the variation in their baryon number ( $A$ ) for (a) fixed value of the gap parameter $\Delta_o$ but two different values of the MIT bag parameter $B$ and for (b) fixed value of the bag parameter but two different values of the gap parameter as indicated in the diagrams. The available volume is chosen to be $\mathcal{V} = 5V_b$ in both the figures at $T = 10$ keV at freeze-out. Here, $A_b = 1 \times 10^{52}$ . . . . .	76
3.2. (a) Variations of $\ln \omega$ vs. baryon number ( $A$ ) of CFL strangelets for the available volume $\mathcal{V} = 5V_b$ at three different temperatures at freeze-out are indicated in the diagram. (b) Difference between the logarithm of multiplicities of CFL strangelets, determined separately from quantum and classical formulae, is shown for a limited range of values of the baryon number of strangelets and only for the lowest temperature $T = 1$ keV at freeze-out considered in (a). Available volume and the remaining parameters, considered to draw this diagram, are the same as in (a). In both the figures, $A_b = 1 \times 10^{52}$ . . . . .	77
3.3. Energy per baryon ( $E/A$ ) vs. baryon number ( $A$ ) of strangelets with their parameter values being indicated in the diagram. Here, the available volume is taken as $\mathcal{V} = 5V_b$ at $T = 10$ keV at freeze-out. Also, $A_b = 1 \times 10^{52}$ . . . .	78

4.1. Multiplicity ( $\ln \omega$ ) distribution of strangelets for massless ( $m_s = 0$ ) and massive ( $m_s = 95$ MeV) $s$ quarks both for a fixed value of the bag parameter ( $B^{1/4} = 145$ MeV) at a specific temperature ( $T = 10$ keV) at freeze-out. The $u$ and the $d$ quarks are considered to be massless in both cases. The results are displayed for (a) the full range of the available baryon numbers and (b) for a limited range of baryon numbers of the strangelet-fragments. Fig. 4.1(b) is included to focus on the lower cut-off ( $A \approx 11$ for $m_s = 95$ MeV) in the baryon numbers as well as the baryon number ( $A \approx 4$ ) at which the peak of the distribution (for $m_s = 0$ ) is obtained. Available volume is determined to be $\mathcal{V} \approx 8 \times 10^3 V_b$ , $A_b = 1 \times 10^{53}$ . . . . .	107
4.2. $\ln \omega$ vs. $A$ for the strangelet-fragments with $B^{1/4} = 145$ MeV and $m_s = 95$ MeV at three different temperatures at freeze-out. Variations are displayed for (a) the full range of possible baryon numbers and for (b) a limited range of baryon numbers of the fragments. . . . .	109
4.3. Variations of $\ln \omega$ vs. $A$ for strangelets with $m_s = 95$ MeV at a specific temperature ( $T = 10$ keV) but at two different bag values have been shown for (a) the full range of possible baryon numbers and for (b) a limited range of baryon numbers of the fragments. Approximate value of the quark number chemical potential ( $\mu_b$ ) of the initial bulk matter before fragmentation, that corresponds to each value of the bag parameter at zero external pressure and zero temperature, is also displayed. . . . .	110
4.4. Variation of the energy per baryon ( $E/A$ ) against changing baryon number ( $A$ ) of the strangelet-fragments (with $m_s = 95$ MeV) for three different values of the bag parameter at a specific temperature ( $T = 1$ MeV) at freeze-out. Corresponding value of the quark number chemical potential ( $\mu_b$ ) of the initial bulk matter at zero pressure ( $P_{\text{ext}} = 0$ ) and zero temperature is displayed against each bag value for the sake of comparison. The solid (red) horizontal lines mark the energies per baryon of $^{56}\text{Fe}$ , nucleon and $\Lambda^0$ -hyperon, respectively, that delineate the thresholds for absolute stability, metastability and instability of the fragments. . . . .	112

5.1. A model to study the propagation of strangelets in the Milky Way Galaxy. In the schematic diagram,  $H$  and  $h$  are half-height of the cylinder and half-thickness of the central plane respectively. . . . . 125

5.2. Integral flux vs. rigidity of the strangelet-fragments with  $B^{1/4} = 145$  MeV and  $m_s = 95$  MeV that are formed at three different temperatures at freeze-out. Comparisons with PAMELA results are displayed for (a)  $A = 11$ ,  $Z = 1$  and  $H = 1$  kpc, and for (b)  $A = 30$ ,  $Z = 2$  and  $H = 1$  kpc. . . . . 128

5.3. Integral flux vs. rigidity of the strangelet-fragments with  $B^{1/4} = 145$  MeV and  $m_s = 95$  MeV that are formed at three different temperatures at freeze-out. Comparisons with PAMELA results are displayed for (a)  $A = 11$ ,  $Z = 1$  and  $H = 0.3$  kpc, and for (b)  $A = 30$ ,  $Z = 2$  and  $H = 0.3$  kpc. . . . . 129

List of Tables

1.1. A list of experiments involved in the search of strangelets. . . . . 29

1.2. A list of strange matter phenomenology. . . . . 31

1.3. Summary of Z vs A in different CR experiments. . . . . 32

4.1. Expected ranges of the integrated (over baryon number) intensity of stable strangelets in the solar neighborhood for different intervals of plausible bag values and for the corresponding ranges of the (tentatively) estimated tidally released mass per SS merger. The estimations of ejected masses are inspired by the recent simulations of SS mergers in binary systems in which the limit of mass-resolution was  $\sim 10^{-5}M_{\odot}$ . . . . . 114

# Chapter 1

## Introduction and overview

### 1.1. Prelude

*“Twinkle, twinkle, little star,  
How I wonder what you are!  
Up above the world so high,  
Like a diamond in the sky.  
.....  
Twinkle, twinkle, little star.”*

*Jane Taylor [1]*

Even to-date, those wonderful lines from the poem “The Star” direct the joyful attention of the children to the sparkling “diamonds” in the night sky. That attention, perhaps, creates a lasting impression in the minds of at least some of those children who become inspired enough to scientifically probe into those heavenly objects after they grow up to maturity. In fact, from the ancient times, human beings have encountered various celestial objects and events such that a drive for self-protection from the possible inauspicious events seemingly associated with those phenomena, accompanied by a natural inquisitiveness, have compelled them to ponder over the reasons for those occurrences that eventually gave birth to the specialized discipline of astronomy and astrophysics. This discipline got an

impetus from the advent of modern optical telescopes that were first used to observe the sky by Galileo Galilei in the early seventeenth century. At the present epoch, the highly sophisticated space and ground based telescopes span our field of view from the gamma rays to the radio wavelengths. Instruments are being developed that can even detect highly relativistic, almost non-interacting neutrinos and the gravitational radiations coming from far away corners of the universe. Those modern ‘observing’ equipments are able to resolve distant objects with unprecedented accuracy thus helping us enormously to understand the issues related to the origin, evolution, structure and constituents of the universe having an unimaginable extent.

With the above advancements in astronomy and astrophysics, along with the advances in nuclear and particle physics accompanied by the tremendous improvements in the observational, experimental and the computational resources, the scientific community has reached some consensus about the origin of the universe. The currently prevailing view is that we live in a flat, homogeneous and isotropic universe that originated in a hot (and dense) “Big Bang” about some fourteen billion years ago and it is possibly evolving through an accelerating phase of expansion at its present epoch [2]. Moreover, there is perfect unanimity among the physicists regarding the “standard model of particle physics” that informs us that the fermions, called the quarks and the leptons, along with their antiparticles (having oppositely signed electric charge as well as all the oppositely signed flavor quantum numbers or lepton numbers barring the mass and the total angular momentum or the spin which do not change their signs), are the basic constituent particles of any form of known matter. A list of all the quarks and leptons as well as the quanta (ie., the bosons) of the three fundamental (ie., the strong, weak and the electromagnetic) forces of nature in this standard model of particle physics, along with their crucial properties, are summarized in Fig. 1.1 [3]. According to this standard model, quarks are bound either in the baryons (ie., protons, neutrons, atomic nuclei and the hyperons) or in the mesons (eg., pions, kaons etc.); see Fig. 1.2 [4] for the various possible forms of matter constituted by the two or three of the “light quarks” (ie., the up, down and the strange quarks) and their antiquarks with three different “color quantum numbers” that we will touch upon in Sec. 1.4 below. Quarks can interact *via.* the so-called “strong force (or, the strong interaction)” and the gluons are the mediator of such a force. The so-called “weak interaction” (the famous

The Periodic Table of Elementary Particles and Forces

Three Generations of Matter (Fermions)				
	I	II	III	
mass→	2.4 MeV	1.27 GeV	171.2 GeV	0
charge→	$\frac{2}{3}$	$\frac{2}{3}$	$\frac{2}{3}$	0
spin→	$\frac{1}{2}$	$\frac{1}{2}$	$\frac{1}{2}$	1
name→	<b>u</b> up	<b>c</b> charm	<b>t</b> top (truth)	<b>γ</b> photon (electromagnetic)
Quarks	4.8 MeV $-\frac{1}{3}$ $\frac{1}{2}$ <b>d</b> down	104 MeV $-\frac{1}{3}$ $\frac{1}{2}$ <b>s</b> strange	4.2 GeV $-\frac{1}{3}$ $\frac{1}{2}$ <b>b</b> bottom (beauty)	0 0 1 <b>g</b> gluon (strong force)
	<2.2 eV 0 $\frac{1}{2}$ <b>ν<sub>e</sub></b> electron neutrino	<0.17 MeV 0 $\frac{1}{2}$ <b>ν<sub>μ</sub></b> muon neutrino	<15.5 MeV 0 $\frac{1}{2}$ <b>ν<sub>τ</sub></b> tau neutrino	91.2 GeV 0 1 <b>Z<sup>0</sup></b> weak force
	0.511 MeV -1 $\frac{1}{2}$ <b>e</b> electron	105.7 MeV -1 $\frac{1}{2}$ <b>μ</b> muon	1.777 GeV -1 $\frac{1}{2}$ <b>τ</b> tau	80.4 GeV ±1 1 <b>W<sup>±</sup></b> weak force
Leptons				115-185 GeV ±1 0 <b>H</b> higgs boson

Figure 1.1.: The fundamental particles as well as the quanta of the three fundamental force-fields that act upon those particles according to the Standard model of particle physics [3].

example of which is the beta-decay) involving leptons are mediated by the  $Z^0$  and the  $W^\pm$  bosons while the electromagnetic interactions are mediated by the photons. Fig. 1.1, given above, provides a pictorial representation of these quanta of the three fundamental (excluding gravity) force-fields. Fig. 1.2, displayed below, shows that both the baryons and the mesons together are classified as the hadrons. According to the modern nuclear and particle physics, protons and neutrons (together, they are known as the nucleons) are

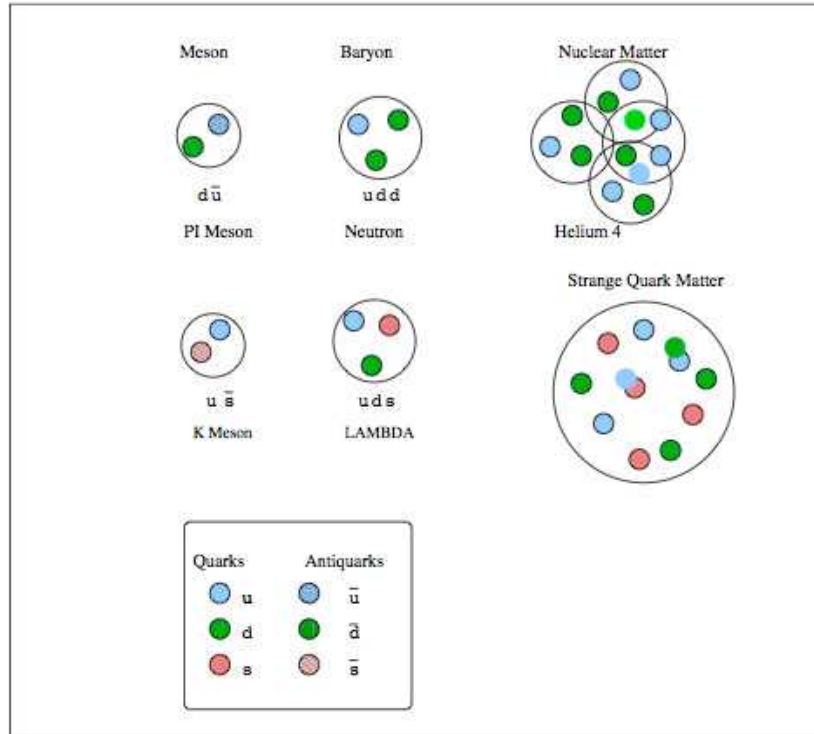


Figure 1.2.: Various combinations of quarks in the hadrons are shown in the figure. Ordinary matter (ie., the nuclear matter) are formed out of the nuclei consisting of the two lightest quarks, namely, the  $u$  and the  $d$  quarks. The combinations of three quarks (or, their antiquarks) are called the baryons (such as the nucleons) and the combinations of only one quark and an antiquark are called the mesons (such as the  $\pi$ -meson). The heavier  $s$  quarks (or, their antiquarks  $\bar{s}$ ) have, so far, been found only in unstable particles, ie., in heavier mesons and in hyperons, such as the K-mesons and the lambda particles respectively, as shown in the figure. Each of the nucleons retains its individuality in ordinary nuclear matter. On the other hand, individual hadrons lose their identity (ie., the hadrons are so close to each other that their separate boundaries get dissolved and the quark degrees of freedom dominate) in the hypothesized SQM that may exist as a more stable form of matter than the nuclear matter [4].

the basic constituents of all the atomic nuclei, that are found to prevail in the terrestrial environment. The nuclear matter is also believed to constitute all the stars - including both the “twinkling” (or, the luminous) stars [5] and the so-called “dead stars”, the latter consisting mainly of the white dwarfs (WDs), neutron stars (NSs) and the black holes

(BHs) [6, 7, 8]; see, Sec. 1.2 for more details about those objects. Some hyperons (such as the lambda particles in Fig. 1.2) may also be present in their metastable state under the extreme conditions of temperature and pressure that are likely to prevail in the interior of the NSs [6, 7]. The galactic cosmic rays (GCR) - the mysterious high energy corpuscular radiation (see Sec. 1.3 for more detail), that possibly originate from some violent stellar explosions called the supernovae (SNe; see Sec. 1.3) in our Galaxy, before arriving at the top of the Earth's atmosphere are also found to be dominated by the protons, neutrons and the atomic nuclei (along with some unstable mesons, unstable hyperons and also some leptons, of course) thus giving evidence of the predominant presence of the baryons in the Galaxy. However, several past and contemporary records, such as the Price's event [9] and the AMS-01 [10] experiment (see Sec. 1.7 for a brief account of several such events) have indicated the possible existence of certain exotic particles with unusual (in comparison with the normal nuclei) charge to mass ratio in the observations of GCR and their ground-based counterparts, namely, the "secondary cosmic rays" or the "atmospheric cosmic rays" (arising out of the interactions of GCR with the Earth's atmosphere), which can not be explained away in terms of the known baryons, mesons or the leptons. Small lumps of a novel form of yet hypothesized matter, namely the "Strange Quark Matter (SQM)" [11, 12], may, in fact, be the potential candidates of such unusual events in GCR; see Secs. 1.5 and 1.6 for some more detail. A possible mode of origin of such strangelets in GCR and the theoretical possibility of their detection by the space-borne detectors above the atmosphere of the Earth is the subject matter of the present thesis.

The topic of this thesis is, in fact, based on the conjecture, known as the "strange matter hypothesis (SMH)" [11, 12], that arose from the realization that the standard model of particle physics allows the existence of a new form of matter, namely the SQM, with the strange ( $s$ ) quarks being one of its essential ingredients that make it more stable than the normal nuclear matter such as a gas of neutrons [13]. This matter is obviously colorless and a baryon number may be attached to it so that they are sometimes called the "quasi-baryonic matter" [4] in the literature. SMH, in fact, claims that the SQM, on its own right, may be the true ground state of hadronic matter instead of the hitherto experienced most stable form of hadronic matter, namely, the  $^{56}\text{Fe}$  nuclei; SQM is incorporated in Fig. 1.2 above, along with the other known forms (viz. baryons and mesons) of hadrons, for the

sake of completeness.

The SQM was originally proposed to be a possible candidate for the cosmological dark matter - the yet unidentified form of matter that fails to absorb or emit electromagnetic radiation but still accounts for about 27% of all the matter and energy in the universe [14]. Some authors [15, 16] are of the opinion that the SQM might have been produced during the cosmological quark-hadron phase transition in the early universe, i.e., some  $10^{-5}$  s after the Big Bang [17], even if such a phase transition were not of the first order. Some chunks of those originally produced SQM may still survive in the present epoch of the universe to potentially account for the cosmological dark matter problem [16]. The above idea, though not at all ruled out, is seldom found to appear in the recent literature [18]. In this thesis, we, therefore, leave that (albeit important) particular issue aside without further justification. Even without that aspect, the SMH has other astrophysical implications, perhaps the most important of them being the possible existence of stable, self-bound strange stars (SSs) with vanishing external pressure on the surface of those stars [6, 7, 11, 19, 20]. A theoretical examination of the possible consequences of this implication and the simultaneous experimental efforts to find the signatures of those consequences are necessary to ultimately vindicate the SMH. The present thesis focuses on such astrophysical relevance of SMH in the light of modern experimental observations.

The remaining part of this introductory chapter is essentially an outline describing some of the basic concepts used later in this thesis. There, we would review the basic facts about the compact stars and the cosmic rays (CR). We would also review those properties of the SQMs that have some bearings on our theoretical calculations elaborated in the subsequent chapters of this thesis. In the following sections of this chapter, we would also outline the possible astrophysical production scenario of the small lumps of SQM, namely the strangelets, and briefly mention the current experimental searches for those strangelets in the galactic and atmospheric CR.

## 1.2. Compact stars

The compact stars are like the corpses of once luminous stars. They are, in fact, the remnant cores of the dead stars that have already completed their lifetimes of about a few

tens to a few thousands of million years [6] as bright objects undergoing nuclear fusion reactions.

Nuclear fusion reactions occur in the interior of all luminous stars. In such reactions, hydrogen gets converted to heavier elements during the luminous lifetimes of the stars. For the massive ( $M_{\text{star}} \gtrsim 8M_{\odot}$  with  $M_{\odot} \approx 2 \times 10^{33}$  gm being the solar mass) stars, the end point (called the iron point) of the exothermal nuclear fusion reaction is reached when the star finally gets transformed to an NS after passing through several complex stages of its evolutionary track [6]. For the light ( $M_{\text{star}} \lesssim 8M_{\odot}$ ) stars, the combustion process is incomplete in the sense of not reaching the iron point. The star is generally converted to a WD [6] in this particular situation. The black holes (BHs), on the other hand, are believed to form mostly from the stars that were initially more massive ( $M_{\text{star}} \gtrsim (20 - 30) M_{\odot}$ ) than the NS progenitors. In such BHs, the material of the stellar core collapses under its self-gravity to such a high density that its escape velocity reaches the speed of light. It should, however, be borne in mind that such categorization of the end states of the stars according to their progenitor masses alone cannot be in complete agreement with reality as it leaves out many other important parameters of the stars.

Apart from the BHs, the WDs and NSs are the two major groups in the family of compact stars. WDs are composed of the nuclei immersed in a degenerate electron gas. This degenerate gas provides the necessary inward gradient of the Fermi pressure to support the WD against collapse under its self-gravity [6, 8]. In contrast, the protons and electrons supposedly fuse together to form neutrons under the force of gravity in the dense core of an NS. The outwardly directed radial gradient of the neutron degeneracy pressure inside the NS, along with its inwardly directed self-gravity, principally maintains the equilibrium of an NS [6]. They are supposedly composed mainly of the nucleons and the hyperons but, in some cases, the core of an NS may also contain the strange quark matter [6]. It follows that, apart from their conventional form that gives them their name, the NSs can theoretically take several other forms like the hyperon stars, hybrid stars and the strange stars (SSs) [6]. If SMH is true, then the SSs (ie., the stars comprising almost entirely of SQM except perhaps a thin crust made out of the ordinary nuclei [6]) would be the most likely fate of the NSs so that all the existent NSs would ultimately be transformed into the SSs. Various routes for such NS to SS conversion process have been put forward by different

authors [21, 22]. Without going through a detailed review of all such processes, we simply note that, according to most of those authors, the time scale for the possible conversion processes is at the most of the order of a few seconds to a few minutes [21, 22] which is, in fact, minuscule in comparison with the luminous life-time of the star or with the present age of the universe. Therefore, we are, perhaps, justified in assuming that, a very large number (if not all) of the supposed NS candidates in our galaxy are, in reality, the already converted SSs. Similarly, the majority of the compact binary stellar systems in the Galaxy, that are believed to consist of two NSs, may actually be comprised of two SSs. In this context, it is important to note that it may be quite difficult, if not impossible, to observationally confirm whether a star is an SS or an NS. A few plausible diagnostic tools, arising out of the preliminary numerical simulations, have, however, been suggested to distinguish a merger event between two NSs from the one between two possible SSs in a compact binary stellar system [23, 24]. Firstly, the characteristic frequencies of the gravitational wave-signals generated during the simulated merger events are found to be different in the two cases mentioned above [23, 24]. Secondly, the quasistatic evolution of the combined system after merger has been found to be very different in the two cases [23, 24] so that they might be observationally distinguishable. Finally, a simulated tidal interaction between two SSs has been found to spew appreciable SQM material out of the gravitational influence of the merged system for the standard values of the quantum chromodynamical (QCD) bag constant  $B$  (see Sec. 1.4 for more details), which is a crucial parameter in the theoretical description of the SSs [23]. The above numerical simulations further predict that the SQM, thus ejected in an SS merger event, would eventually fragment into charged strangelets of various sizes to mix with the GCR, the detection of which in the vicinity of the solar system might provide us with a decisive proof of the existence of SSs in the compact binary stellar systems of the Galaxy thus, in turn, vindicating the SMH [23, 24, 25].

### 1.3. Connection between cosmic rays (CR) and strangelets

Several authors [26, 27, 28, 29, 30] have pointed out the possibility of detecting strangelets in the observations of the CR both above and within the Earth's atmosphere. Recent simulations of SS mergers (see Sec. 1.8 for detail) in the compact binary stellar systems

have predicted the formation of tidal arms and the ejection of appreciable amounts of SQMs from the tips of those tidal arms in a number of such merger events [23, 24] that are likely to fragment into strangelets to eventually mix with the GCR [23]. In this section, we would, therefore, like to provide a very brief account of the CR before we actually discuss the possibility of finding strangelets in CR.

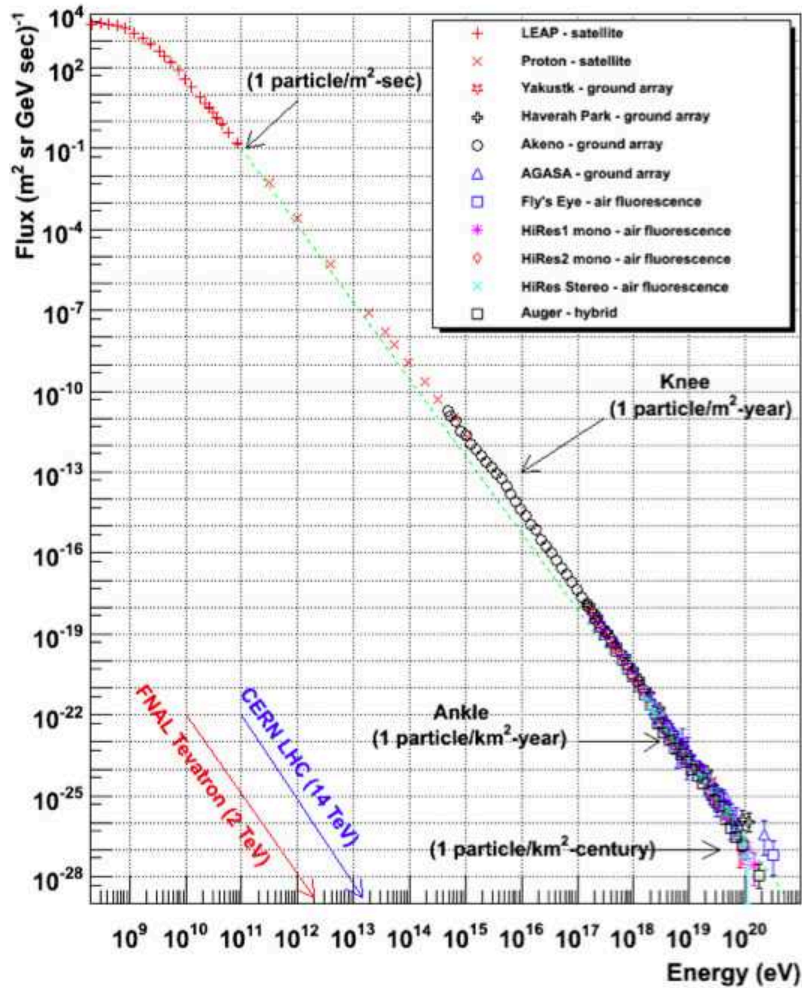


Figure 1.3.: Observed differential spectrum of CR above the Earth's atmosphere [31].

Fig. 1.3 [31] shows the differential spectrum (ie., the ratio between the differential change in the flux of CR particles for an infinitesimal increment in the energy per nucleon of those

particles and the aforesaid increment in energy as plotted against the energy per nucleon of CR particles) of CR above the Earth's atmosphere that indicates that the CR has a very wide range of energy, from  $\sim 10^9$  eV/nucleon to  $10^{20}$  eV/nucleon. CR particles, having energies (per nucleon)  $\lesssim 10^{18}$  eV [32] are most likely to be the GCR, while those having their energies above this limit are supposed to come from the extragalactic sources [33, 34]. In this thesis, we would confine our attention to GCR alone. The GCR particles are energetic, ionized nuclei that consist mostly of protons along with a small fraction of alpha particles and the heavier nuclei [33]. GCR presumably originates at the SNe [35] and gets accelerated at the shock waves associated with those SNe [33, 36]. In the following paragraph, we provide a very brief account of the SNe and the particle acceleration at the shocks associated with them as we would use very similar concepts for the acceleration of strangelets in Chap. 5 of this thesis.

SNe [35] are among the most energetic phenomena in the Galaxy in which the outer crusts of the luminous stars are ejected at almost relativistic speeds either due to sudden re-ignition of nuclear fusion in a degenerate star owing to the accretion of new material from its binary companion or due to the sudden gravitational collapse of the core of a massive star at the end of its luminous life time. The ejected material would then collide either with the interstellar medium (ISM) or with the wind generated by the parent star that creates a powerful shock wave [31]. GCR particles originating at the ejected material of the SNe are presumably accelerated at this shock by the first order Fermi acceleration mechanism [33, 37], in which the particles cross the shock front several times in the course of their random thermal motion in the vicinity of the shock. After gaining sufficient energy, the particles leave their sites of generation and they are accelerated to get injected in the ISM with their energies following a characteristic power law distribution; note the approximate power law behavior of the differential flux of GCR with energy in Fig. 1.3. The accelerated and charged GCR particles then propagate randomly in the inhomogeneous magnetic field of the ISM before they arrive in the solar neighborhood. In Chap. 5 of this thesis, we would adopt a somewhat similar mechanism for the production and acceleration of galactic strangelets and their eventual propagation in the ISM so that we can approximately determine the flux of those strangelets in the vicinity of the solar system. There, we consider that the strangelets originate from fragmentation of the SQM material tidally released out of the

coalescence of two SSs in a compact binary stellar system. The produced strangelets are likely to be adjacent to the shock front that has been generated by the merger process itself, perhaps by the impact of the tidally released matter with the ISM. Due to their random motion in the inhomogeneous magnetic field of the ISM, the charged strangelets cross this shock front several times so that they are accelerated by the first order Fermi mechanism in a way similar to the GCR particles. Apart from the possibility of obtaining strangelets from SS mergers as suggested above, a few authors have proposed that some SQMs might get mixed with the material ejected in certain core-collapse SNe [38], that should also contribute to the galactic strangelet-flux above the Earth's atmosphere. In that particular scenario, a detonation wave should be triggered during the conversion of nuclear matter to SQM in the NS core of an SN with a massive ( $> 8M_{\odot}$ ) progenitor star. The detonation front would propagate from the center of the core towards its surface. This detonation wave is supposedly energetic enough to catch up with the original SN shock thus contaminating the initial SN ejecta with SQM due to turbulent mixing [39]. In Ref. [25], J. Madsen, however, opined that the possible flux of strangelets, that may be available near the solar system from such core-collapse SNe, would probably be insignificant in comparison with the one arising from the possible SS merger events. Moreover, recent three dimensional hydrodynamical simulations of the NS to SS combustion [40] process have also shown that the resulting conversion front may stop well before it reaches the surface of the core of the NS thus suggesting that the mixing of SQM with the SNe ejecta is quite unlikely. In this thesis, we, therefore, leave such possibility of obtaining strangelets from the SNe ejecta out of our consideration in favor of the possibility of their production in stellar mergers alone. The model of SQM fragmentation, that we develop in this thesis, is, however, generalized enough to be useful in the former scenario as well. To work out the detailed consequences of the particular production scenario endorsed in this thesis, we are now required to filter out the most relevant features from our phenomenological knowledge of the strong force (see Sec. 1.1 above) binding the quarks together thus enabling us to mathematically describe the approximate properties of strange matters and their fragmentation into strangelets of a wide array of sizes in a satisfactory way. Such an identification of the important aspects of QCD (that is the fundamental theory of the strong force) and the choice of a simple mathematical model simulating those aspects into a description of SQM and its

fragmentation is undertaken in the next section of this introductory chapter.

## 1.4. Quantum Chromodynamics (QCD) & the MIT bag model of SQM

Quarks are bound together in hadrons by the so-called strong force in such a manner that a single quark alone can never escape from those multi-quark systems. The strong force binds only the quarks together and does not affect the leptons. The resulting interaction between the quarks under this force-field is called the strong interaction. The strength of this strong force varies with distance. This distance dependence is much stiffer than the one for gravity or the electromagnetic force which obey the inverse-square law. The strong force effectively disappears once the quarks are separated by more than about 1 fm ( $= 10^{-13}$  centimetre), which is approximately the radius of a nucleon. QCD is the theory that is supposed to describe the properties of this strong interaction between quarks. However, this theory is so complex that it is amenable neither to an analytical approach nor to some form of numerical computations that are suitable for providing an insight into the “working” of this theory from its basic principles at the relevant energy scale ( $\gtrsim 1$  GeV). As a consequence of the above, even though QCD is claimed to be the fundamental theory for the strong interaction, many basic questions regarding the detailed nature of such strong interaction inside the hadrons remain yet unanswered. As a result of this complexity of the theory of strong force, although a broad range of physical properties of the strongly interacting systems are now tentatively understood, only a very few results have actually been rigorously proved within the QCD framework. For example, according to QCD, each quark carries a color quantum number. Baryonic systems, in particular, seem to be made of the combinations of three different colored quarks, usually denoted as the red, green and the blue quarks with their antiquarks having the corresponding anticolors, so that the whole system becomes color-neutral. A single quark can not fulfil the criteria of color neutrality which introduces the concept of spatial and color confinement of the quarks thus explaining the fact that no isolated or free quark has, so far, been detected in the past efforts and also in the presently performed experiments.

As we are unable to derive the physical properties of strongly interacting systems from first principles, a different route is usually taken by exploiting the phenomenological knowledge of QCD. One may thus construct models so that they resemble the true theory as closely as possible. The standard MIT bag model [41] is one of such phenomenological models that we use in this work.

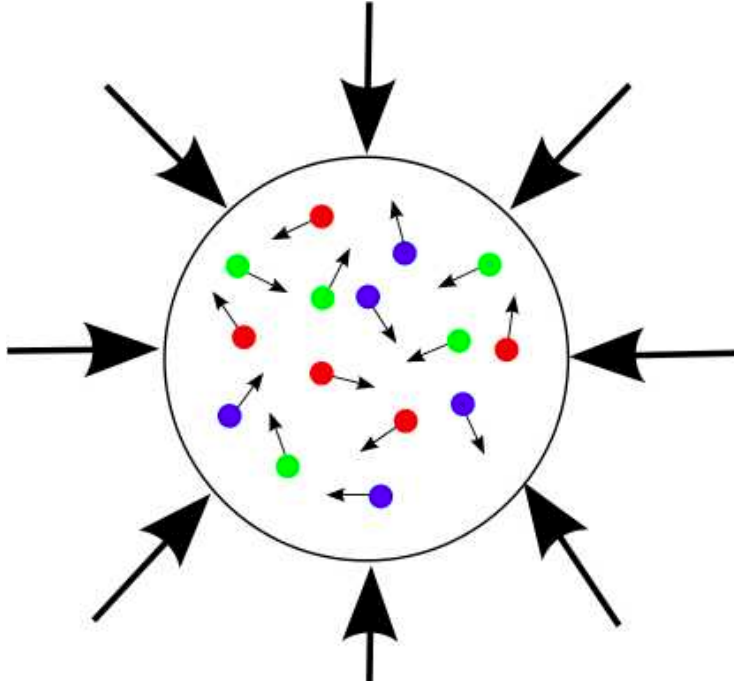


Figure 1.4.: A pictorial representation of the MIT bag model showing free quarks inside the bag that can not escape from the bag. The quarks are confined inside the bag due to the pressure exerted on them by the QCD vacuum from outside the bag boundary on the system of quarks inside the bag [42].

In 1974, the standard MIT bag model was proposed by a group of physicists of the Massachusetts Institute of Technology, USA to explain the properties of hadrons. In this model, the spatial and color confinement of QCD in long distance scales ( $\gtrsim 1$  fm) is phenomenologically modelled by a ‘bag’ that acts as an enclosure for the color-constituents (ie., the quarks) of the strongly interacting systems such that they can not escape from those systems as shown in Fig. 1.4 [42]. The relativistic quarks are, however, free to move inside the bag thus simulating the “asymptotic freedom” of the quarks in QCD at small

(< 1 fm) distances as measured from the centre of the hadrons. The bag constant  $B$  is the major parameter in this model that may be physically realized as the pressure exerted by the surrounding non-perturbative QCD vacuum outside the bag boundary on the quarks inside the bag. The bag provides a barrier for the color-constituents and hence mimics the spatial and color confinement of a strongly bound system. Apart from the bag parameter, other parameters in the MIT bag model are the current mass ( $m_s$ ) of the  $s$  quarks and the interaction strength ( $\alpha_s$ ) representing the force exerted by the perturbative (QCD) vacuum inside the bag on the multiquark system. The parameter  $\alpha_s$  has uncertain values but, fortunately, we can approximately handle it by choosing  $\alpha_s = 0$ . This is because of the fact that the effect of finite  $\alpha_s$  may, to a reasonable approximation, be absorbed into the bag constant ( $B$ ) [12] which itself is an uncertain parameter and, therefore, must be kept flexible within certain empirically determined range of values. With the above simplification, the properties and stability of the hadrons in the MIT bag model are determined only by the bag constant ( $B$ ) and current-mass  $m_s$  of the  $s$  quarks. Although the MIT bag model addresses only selective features of QCD, namely, the asymptotic freedom and the confinement property of strongly interacting systems, it has become successful in interpreting the mass spectrum of the light hadrons (except that it fails to explain the mass of pions) and various other experimental results related to the properties of those hadrons [43]. In this thesis, we do not take into account the contribution of zero-point energy (it is also ignored by several authors to study the properties of strangelets [42, 44, 45]), a phenomenological term originally introduced in the MIT bag model to fit the properties of light hadrons, which vanishes rapidly (compared to other finite size effects, such as surface and curvature, in strangelets) with increasing radius (ie., the zero-point energy is inversely proportional to radius) of the bag [42].

In this thesis, we have used the MIT bag model to describe the physical properties of SQM as well as those of the strangelets. This is because of the fact that, we are primarily interested in the fragmentation of SQM into strangelets with a wide array of their possible baryon numbers ( $A$  is denoted as baryon number) in this thesis. To describe such fragmentation pattern for the first time in the literature, we find it convenient to distil two essential features of the complex QCD theory into our modelling. Firstly, we are required to exploit the property of asymptotic freedom of the quarks well inside each of

the strangelets so that we may approximate those quarks as belonging to a free, relativistic fermi gas within that strangelet. Secondly, we exploit the spatial and color confinement of the quarks within each of the myriad number of strangelets that may be obtained from the thermodynamically motivated reorganization of the quarks originally residing inside the dilute and warm bulk strange matter before fragmentation. We believe that the resultant simple, two parameter MIT bag model of SQM would be able to provide us some physical insight into the trend in the fragmentation pattern that would not have been available by straight way employing more complex, multiparameter models of SQM, such as, the effective field theoretical models or the Nambu-Jona-Lasinio (NJL) models [46]. On the other hand, once the basic trend in the fragmentation pattern of SQM and the nature of its dependence on various physical parameters, such as the bag constant ( $B$ ), the mass ( $m_s$ ) of the  $s$ - quarks and also the temperature ( $T$ ), representing thermodynamic equilibrium of the fragmenting complex, are already known from the MIT bag model, it would perhaps be useful to investigate how such basic pattern is changed by using more complex QCD-motivated models. In the next section, we, therefore, give an outline of the properties of SQM within the framework of the MIT bag model.

## 1.5. Strange quark matter (SQM)

Within the framework of the MIT bag model [41], the SQM may be considered to be a large collection of comparable numbers of up ( $u$ ), down ( $d$ ) and strange ( $s$ ) quarks enclosed in a bag. These quarks can move around freely inside the enclosure (ie., the bag) that does not allow the quarks to escape thus forming a multiquark bound system (see Fig. 1.4 [42]).

In our everyday experience, we confront stable baryonic matter, ie., the nuclei of our familiar matter, that consists of the nucleons (protons and neutrons) - each of which may be envisaged as consisting of three of the two types of the lightest quarks, namely the  $u$  and the  $d$  quarks, enclosed in an MIT bag. We may, therefore think that it is quite unlikely to find stable bags consisting of more than three quarks. Consider, for example, a stable deuteron nucleus comprising of a proton and a neutron that are, in fact, two adjacent but distinct quark bags according to the MIT bag model. We have no evidence, whatsoever, of any stable system, consisting of the  $u$  and the  $d$  quarks, in which a single quark bag holds

all those six quarks simultaneously - still having an energy per baryon that is lower than that for the deuteron nucleus.

A.R. Bodmer [47] was the first person to theoretically envisage the possibility of the existence of the nuclei of a new form of matter in which the  $s$  quarks are added to the quark bag consisting of the  $u$  and the  $d$  quarks. According to his proposal, such a novel form of nuclei may exist as the long-lived exotic nuclei under large pressure within the cores of the compact stars with the sizes of their bag (ie., the sizes of the exotic nuclei) being more compressed than those for the ordinary nuclei.

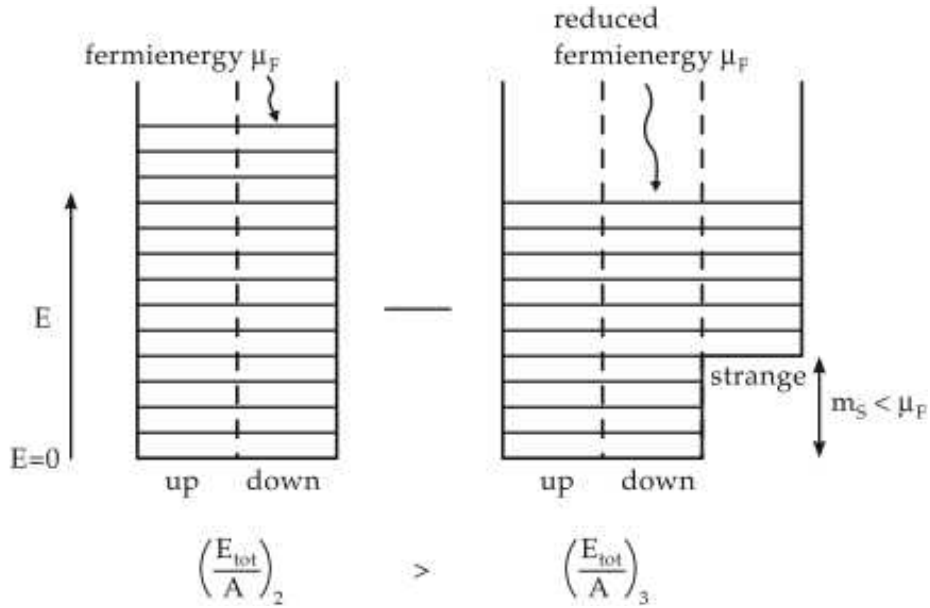


Figure 1.5.: The presence of an additional Fermi well lowers the energy per baryon of a 3-flavor system in comparison with the 2-flavor system [49].

Later, S.A. Chin and A.K. Kerman [48], and independently, L.D. McLerran and J.D. Bjorken [26], came up with some general arguments in support of the possibility of having stable hadronic states consisting of three quark flavors even at zero external pressure [49]. The postulates given by them regarding such a stable system are stated as in the following.

1. In such a configuration, the weak decay of an  $s$  quark into a  $d$  quark would be forbidden due to the unavailability of the lowest single quark states as all those

states may be occupied.

2. The  $s$  quark mass \* would be less than the Fermi energy of the  $u$  and the  $d$  quarks in such a system. The  $s$  flavor, being different from the  $u$  and the  $d$  flavor, would insert an additional Fermi well in the system. Thus, the system would lower its overall Fermi energy by distributing the quarks in all the three Fermi wells (shown in Fig. 1.5 [49]).

According to this picture, an SQM is likely to be charge-neutral as any net charge arising from the difference between the number of the massive  $s$  quarks and the (equal) numbers of each of the (almost) massless  $u$  and the  $d$  quarks would be neutralized by electrons residing inside the SQM. If we ignore the mass of the  $s$  quarks, then the numbers of the  $u$ ,  $d$  and the  $s$  quarks should be exactly equal so that the SQM becomes absolutely charge-neutral without the necessity of having electrons in the system.

In 1984, E. Witten [11] resurrected the above ideas in his seminal paper in which he had put forward the conjecture that a system of  $3A$  ( $A$  being the baryon number of the SQM) quarks consisting of roughly equal numbers of the  $u$ ,  $d$  and the  $s$  quarks may have an energy per baryon that is lower than that of the normal nuclear matter (ie., a gas of neutrons, say) with a mass number  $A$  [11]. The SQM may even be more stable than the iron nuclei. A SQM blob of a reasonably large baryon number  $A$  (so that the finite size effects remain reasonably small; see the next section) would, therefore, represent the true

---

\*Here, the mass of each of the quark-flavors is considered to be its current quark-mass, ie., the mass of the bare quark, as considered in the MIT bag model [18]. The actual mass of a quark in a hadron, which is its constituent quark-mass in that hadron, may be much larger than its current quark-mass due to various QCD effects that have not been taken into account in the MIT bag model [6, 12, 18, 24]. We, therefore, do not consider such constituent quark-mass in this thesis. The current quark-mass of the  $u$ ,  $d$  and the  $s$  quarks are  $m_u \approx 3$  MeV,  $m_d \approx 5$  MeV and  $m_s \approx 100$  MeV, respectively. The chemical potentials of the  $u$ ,  $d$  and the  $s$  quarks at  $T = 0$ , that are the highest energies of those quarks in their respective Fermi-wells at chemical equilibrium at zero temperature, are given by  $\mu_u \approx \mu_d \approx \mu_s \sim 300$  MeV. A quark can be considered as massless if the square of the ratio of its current quark-mass to its chemical potential is much smaller than one. This approximation seems to be a reasonable one for the  $u$  and the  $d$  quarks but it seems to break down for the heavier  $s$  quarks. In Chaps. 2 and 3 of this thesis, we have, however, considered  $m_u \approx m_d \approx m_s \approx 0$  as a simplifying first approximation that is hoped to serve as a guidance to our further complicated calculations presented later in Chaps. 4 and 5 of this thesis. Similar approximations have earlier been considered by various authors [6, 18] to get a feeling for the physical nature of their complicated results obtained later with more realistic parameter values.

ground state of hadronic matter. This hypothesis of Witten (1984) is known as the strange matter hypothesis (SMH) in the literature that forms the basis of the present thesis. In the next section, we would like to discuss the thermodynamic properties of such an SQM.

## 1.6. Properties of Strange Quark Matter (SQM)

### 1.6.1. Bulk SQM

Bulk SQM can be considered to be a free Fermi gas of a large total number ( $3A$ ) of the  $u$ ,  $d$  and the  $s$  quarks under spatial and color confinement in a quark bag that separates the gas from the QCD vacuum by a phase boundary. In this case, as the volume of the system is sufficiently large, the finite size contributions, such as the contributions from the surface and curvature of the bag, to the system's thermodynamic potential may be ignored as a first approximation in comparison with the contribution from its volume. Actually, if we consider the energy per baryon of SQM, then the volume, surface and the curvature contributions vary with its baryon number as independent of  $A$ ,  $A^{-1/3}$  and  $A^{-2/3}$  respectively [18]. For bulk approximation (ie.,  $A \rightarrow \infty$ ), the surface and curvature contributions are, therefore, much smaller than the volume contribution, so that, we can ignore the surface and curvature contributions altogether in comparison with the volume (or, the bulk) term. For the sake of simplification, we here consider this bulk matter to be at zero temperature and zero external pressure (apart from the bag pressure). Due to the presence of the  $s$  quarks, the bulk SQM is relatively more stable than a collection of the  $u$  and the  $d$  quarks having the same baryon number  $A$ . If we further consider the  $s$  quarks to be massless (ie.,  $m_s = 0$ ), then the identical number (ie.,  $n_u = n_d = n_s$ ) of each of the three quark-flavors makes for a perfect charge-cancellation (ie.,  $\frac{2}{3}n_u - \frac{1}{3}n_d - \frac{1}{3}n_s = 0$ ) in the bulk matter. If, on the other hand, we consider a finite mass ( $m_s \neq 0$ ) of the  $s$  quarks, then the number of those quarks is somewhat lesser than the number of each of the massless  $u$  and  $d$  quarks inside the SQM at a specific baryon number ( $A$ ) of the bulk matter. In this situation, the small positive charge arising from such an imbalance in the numbers of different quark-flavors is neutralized by the presence of electrons inside the bulk matter. Chemical equilibrium in the system (chemical potential can be associated

with each flavor of the quark, electron, and neutrino) is maintained by weak interactions through the following flavor conversions:

$$d \leftrightarrow u + e^- + \bar{\nu}_e \tag{1.1a}$$

$$s \leftrightarrow u + e^- + \bar{\nu}_e \tag{1.1b}$$

$$u + s \leftrightarrow d + u. \tag{1.1c}$$

Here, the contribution from the neutrinos (actually those are antineutrinos) in the above reactions is not taken into account as those neutrinos leave the system after their production in the above reactions without any further interactions with the quarks inside the bag. In Secs. 1.4 and 1.5, we have provided heuristic arguments in favor of the hypothesis that the bulk SQM can become more stable in comparison with the nuclear matter, or even in comparison with the iron nuclei, for a certain region of the two dimensional parameter ( $B$  and  $m_s$ ) space. If we further consider the  $s$  quarks to be massless, the bulk SQM would then be absolutely stable (ie., more stable than the  $^{56}\text{Fe}$  nuclei) for the values of the bag parameter lying within a range given by [18]

$$145 \text{ MeV} \lesssim B^{1/4} \lesssim 163 \text{ MeV}. \tag{1.2}$$

Here, the lower limit of  $B^{1/4}$  corresponds to the minimum of the physically significant values for the bag constant ( $B$ ). For  $B^{1/4} < 145 \text{ MeV}$ , the calculated values of the energy per baryon of the bulk SQM would become more than that for a bulk matter consisting of the  $u$  and the  $d$  quarks alone. In that case, the SQM would be spontaneously converted to an  $ud$  quark matter which would become the most stable configuration of hadronic matter for such values of the bag constant. As for an example, the deuteron nucleus, consisting of one proton and one neutron, would spontaneously convert to a large conglomeration of three  $u$  quarks and three  $d$  quarks within a single QCD bag for such low values of the bag constant  $B$ . Such possibility is, however, in disagreement with our everyday experience and must, therefore, be ruled out. On the other hand, the upper limit of  $B^{1/4}$  in the above inequality corresponds to the maximum possible value of the bag constant for which the bulk SQM remains absolutely stable, ie., its energy per baryon remains lower than that for the iron

nuclei. This, in turn, implies that SMH is inapplicable for values of  $B^{1/4}$  that are more than the above upper limit. The above arguments in favor of the possible window of absolute stability (expressed by the inequality 1.2) of an SQM in terms of the values of its bag constant  $B$  in the simplifying case  $m_s = 0$  have, in fact, been analytically demonstrated in Ref. [18], that is not reproduced again in this thesis. More detailed calculations have shown that the above range of plausible values of the bag constant  $B$  is not significantly altered even when we incorporate the finite size effects in our calculations to consider the exotic nuclei of small  $A$  values that we would classify as the strangelets [18]. The upper bound of  $B$  in the inequality (1.2) is, however, found to decrease as we take a finite mass ( $m_s \neq 0$ ) of the s quarks into account [18].

### 1.6.2. Strangelets

Small lumps of SQM, whose baryon numbers usually satisfy the condition  $A \ll 10^7$ , are classified as the strangelets. The dimension of such a lump is simply given by  $\sim r_0 A^{1/3}$ , where  $r_0 \approx 1$  fm [45] is the radius parameter of the strangelet. For a baryon number  $A \sim 10^7$ , the size of the strangelet turns out to be  $\sim 215$  fm, which is less than an order of magnitude smaller than the Compton wavelength of the electrons given by  $\sim \frac{h}{m_e c} \sim 2478$  fm, where  $h$ ,  $m_e$  and  $c$  are the Planck's constant, the mass of the electron and the speed of light, respectively. Unlike in the case of the bulk SQM with  $m_s \neq 0$  (described in the previous section), in which the localized electrons within the SQM ensure its charge-neutrality, the charge-neutrality of the strangelets can no longer be maintained by the electrons that now reside well-outside the strangelets. Due to this fact, the strangelets would be slightly positively charged in the case  $m_s \neq 0$ . The charge ( $Z$ ) of the strangelets is, however, very small such that  $Z/A \ll 1/2$ , this being the key diagnostic feature for the strangelets, that makes them different from the normal cosmic rays nuclei, for which  $Z/A \sim 1/2$ . In the case of a strangelet, the finite size effects (ie., the contributions from its surface and curvature to its total energy) and the internal coulomb interactions between the charged quarks inside that strangelet (the effect of which is usually smaller than the surface and the curvature effects) will come into play that would try to destabilize the strangelet by tending to increase its energy per baryon above that for the iron nucleus or even those

for the nucleons. For the same values of the bag constant and the strange quark mass, a strangelet of an arbitrary baryon number may, therefore, be unstable even though the corresponding bulk SQM is absolutely stable. The strangelets of a specific baryon number ( $A$ ) may still be absolutely stable for certain specific intervals of values of the bag constant ( $B$ ) and the mass of the strange quarks ( $m_s$ ) [12, 18, 50] in those strangelets. Strangelets can be studied by the Shell model (analogous to the case of the normal nuclei) [12, 51, 52, 53]. It is known from the literature that the calculations performed by using the shell model, though tedious, usually provide more rigorous and detailed results [18] regarding the properties of an individual strangelet. In this thesis, we, however, have to deal with a collection of strangelets consisting of a vary large number of the strangelet-species, each of them having different values of the baryon number and the charge, so that it would, perhaps, be adequate to find the average properties of each species that are found to be satisfactorily provided by the so-called liquid drop model [18] of the strangelets. Finite size effects, such as the surface tension and the curvature coefficients stemming from the depletion of the surface and curvature density of states due to the finite value of  $m_s$ , are here derived by using the multiple reflection expansion procedure [54] within the frameworks of the liquid drop model and the standard MIT bag model [18].

### 1.6.3. Color Flavor Locked (CFL) SQM and the corresponding strangelets

The SQM described in the item number 1.6.1 of section 1.6 above may be termed as the “ordinary” or the “unpaired” SQM. This is in contrast with the other variant of SQM in which the quarks of three different flavors with their different color (see Fig. 1.6 [55]) quantum numbers form condensates [55] near the Fermi surface of the SQM with the SQM now showing new properties that are somewhat analogous to the appearance of superconductivity due to the BCS-pairing (eg. electrons in metals,  $^3\text{He}$  atoms etc. [55]) in solid state physics. Such SQMs are called the color-flavor-locked (CFL) SQM. This variety of SQM has been shown by Rajagopal and Wilczek [56] to be feasible for quite a significant ranges of values of the chemical potential (representing the values of the bag constant  $B$ ) and the mass of the strange quarks ( $m_s$ ). The bulk CFL SQM is electrically neutral even without having to have electrons inside that bulk matter unlike in the case of SQM of the ordinary variety; see item 1.6.1 above. This charge-neutrality is the outcome of the “BCS-

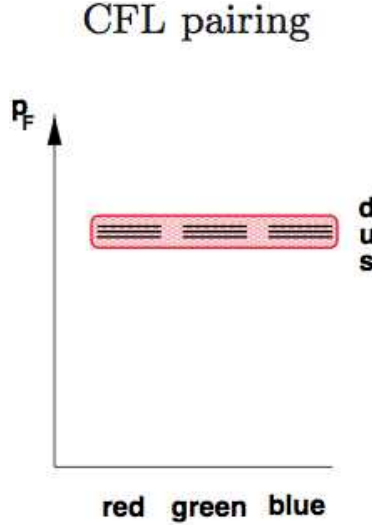


Figure 1.6.: CFL phase is shown in the figure in which the quarks of all the flavors ( $u$ ,  $d$  and  $s$ ) and the colors (red, green and blue) in an SQM together form the condensates with a common Fermi momentum  $p_F$  [55].

like pairing” between quarks of distinctly different flavors and the color quantum numbers having zero net momentum inside the SQM with the energy of the paired system being minimized only if the Fermi momenta of those quarks are equal [57]. One important aspect of the CFL phase is that the CFL SQM is denser and more stable than the corresponding ordinary SQM. The lower limit of bag constant for stable CFL SQM corresponds to  $B^{1/4} \gtrsim 156$  MeV, below which the strange matter decays to a two flavor color-superconducting phase in which only the two, instead of the three colors of the  $u$  and the  $d$  quarks are paired up. The upper limit of the bag constant for the CFL SQM has been found theoretically to approximately corresponds to  $B^{1/4} \sim 180$  MeV for  $m_s = 0$  with a typical value of the pairing or the gap energy (ie., the strength of the pairing of quarks [55]) being  $\sim 100$  MeV [57]. As in the case of the unpaired or the ordinary SQM, finite  $m_s$  lowers the upper limit of bag constant for CFL SQM also. Similar to the situation found in the case of ordinary strangelets, finite size effects increase the energy per baryon of the CFL strangelets [11, 12, 47, 48, 50, 51, 57, 58, 59] simultaneously yielding a small positive charge for those strangelets [59]. The charge to mass ratio for CFL strangelets with the electric charge number being  $Z \sim 0.3A^{2/3}$  [25], is, however, significantly different from those of

the ordinary strangelets. This difference in the charge to mass ratio may provide us with a diagnostic tool to test the existence of the CFL strangelets as opposed to the ordinary strangelets in the cosmic rays. The possible existence of CFL SQM in the stellar core is supposed to have significant consequences for the physics of the compact stars [60]. Here, we would like to add that a finite value of the temperature would increase the energy (per baryon) of both of the normal and the CFL strangelets [45, 61].

Having discussed the possibility of the existence of strange matter and strangelets (in Secs. 1.4-1.6) as the true ground state of hadronic matter, we must now find a satisfactory answer to the fundamental question as to why the various known baryonic forms of matter in our part of the universe have not already decayed to their natural ground state, namely, the SQM. One straightforward answer to this question is that such a decay to the SQM phase would require the presence of a significant fraction of  $s$  quarks in this part of the universe. The conversion of an iron nucleus with  $A = 56$  into a strangelet, for example, would require a very high order of weak interactions for the simultaneous conversions of a large number of the  $u$  and the  $d$  quarks (ie., roughly 56  $u$  and  $d$  quarks) into the  $s$  quarks. The probability of such simultaneous conversions is very rare in nature unless the environment in which such conversion might take place is already rich in its strangeness content (ie., a large fraction of the  $s$  quarks are already present in the environment) like the situation that possibly prevails in the interior of the neutron stars. For lower  $A$  values, however, lower order weak interaction is needed for the conversion, but finite size effects will also make the system unstable [18] in that situation. A simple calculation has estimated that in the normal environment, nuclei with  $A \gtrsim 6$  can exist for more than  $10^{60}$  years [7] before its possible conversion to a strangelet. From the above arguments, we can conclude that, the stability of SQM does not contradict with our everyday experience of baryonic matter (ie., composed with ordinary nuclei) in the visible universe.

## 1.7. Experimental searches for strangelets and a few possible evidences of their existence

### 1.7.1. Experimental searches

Experimental physicists have been searching for the evidence of SQM, the hypothesized ground state of hadronic matter, over the past three decades. Despite the fact that several strangelet-like exotic events have been reported within this time span, scientists could not draw any firm conclusion regarding the existence of strangelets from all those events. Such experimental searches for exotic particles fall mainly in two different categories, namely, 1) the attempts to produce strangelets in the Heavy-ion collision experiments [7] and 2) the searches for strangelets in CR. In the following, we mention a few selected experiments belonging to each of those categories, along with Table 1.1 [7], in which we provide a concise list of all those searches known to us.

#### 1.7.1.1. Heavy-ion collision experiments

High energy physicists are often of the opinion that strangelets of very low baryon numbers might actually be formed in the ultrarelativistic heavy-ion collision (UHIC) experiments. Even if we accept this possibility as being a plausible one, the finite size effects on the strangelets produced in that way are likely to destabilize those light strangelets. Apart from such finite-size effects, the ambient temperature of the region within the experimental set-up, in which the strangelets are formed, are likely to be high enough to severely reduce the stability of the produced strangelets so that those unstable or metastable strangelets would possibly decay into nuclei within about a weak interaction time-scale. Here, we would like to add that a number of such accelerator or collider-based experiments have, in fact, been already performed to produce strangelets in the laboratory, all of which have, however, ended up with null results [72].

### 1.7.1.2. Search for strangelets in CR

- Alpha Magnetic Spectrometer (AMS)



Figure 1.7.: The picture shows the cargo bay of the Discovery space shuttle in which AMS-01 detector was placed at the tail part of the cargo bay [64].

The Alpha Magnetic Spectrometer (AMS) is a space based particle tracker and detector, in which different charged particles follow different trajectories due to the applied magnetic field so that those charged particles are separated from each other depending on their charges and their baryon numbers.

In June 1998, the space shuttle ‘Discovery’ flew with a prototype of a particle detector (AMS-01) (see Fig 1.7 [64]) [65]. The analysis of data collected from that mission has

given the hints of a few events with unusually low  $Z/A$  ratio. One of such events had a signature of  $Z = 2$  and a mass of about 16.5 GeV. From the detector sensitivity, AMS-01 has predicted the flux of the order of  $1.5 \times 10^3 \text{ m}^{-2} \text{sr}^{-1} \text{yr}^{-1}$  [10] for those particles.



Figure 1.8.: The picture shows the AMS-02 detector (shown in the red circle). The detector has been installed at the International Space Station (ISS) [66].

Recently, a second generation detector of AMS, namely the AMS02, has been successfully installed at the International Space Station (ISS) (as shown in Fig 1.8 [66]). One of its many scientific goals is to search for strangelets in GCR. The sensitivity of the AMS-02 detector (for  $Z \lesssim 30$  and  $A \lesssim 10^3$ ) is about 1 particle  $\text{m}^{-2} \text{sr}^{-1} \text{yr}^{-1}$  [67].

- **PAMELA**

Like the AMS, the Payload for Antimatter Matter Exploration and Light-nuclei Astrophysics (PAMELA) is another space-borne detector which was launched by the European space agency. It also contains a magnetic spectrometer that can detect unusual events with low  $Z/A$  in GCR. Based on the null result of their attempt to

detect strangelets with their detector, the PAMELA collaboration has recently provided an upper limit for the possible flux of strangelets with their charge numbers being in the range  $1 \leq Z \leq 8$  [68]. In Chap. 5, we will compare our theoretically determined strangelet flux with the aforesaid upper limit of the flux reported by the PAMELA collaboration.

- **LSSS**

The surface layer of the moon is known to have a large cosmic ray exposure time of around 500 million years. Due to the absence of a magnetosphere of the moon, the expected strangelet concentration on the surface of the moon would be some four orders of magnitude larger than the one on the Earth [69]. The Lunar Soil Strangelet Search (LSSS) was, therefore, conducted to find the evidence of strangelets in a sample of about 15 grams of lunar soil, that is the part of a larger sample brought by the Apollo 11 mission from the moon. The analysis of the above sample was done by using the tandem accelerator at the Wright Nuclear Structure Laboratory at Yale University [69]. The analysis covered the charge numbers 6, 8 and 9, respectively in a mass range of about (42-70) amu (ie., atomic mass unit). From the null results of the above search, the upper limit of strangelet flux in the vicinity of the Earth is calculated to be about  $\sim 10^2 \text{ m}^{-2}\text{sr}^{-1}\text{yr}^{-1}$  [69].

- **SLIM**

Assuming that the strangelets are more likely to be found in CR at the mountain altitude, where they are less likely to interact with a very large number of atmospheric particles, the SLIM experiment was carried out at the Mt. Chacaltaya High Altitude Laboratory (5230 m above the sea level (asl)) at Bolivia during the years 2001-2005. In this experiment, some 427  $\text{m}^2$  wide array of nuclear track detectors in the modules of  $24 \times 24 \text{ cm}^2$  area each was laid exposed to the atmospheric CR for 4.22 years. The detectors were then etched and analyzed at the laboratory of Bologna, Italy resulting in null results. From such results, the upper limit of the possible strangelet flux in CR at the Mt. Chacaltaya altitude was estimated to be  $\sim 4.1 \times 10^{-4} \text{ m}^{-2}\text{sr}^{-1}\text{yr}^{-1}$  [70].

- **Indian experiment for searching strangelets in CR**

Like the experimentalists of the SLIM experiment, the researchers from the Centre

for Astroparticle Physics and Space Science (CAPSS) of Bose Institute, Kolkata and Darjeeling, India, have also been involved in a project sponsored by the Department of Science and Technology (DST), Govt. of India, with a goal to detect strangelets in atmospheric cosmic rays at the mountain altitudes of Darjeeling (2042 m asl), Ooty (2240 m asl) and Hanle (4500 m asl) in India. In this particular experiment, the detectors are made out of a low-cost polymer, namely the polyethylene terephthalate (PET), that is being used as the passive solid-state nuclear track detector (SSNTD) systems. Normally, a charged CR particle would leave behind it a narrow damaged trail during its passage through the SSNTD [82]. As the damaged trails are chemically more reactive than the undamaged parts of the detectors, those trails are etched out with the help of chemical reagents. A detailed study of the geometry of the etch-pits is expected to reveal the identity of the charged particles [82, 83] that caused the damages. In the first half of the project, the PET detectors were exposed to known ion beams available at different particle accelerator facilities in India and abroad to study the charge response of PET and the detectors were calibrated accordingly. The aim of the currently ongoing second stage of the project is to identify anomalous events in CR and to determine their approximate  $Z/A$  ratio with the help of the calibration curve drawn during the first half of the project. Some anomalous events in CR have, so far, been detected by using the above detectors, a detailed analysis of which is presently in order [83]. It is, however, important to note that the choice of the detector material (ie. its sensitivity on the charge and the kinetic energy of the desired strangelets) in the above experiment has been, to some extent, motivated by a plausible theoretical model [4] regarding the interaction of strangelets with the atmospheric molecules that may, as well, limit the validity of the above experiment only to a certain class of events. Also, at least an approximate theoretical estimate of the plausible flux of strangelets above the Earth's atmosphere, along with the theoretical model given in Ref. [4], may be necessary for a better assessment of the results obtained from the experiment under consideration. The work presented in this thesis is, in fact, a preliminary attempt towards that particular direction.

Table 1.1.: A list of experiments involved in the search of strangelets.

Experiment	References
Search for strangelets at Heavy-ion experiments: Strangelet searches E864, E878, E882-B, E896-A, E886 Pb+Pb collisions	[62] [63]
Cosmic ray searches for strangelets: Alpha Magnetic Spectrometer (AMS)  PAMELA LSSS SLIM Cosmic Ray And Strange Hadronic matter (CRASH) Extremely-heavy Cosmic-ray Composition Observer (ECCO) HADRON Irvine Michigan Brookhaven proton-decay detector (IMB) Japanese-American Cooperative Emulsion Chamber Ex- periment (JACEE) Monopole, Astrophysics and Cosmic Ray Observatory (MACRO) Extreme Universe Space Observatory will be accommo- dated in Japanese Experimental Module (JEM-EUSO) Strangelet search with passive detector (PET)	[10, 65, 67, 71, 72] [68] [69] [70] [30, 73, 74] [75]  [76] [77] [78, 79] [80] [81] [83]
Search for strangelets in terrestrial matter Tracks in ancient mica Rutherford backscattering	[84] [27, 85] [86]

### 1.7.2. Existing reports of exotic events

In the context of the possibility of detection of strangelets in CR, that is the subject matter of this particular thesis, we should also mention a number of observed events, with unusually small charge to mass ratios in comparison with the ones for the ordinary nuclei, that have, so far, been reported in the CR observations. These events are listed in the

following.

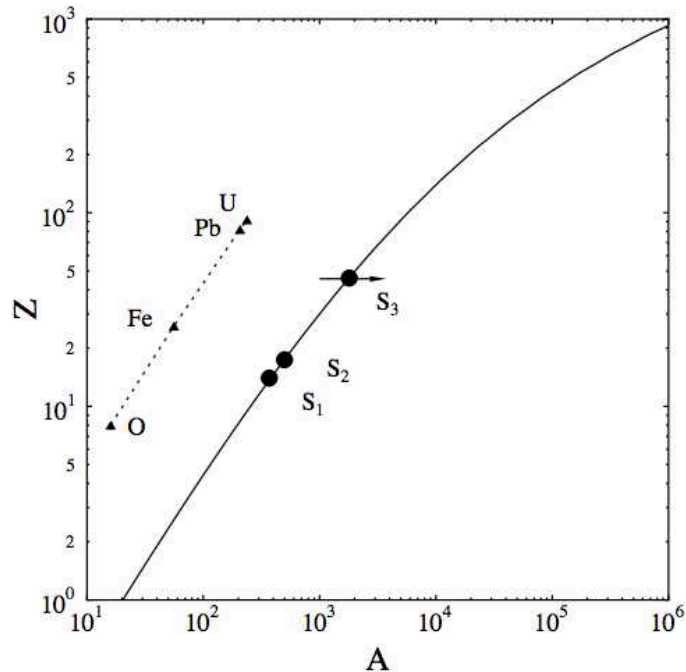


Figure 1.9.: Three unusual events detected in CR, along with normal CR nuclei like O, Fe, Pb and U, are displayed in the  $Z$  vs.  $A$  diagram [89].

The earliest recorded account of the observation of an anomalous event detected in the atmospheric CR is perhaps the famous ‘Price’s Event’ [9]. This particular event, that has been associated with an unusual particle with a charge number  $Z \sim 46$  and a baryon number  $A \sim 1000$ , was recorded in a 1978 CR observation. Almost around the same time, a few more events, known as the ‘Centauro cosmic ray events’ [87], were detected in emulsion exposures in an experiment carried out by a joint Brazil-Japan collaboration group at the observing station at Mt. Chacaltaya, Bolivia. The Centauro events are particularly interesting as the recorded events contained hundreds of baryons with almost no  $\pi^0$  and the  $\gamma$  photons associated with them which is not normally observed in ground based CR detectors.

In 1990, Saito *et al.* [30] analyzed the data collected from the HECRO-81 balloon borne experiment equipped with Cherenkov and scintillation counters. These authors claimed to

have identified two unusual events with  $Z \sim 14$  and  $A \sim 370$  that could not be explained in terms of any nuclei that are known to be available in CR. Fig 1.9 [89] displays three events in a  $Z$  vs  $A$  diagram along with a few normal nuclei like O, Fe, Pb and U to show the unusual nature of the above three events and their difference from the ordinary nuclei.

Table 1.2.: A list of strange matter phenomenology.

Phenomenon	References
Centauro cosmic ray events	[26, 29, 48, 87, 88]
High-energy gamma ray sources: Cyg X-3 and Her X-3	[90]
Strange matter hitting the Earth: Strange meteors	[27]
Nuclearite-induced earthquakes	[27, 91]
Unusual seismic events	[92]
Strange nuggets in cosmic rays	[28, 89, 93]
Strange matter in supernovae	[94]
Strange star phenomenology	[7, 20, 95, 96]
Strange dwarfs: Static properties and stability	[96, 97, 98]
Thermal evolution	[99]
Strange planets	[96, 97]
Strange MACHOS	[100]
Strangeness production in dense stars	[101]
Burning of neutron stars to strange stars	[102]
Gamma-ray bursts, Soft Gamma Repeaters	[19, 103]
Cosmological aspects of strange matter	[11, 104]
Strange matter as compact energy source	[105]
Strangelets in nuclear collisions	[49, 106]

In 1993, an ‘exotic track event’ with  $Z \sim 20$  and  $A \sim 460$  was reported by Ichimura *et al.* [74] after the analysis of a balloon borne experiment performed in the year 1989 in which CR39 (Columbia Resin 39) was used as the SSNTD. Recently, the AMS-01 (see Fig 1.7 [64]) experiment has reported two events (apart from the one discussed in Sec. 1.7.1.2) with

their charge numbers and the baryon numbers being given as  $Z \sim 8$ ,  $A \sim 20$  and  $Z \sim 4$ ,  $A \sim 50$  [10], respectively. Additionally, several exotic events have also been reported with their baryon numbers lying in the range  $Z \sim (10 - 20)$  and  $A \sim (350 - 500)$  in the CR experiments [9, 74, 78, 107, 108]. A compact list of such unusual events, detected in the CR experiments, has been displayed in Table 1.2 [7]. A synopsis of all such unusual events, along with the observed ranges of their masses (baryon number) and the charge numbers, is presented in Table 1.3 [4]). Here, we may note that all the events presented in Table 1.3 are characterized by their small ( $Z/A \ll 1/2$ ) charge to mass ratio, that is supposed to be the characteristic feature of the strangelets; see Sec. 1.6.

Although the above observations have been performed by different experimental groups at different times, the agreement on their possible connection with the existence of SQM is almost unequivocal. The aforesaid observational results were, however, shredded with a lot of uncertainties, such as the ambiguities related to the calibration of Cherenkov counter output, detector noises, dead times etc. that differed from one experiment to the other so that the existence of SQM could not, so far, be confirmed from those experiments. We are hopeful that the ongoing and the upcoming experimental projects will be able to draw some decisive conclusions regarding this matter.

Table 1.3.: Summary of Z vs A in different CR experiments.

Event	Charge (Z)	Mass (Baryon Number) (A)
Counter Experiments ([107])	14	350-450
Exotic Track ([74])	20	460
Price's Event [9]	46	1000
Balloon Experiment ([78, 108])	14	370
AMS 01 ([10])	4	50
	8	20

The discussion presented in this section seems to suggest that the astrophysical or cosmic ray observations, particularly at high altitudes or above the Earth's atmosphere, perhaps offer a better possibility of the detection of strangelets in comparison with their possible production in various accelerator or collider based experiments. This is the reason for our emphasis on the astrophysical scenario of production of strangelets in the present thesis. In the next section, we would present a brief review of the results from some of the recent numerical simulations, that are concerned with the possibility of the production of strangelets in the merger between two SSs in the compact binary stellar systems of the galaxy. The strangelets, thus produced, would possibly propagate in the random magnetic field of the galaxy to ultimately arrive in the vicinity of the solar system where they may be detected in the CR by the detector systems installed on-board various space-based observing stations. An approximate estimate of the flux of such strangelets of an wide array of plausible sizes in GCR in the solar neighborhood is the actual aim of this thesis.

## 1.8. A possible scenario for the production of astrophysical strangelets

Apart from the normal NSs and WDs, SMH predicts the existence of an additional family of compact stars, namely the SSs [6, 7, 19, 20, 109] (see the discussion in Sec. 1.2). Furthermore, most of the WDs and the NSs are likely to convert into their stable SS counterparts within time-scales that are much shorter in comparison with the luminous life times of their progenitor stars. A likely scenario for the production of galactic strangelets is that those strangelets are possibly the debris of collisions between the SSs in the compact binary stellar systems of the Galaxy. Recent simulations of SS mergers have demonstrated the formation of tidal arms during many of such merger processes (as shown in Fig.1.10 [23]). Fig. 1.10 [23], in fact, shows the different steps of a typical binary SS merger event, obtained in the numerical simulations of the coalescence between a  $1.2 M_{\odot}$  and a  $1.35 M_{\odot}$  companion SSs in a compact binary stellar system at different time steps of its evolution. The upper left panel of the figure shows the inspiral phase of the companion stars. In this phase, the binary SSs, rotating in counter-clockwise direction with respect to each

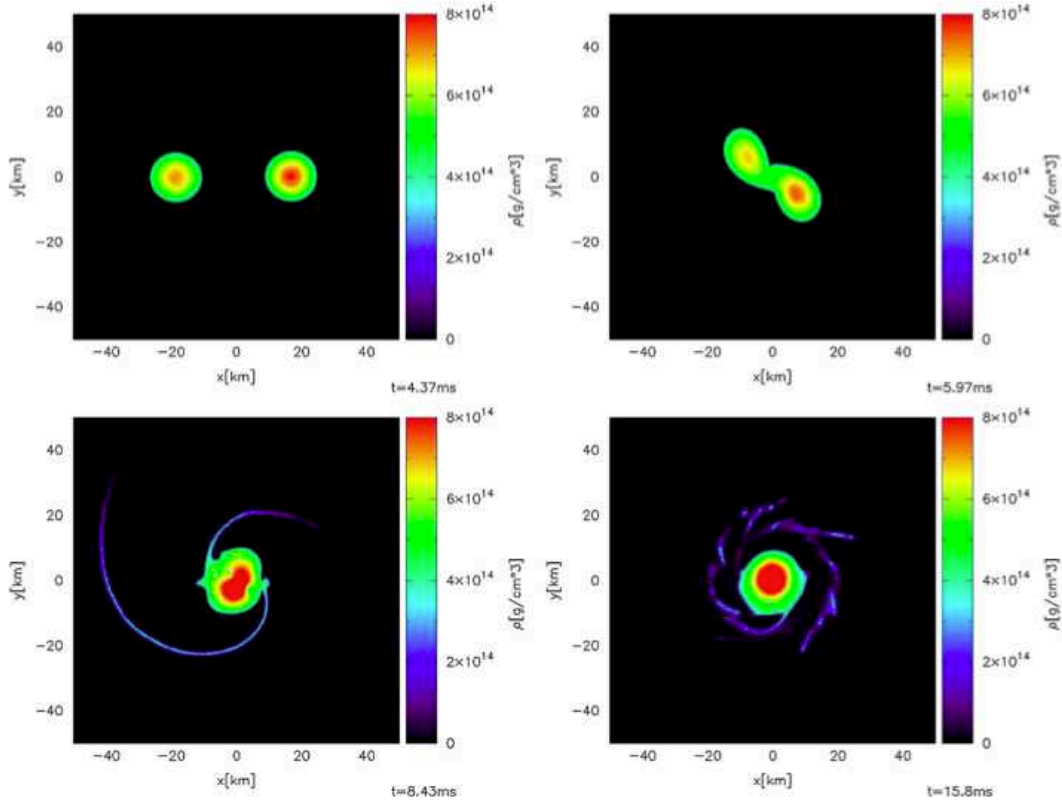


Figure 1.10.: Different possible stages of a binary SS merger are shown in the figure that actually displays the quark matter density contours at different time steps obtained in the simulations of such merger between two model SSs. The formation of the tidal arms is shown at the bottom left panel of the diagram. A fraction of the strange matter located at the tips of those tidal arms becomes gravitationally unbound of the merged stellar remnant to escape freely in the ISM [23].

other, lose angular momentum and energy due to gravitational wave emission which leads to their shrinking orbits until the SSs finally merge (shown in the upper right panel of the Fig 1.10) to each other. The above simulations of SS mergers have also demonstrated the formation of tidal arms during that merger process (shown in the bottom left panel of the Fig.1.10). A fraction of the SQM, located near the tips of those tidal arms, become gravitationally unbound to get injected in the ISM [23, 24]. Most of the SQM in the spiral arms is, however, gravitationally bound thus ending up in an orbit around the remnant of the combined (ie., merged) stellar system (shown in the bottom right of the Fig.1.10) by

forming a geometrically thin accretion disc around that merged stellar system. The ejected SQM, on the other hand, may be further fragmented to form strangelets of a large array of sizes (or, masses) such that the produced fragments would eventually mix with the GCR particles and propagate in the stochastic magnetic field of the galaxy to ultimately arrive in the vicinity of the solar system. J. Madsen [25] predicted the flux of such strangelets, produced in stellar mergers, above the Earth’s atmosphere by assuming all the strangelets, fragmented out of the tidally released bulk SQM, to be of equal sizes. In this thesis, we, however, assume that the initial SQM would produce strangelets of a large distribution of sizes after fragmentation. In the next section, we would briefly mention the statistical multifragmentation model (SMM), that we adopt in this thesis, for the description of the system, that is about to be permanently fragmented into strangelets of large an array of sizes at its thermodynamic equilibrium at freeze-out.

## 1.9. Statistical multifragmentation model (SMM)

For the determination of the mass spectrum (or, the baryon number distribution) of strangelets, we adopt a statistical multifragmentation model (SMM), which is also known as the ‘Copenhagen model for nuclear fragmentation’ in the literature. The model is often used to explain the experimental data related to the distribution of the lighter nuclei, that are the results of collisions between two heavier nuclei. In nuclear SMM [110, 111, 112], it is primarily assumed that an initially compressed warm nuclear matter, containing  $N'_o$  neutrons and  $Z'_o$  protons with a total baryon number  $A_0 = N'_o + Z'_o$ , evolves in quasi-thermodynamic equilibrium. The expanding matter undergoes disassembly when it reaches the ‘freeze-out volume’ at a constant temperature  $T$  over the volume of the fragmenting system, so that the residual strong interactions between the neighboring fragments cease (see Fig. 1.11 [110]) to exist. Here, the fragmenting system (ie., the expanding nuclear matter) is assumed to expand quasi-statically [113], for which the expansion time scale of the fragmenting complex is much larger in comparison with the relaxation time-scale of that complex. In the statistical disassembly model, the total charge and the baryon number of the fragmenting system are conserved. Thermodynamic equilibrium also implies chemical equilibrium, so that the chemical potentials of protons ( $\mu_p$ ) and neutrons ( $\mu_n$ )

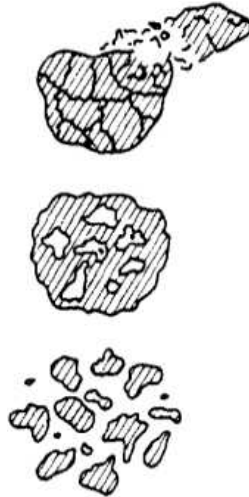


Figure 1.11.: A schematic diagram depicting the process of fragmentation, in which a warm and excited nuclear or strange matter expands in quasi-thermodynamic equilibrium and cools down simultaneously. Fluctuations in the bulk matter produce fractures that develop into lumpy structures (or, the quasi-fragments) with the further expansion of the fragmenting system. At the freeze out, the residual strong interactions between those lumpy structures cease to exist so that the fully developed fragments are produced [110].

attain their constant values throughout the body of the fragmenting system at freeze-out. At such freeze-out, the system is also assumed to have achieved its mechanical equilibrium under zero external pressure so that there can not be any radial collective flow in the fragmenting system at this particular state. The total thermodynamic potential of the system at freeze-out may then be written as [112, 114, 115]

$$\Omega = E - TS - \sum_{i=1}^{N'_s} \mu^i \omega^i. \quad (1.3)$$

Here,  $E$  and  $S$  are, respectively, the internal energy and the entropy of the fragmenting system. In Eq. (1.3),  $i$  denotes a particular fragment species with multiplicity  $\omega^i$  and chemical potential  $\mu^i = Z_p^i \mu_p + N_n^i \mu_n$ ;  $Z_p^i$  and  $N_n^i$  being the numbers of protons and neutrons in each fragment belonging to the  $i^{\text{th}}$  species. Moreover,  $N'_s$  is the total number of all the species available in fragmentation. The results obtained from this model correlates

extremely well with the relevant experimental observables [110].

The minimization of total thermodynamics potential in Eq. (1.3) leads to the occupancy function of a particular fragment-species. A phase-space integration of this occupancy function ultimately yields an expression for the multiplicity [112] of that particular species. This expression is given by [112, 115]

$$\omega^i = \frac{2\mathcal{V}}{\sqrt{\pi}(\mathcal{L}^i)^3} \sum_{j=0}^{\infty} g_j^i J_{1/2}^+(\eta_j^i), \quad (1.4)$$

or,

$$\omega^i = g_0^i \frac{1}{(e^{-\eta_0^i} - 1)} + \frac{2\mathcal{V}}{\sqrt{\pi}(\mathcal{L}^i)^3} \sum_{j=0}^{\infty} g_j^i J_{1/2}^-(\eta_j^i), \quad (1.5)$$

depending on whether the species is a fermion or a boson. The first term on the right hand side of Eq. (1.5) represents the contribution from the Bose-condensation. In Eqs. (1.4) and (1.5),  $\mathcal{V}$  is the available volume (ie., freeze-out volume minus the volume of the produced fragments) and  $\mathcal{L}^i = h/\sqrt{2\pi m^i T}$  is the thermal de Broglie wavelength of the  $i^{\text{th}}$  species;  $m^i$  being the effective mass of a fragment belonging to that species and  $h$  is the Planck's constant. We can consider  $m^i \approx m_n A^i$ , where,  $A^i$  is the baryon number of the  $i^{\text{th}}$  species and  $m_n = 938$  MeV is the average nucleon mass. In Eqs. (1.4) and (1.5), the freeze-out volume may be considered as a free parameter in the model. It is normally taken as about 3-10 times the initial volume of the fragmenting system [116]. In the above equations, the summation over  $j$  implies the summation over all the possible energy states of the fragment including the ground state and  $g_j^i$  is the degeneracy of the states. In Eqs. (1.4) and (1.5),  $J_{1/2}^{\pm}(\eta_j^i)$  denotes the Fermi or the Bose Integral; ie. [112],

$$J_{1/2}^{\pm}(\eta_j^i) = \int_0^{\infty} \frac{(x^i)^{1/2}}{e^{x^i - \eta_j^i} \pm 1} dx^i, \quad (1.6)$$

where,  $x^i = \frac{(p^i)^2}{2m^i T}$ ,  $p^i$  being the momentum of  $i^{\text{th}}$  species [112]. The ‘fugacity’  $\eta_j^i$  can be designated as [115]

$$\eta_j^i = (\mu^i - E_j^i)/T \quad (1.7)$$

with  $E_j^i$  is the energy of the  $i^{\text{th}}$  species in the  $j^{\text{th}}$  state.

If  $\eta_j^i < 0$  and  $|\eta_j^i| \gg 1$ , then  $J_{1/2}^\pm \simeq (\sqrt{\pi}/2)e^{\eta_j^i}$ ; Eqs. (1.4) and (1.5) can then be rewritten as the Maxwell-Boltzmann distribution for the fragments; ie. [115],

$$\omega^i = \frac{\mathcal{V}}{(\mathcal{L}^i)^3} e^{\mu^i/T} \sum_{j=0}^{\infty} g_j^i e^{-E_j^i/T}. \quad (1.8)$$

The sum in Eq. (1.8) can be correlated with the total canonical partition function  $\mathcal{Z}^i$  of the fragment of  $i^{\text{th}}$  species and defined as  $\mathcal{Z}^i = e^{-F^i/T}$ , where,  $F^i$  is the Helmholtz free-energy of the  $i^{\text{th}}$  species. The expression for the multiplicity of the  $i^{\text{th}}$  species may, therefore, be reframed as [115, 117]

$$\omega^i = \frac{\mathcal{V}}{(\mathcal{L}^i)^3} e^{(\mu^i - F^i)/T} = \frac{\mathcal{V}}{(\mathcal{L}^i)^3} e^{(-\Omega^i/T)}, \quad (1.9)$$

in which  $\Omega^i$  is the thermodynamic potential of the  $i^{\text{th}}$  fragment.

In this thesis, we adopt SMM to obtain a plausible size (or, the baryon number) distribution of strangelets resulting from the fragmentation of strange matter tidally released due the SS merger. In that particular application,  $i$  denotes the strangelet-species with baryon number  $A^i$  and  $m^i$  is the mass of that species. For massless quarks, the chemical potential of  $i^{\text{th}}$  species can be denoted as  $\mu^i = \sum_f \mu_f N_f^i$ , where,  $f$  denotes the flavor of the quark and  $N_f^i$  is the number of quarks of  $f^{\text{th}}$  flavor in the  $i^{\text{th}}$  species. This simple expression of  $\mu^i$  is modified for massive  $s$  quarks and the consequent presence of the electrons in the SQM (see Chap. 4). For massless antiquark, the number density of that antiquark (of a particular flavor) is proportional to  $T^3 e^{-\mu_q/T}$  [118], where,  $-\mu_q$  is the chemical potential of antiquark. The production of antiquark, for the temperature range we consider in this thesis, is negligible. For this reason, we do not consider the numbers of antiquarks and antibaryons in this thesis.

## 1.10. The outline of the thesis

The content of this thesis is organized as the following. In Chap. 2, we examine the thermodynamic properties of bulk SQM as well as those of the finite-sized strangelets by using the multiple reflection expansion procedure within the theoretical framework of

the MIT bag model with the additional assumption of massless quark-flavors within the MIT bag. In that chapter, we also provide a fragmentation model of the bulk SQM with massless quarks to find out the size distribution of the resulting strangelets and their approximate flux in the vicinity of the solar system. We hope that, the simplifying zero quark-mass approximation would provide us with some insight regarding the basic nature of the distribution pattern of the strangelets of varying sizes that may fragment out of the bulk matter tidally released in stellar merger. Some objections to this basic fragmentation pattern have recently been raised in Ref. [119] in which it has been claimed that, the fragmentation pattern would be altogether different from the one given in Chap. 2, if the color superconductivity of strange matter and the finite mass of strange quarks are taken into account in the calculations. In this thesis, we separate out the influences of those two factors on the fragment-size distribution of SQM. In Chap. 3, we examine the effect of the color-flavor-locking (CFL) alone on the fragmentation pattern of SQM in the limit of vanishingly small quark-masses. There, we find that the incorporation of the effect of color superconductivity of quark matter does not fundamentally change the nature of variation of the fragmentation pattern with the changes in the basic physical parameters of the problem. We, however, do not pursue the question of fragmentation of CFL matter in any more detail in this thesis. This is because of the fact that the recent theoretical research, along with the results obtained from numerical simulations, seems to suggest the near impossibility of obtaining CFL strangelets out of the stellar merger events. These reasons have been touched upon by us particularly in the concluding section of Chap. 3. The possibility of obtaining ordinary or unpaired strangelets in GCR seems, on the other hand, to be quite promising. In this thesis, we, therefore, confine ourselves mostly to those ordinary strangelets. In Chap. 4, we discuss the influence of finite mass of the  $s$  quarks on the fragment-size distribution of those ordinary strangelets. There, we find that the basic nature of the dependence of the fragmentation-pattern on various parameter values remains practically unaltered in the case of massive  $s$  quarks from the  $m_s = 0$  case described earlier in Chap. 2. The numerical values of the sizes would, however, depend on specific value of  $m_s$  chosen so that we have considered the current experimental estimate of a such value in Chap. 4. In Chap. 5, we used the fragment-size distributions obtained in Chap. 4 as inputs in a diffusive model of galactic propagation of strangelets to find an approximate

integral flux of galactic strangelets in the neighborhood of the Sun. There, we also compare the theoretically determined strangelet flux with the possible upper limit of the integral flux determined from the null results obtained, so far, in the PAMELA strangelet search experiment. In Chap. 6, we summarize the important features of the results obtained in this thesis. The future outlook for the theoretical strangelet research is also presented in that final chapter of the thesis. Throughout this work, we choose natural units such that  $\hbar = c = k_B = 1$ , where,  $\hbar$  is the reduced Planck's constant,  $c$  is the speed of light and  $k_B$  is the Boltzmann constant.

## Bibliography

- [1] <https://www.poetryfoundation.org/poems-and-poets/poems/detail/43200>.
- [2] M.H. Jones, R.J. Lambourne, and D.J. Adams, *An Introduction to Galaxies and Cosmology*, Cambridge University Press (2004); J.A. Frieman, M.S. Turner, and D. Huterer, *Ann. Rev. Astron. Astrophys* **46** (1), 385 (2008).
- [3] <https://mbhs.edu/~jeglick/Images/Information/Periodic%20Tables/The%20Periodic%20Table%20of%20Elementary%20Particles%20and%20Forces.jpg>.
- [4] S. Banerjee, *Some Aspects of Strange Matter In Astrophysics*, Ph.D. Thesis, Jadavpur University, India, 2003 [arXiv: 1408.6389].
- [5] P. S. Conti, P. A. Crowther, and C. Leitherer, *From Luminous Hot Stars to Starburst Galaxies*, Cambridge University Press (2008).
- [6] N.K. Glendenning, *Compact Stars: Nuclear Physics, Particle Physics and General Relativity* (Second Edition), Springer-Verlag, New York, USA (2000).
- [7] F. Weber, *Prog. Part. Nucl. Phys.* **54**, 193 (2005).
- [8] S.L. Shapiro and S.A. Teukolsky, *Black Holes, White Dwarfs, and Neutron Stars: The Physics of Compact Objects*, WILEY-VCH Verlag GmbH & Co. KGaA, Weinheim (2004).
- [9] P. B. Price, E. K. Shirk, W. Z. Osborne, and L. S. Pinsky, *Phys. Rev. D* **18**, 1382 (1978) ; T. Saito, *Proc. 24th ICRC, Rome* **1**, 898 (1995).
- [10] V. Choutko, in *28th International Cosmic Ray Conference* (University Academy Press, 2003) **4**, 1765 (2003).
- [11] E. Witten, *Phys. Rev. D* **30**, 272 (1984).
- [12] E. Farhi and R. L. Jaffe, *Phys. Rev. D* **30**, 2379 (1984).
- [13] J. Alam, S. Raha, and B. Sinha, *Astrophys. Jour.* **513**, 572 (1999).

- [14] A.V. Mitsou, *Int. Jour. Mod. Phys. A* **28**, 1330052 (2013); P. A. R. Ade *et al.* (Planck Collaboration), Planck 2013 results. XVI. Cosmological parameters, [arXiv:1303.5076 (astro-ph.CO)]; S. M. Carroll, W. H. Press, and E. L. Turner, *Ann. Rev. Astron. Astrophys.* **30**, 499 (1992).
- [15] S. Banerjee, A. Bhattacharyya, S.K. Ghosh, S. Raha, B. Sinha, and H. Toki, *Mon. Not. Roy. Astron. Soc.* **340**, 284 (2003); S. Banerjee, A. Bhattacharyya, S.K. Ghosh, S. Raha, B. Sinha, and H. Toki, *Nucl. Phys. A* **715**, 827 (2003).
- [16] P.W. Gorham, *Phys. Rev. D* **86**, 123005 (2012); P. Astone *et al.*, astro-ph/1306.5164 (2013); A. Atreya, A. Sarkar, and A.M. Srivastava, *Proc. Indian Natn. Sci. Acad.* **81**, 237 (2015).
- [17] D.J. Schwarz, *The Cosmological QCD Transition*, a thesis submitted for ‘venia legendi’, Institute for Theoretical Physics, Johann Wolfgang Goethe-University, Frankfurt, Germany, 1999.
- [18] J. Madsen, in: J. Cleymens (Ed.), *Lecture Notes in Physics: Physics and Astrophysics of Strange Quark Matter*, vol. **516**, Springer Verlag, Heidelberg, 1999, p. 162, arXiv:9809032v1(astro-ph) (1998).
- [19] C. Alcock, E. Farhi, and A. Olinto, *Astrophys. Jour.* **310**, 261 (1986).
- [20] P. Haensel, J.L. Zdunik, and R. Schaeffer, *Astron. Astrophys.* **160**, 121 (1986).
- [21] A. Bhattacharyya, S. K. Ghosh, P.S. Joarder, R. Mallick, and S. Raha, *Phys. Rev. C* **74**, 065804 (2006).
- [22] I. Bombaci and B. Datta, *Astrophys. Jour.* **530**, L69 (2000); G. Pagliara, M. Herzog, and F. K. Roepke, *Phys. Rev. D* **87**, 103007 (2013).
- [23] A. Bauswein, R. Oechslin, and H.-T. Janka, *Phys. Rev. D* **81**, 024012 (2010).
- [24] A. Bauswein, H.-T. Janka, R. Oechslin, G. Pagliara, I. Sagert, J. Schaffner-Bielich, M.M. Hohle, and R. Neuhaeuser, *Phys. Rev. Lett.* **103**, 011101 (2009).
- [25] J. Madsen, *Phys. Rev. D* **71**, 014026-(1-9) (2005).

- [26] J.D. Bjorken and L.D. McLerran, Phys. Rev. D **20**, 2353 (1979).
- [27] A. De Rujula and S.L. Glashow, Nature **312**, 734 (1984).
- [28] F. Halzen and H.C. Liu, Phys. Rev. D **32**, 1716 (1985); P.B. Price, Phys. Rev. D **38**, 3813 (1988); O.G. Benvenuto and J.E. Horvath, Phys. Rev. Lett. **63**, 716 (1989); O.G. Benvenuto and J.E. Horvath, Int. Jour. Mod. Phys. A **6**, 4769 (1991); R.R. Caldwell and J.L. Friedman, Phys. Lett. B **264**, 143 (1991); D.M. Lowder, Nucl. Phys. B (Proc. Suppl.) **24**, 177 (1991); R.N. Boyd and T. Saito, Phys. Lett. B **298**, 6 (1993); G.A. Medina-Tanco, and J.E. Horvath, Astrophys. Jour. **464**, 364 (1996); S. Banerjee, S.K. Ghosh, S. Raha, and D. Syam, Jour. Phys. G **25**, L15 (1999); S. Banerjee, S.K. Ghosh, S. Raha, and D. Syam, Phys. Rev. Lett. **85**, 1384 (2000).
- [29] G. Wilk and Z. Wlodarczyk, Jour. Phys. G **22**, L105 (1996); *ibid.* **32**, 105 (1996) ; Nucl. Phys. B (Proc. Suppl.) **52**, 215 (1997).
- [30] T. Saito, Y. Hatano, Y. Fukada, and H. Oda, Phys. Rev. Lett. **65**, 2094 (1990).
- [31] W.F. Hanlon, Updated cosmic ray spectrum. Personal site. <http://www.physics.utah.edu/whanlon/spectrum.html>.
- [32] J. Blumer, R. Angel, and J. Horandel, Prog. Part. Nucl. Phys. **63**, 293 (2009).
- [33] T. K. Gaisser, *Cosmic Rays and Particle Physics*, Cambridge University Press, Cambridge, England (1990).
- [34] M. Vereecken, *Cosmic ray shock acceleration in galactic and extragalactic sources*, Master Thesis, Universiteit Gent 2014.
- [35] W. Baade and F. Zwicky, Phys. Rev. **45**, 138 (1934).
- [36] W. Baade and F. Zwicky, Proc. Nat. Acad. Sci. USA **20**, 259 (1934); A.R. Bell, Roy. Astron. Soc. **182**, 147 (1978), A&AA ID. AAA021.143.001; A.R. Bell, Roy. Astron. Soc. **182**, 443 (1978), A&AA ID. AAA021.143.002; R. Blandford and D. Eichler, Phys. Rep. **154**, 1 (1987).
- [37] E. Fermi, Phys. Rev. **75**, 1169 (1949).

- [38] O. G. Benvenuto and J. E. Horvath, Phys. Rev. Lett. **63**, 716 (1989); L. Paulucci, J. E. Horvath, and F. Grassi, Proc. Sci. International Symposium on Nuclear Astrophysics - Nuclei in the Cosmos -IX 159 (2006).
- [39] O. G. Benvenuto and J. E. Horvath, Mod. Phys. Lett. A **4**, 1085 (1989).
- [40] M. Herzog and F. K. Ropke, Phys. Rev. D **84**, 083002 (2011); G. Pagliara, M. Herzog, and F. K. Ropke, Phys. Rev. D **87**, 103007 (2013).
- [41] A. Chodos, R.L. Jaffe, K. Johnson, C.B. Thorn, and V.F. Weisskopf, Phys. Rev. D **9**, 3471 (1974).
- [42] R. Jensen, *Searches for Strange Quark Matter* : Masters Thesis, University of Aarhus, Denmark, 2006.
- [43] T. DeGrand, R.L. Jaffe, K. Johnson, and J. Kiskis, Phys. Rev. D **12**, 2060 (1975).
- [44] J. Madsen, Phys. Rev. D **50**, 3328 (1994).
- [45] Y. B. He, C. S. Gao, X. Q. Li, and W. Q. Chao, Phys. Rev. C **53**, 1903 (1996).
- [46] Y. Nambu and G. Jona-Lasinio, Phys. Rev. **122**, 345 (1961); Y. Nambu and G. Jona-Lasinio, Phys. Rev. **124**, 246 (1961).
- [47] A.R. Bodmer, Phys. Rev. D **4**, 1601 (1971).
- [48] S.A. Chin and A.K. Kerman, Phys. Rev. Lett. **43**, 1292 (1979).
- [49] C. Greiner and J. Schaffner-Bielich, arXiv: nucl-th/9801062 (1998).
- [50] M. S. Berger and R. L. Jaffe, Phys. Rev. C **35**, 213 (1987).
- [51] E. P. Gilson and R. L. Jaffe, Phys. Rev. Lett. **71**, 332 (1993).
- [52] C. Greiner, D.-H. Rischke, H. Stöcker, and P. Koch, Phys. Rev. D **38**, 2797 (1988).
- [53] M. G. Mustafa and A. Ansari, Phys. Rev. D **53**, 5136 (1996); Erratum *ibid* **54**, 4694 (1996); M. G. Mustafa and A. Ansari, Phys. Rev. C **55**, 2005 (1997).

- [54] R. Balian and C. Bloch, *Ann. Phys.* **60**, 401 (1970).
- [55] M.G. Alford, K. Rajagopal, T. Schaefer, and A. Schmitt, *Rev. Mod. Phys.* **80**, 1455 (2008).
- [56] K. Rajagopal and F. Wilczek, *Phys. Rev. Lett.* **86**, 3492 (2001).
- [57] J. Madsen, *Phys. Rev. Lett.* **87**, 172003 (1-4) (2001).
- [58] J. Madsen, *Phys. Rev. Lett.* **70**, 391 (1993); J. Madsen, *Phys. Rev. D* **47**, 5156 (1993); J. Madsen, *Phys. Rev. D* **50**, 3328 (1994); J. Schaffner-Bielich, C. Greiner, A. Diener, and H. Stoecker, *Phys. Rev. C* **55**, 3038 (1997).
- [59] J. Madsen, *Phys. Rev. Lett.* **85**, 4687 (2000).
- [60] M.G. Alford, K. Rajagopal, S. Reddy, and F. Wilczek, *Phys. Rev. D* **64**, 074017 (2001) [arXiv: 0105009 (hep-ph)].
- [61] L. Paulucci and J.E. Horvath, *Phys. Rev. C* **78**, 064907 (2008).
- [62] J. Thomas and P. Jacobs, *A Guide to the High Energy Heavy Ion Experiments*, UCRL-ID-119181; A. Rusek *et al.*, (E886 collaboration), *Phys. Rev. C* **54**, R15 (1996); G. Van Buren (E864 Collaboration), *Jour. Phys. G: Nucl. Part. Phys.* **25**, 411 (1999).
- [63] F. Dittus *et al.* (NA52 collaboration), First look at NA52 data on Pb–Pb interactions at 158 A GeV/c, *International Conference on Strangeness in Hadronic Matter*, ed. by J. Rafelski, AIP **340** (American Institute of Physics, New York, 1995) p. 24; G. Appelquist *et al.*, *Phys. Rev. Lett.* **76**, 3907 (1996); G. Ambrosini *et al.*, *Nucl. Phys. A* **610**, 306c (1996); R. Klingenberg, *Jour. Phys. G: Nucl. Part. Phys.* **25**, R273 (1999).
- [64] [https://en.wikipedia.org/wiki/Alpha\\_Magnetic\\_Spectrometer#/media/File:STS-91\\_PLB.jpg](https://en.wikipedia.org/wiki/Alpha_Magnetic_Spectrometer#/media/File:STS-91_PLB.jpg).
- [65] M. Aguilar *et al.* (AMS Collaboration), *Phys. Rept.* **366**, 331 (2002).
- [66] <http://www.ams02.org/ams-and-iss/where/>.

- [67] A. Kounine (AMS-02 Collaboration), in *XVI International Symposium on Very High Energy Cosmic Ray Interactions* (ISVHECRI 2010), Batavia, IL, USA. [arXiv:1009.5349v1.pdf (astro-ph.HE)].
- [68] O. Adriani *et al.* (PAMELA collaboration), *Phys. Rev. Lett.* **115**, 111101 (2015); M. Casolino *et al.* (PAMELA collaboration), in *Proc. 33rd International Cosmic Ray Conference*, Rio de Janeiro, Brazil 2013, [www.cbpf.br/icrc2013/papers/icrc2013-1214.pdf](http://www.cbpf.br/icrc2013/papers/icrc2013-1214.pdf).
- [69] Ke Han (LSSS Collaboration), *Jour. Phys. G* **36**, 064048 (2009).
- [70] S. Cecchini *et al.*, *Eur. Phys. Jour. C* **57**, 525 (2008).
- [71] The AMS home page is <http://ams.cern.ch>.
- [72] J. Sandweiss, *Jour. Phys. G: Nucl. Part. Phys.* **30**, S51 (2004).
- [73] T. Saito, Test of the CRASH experiment counters with heavy ions, *Proc. of the International Symposium on Strangeness and Quark Matter*, ed. by G. Vassiliadis, A. D. Panagiotou, B. S. Kumar, and J. Madsen (World Scientific, Singapore, 1995) p. 259.
- [74] M. Ichimura *et al.*, *Il Nuovo Cim. A* **106**, 843 (1993).
- [75] Information about ECCO can be found at <http://ultraman.berkeley.edu>.
- [76] S. B. Shaulov, *APH N.S., Heavy Ion Physics* 4 (1996) 403.
- [77] A. De Rujula, S. L. Glashow, R. R. Wilson, and G. Charpak, *Phys. Rep.* **99**, 341 (1983).
- [78] O. Miyamura, *Proc. 24th ICRC, Rome* **1**, 890 (1995).
- [79] J. J. Lord and J. Iwai, Paper 515, presented at the *International Conference on High Energy Physics*, Dallas (1992); H. Wilczynski *et al.*, *Proceedings of the XXIV International Cosmic Ray Conference*, HE Sessions, Rome (1995), Vol. **1**, p. 1.

- [80] MACRO Collaboration, Phys. Rev. Lett. **69** , 1860 (1992); M. Ambrosio *et al.*, Eur. Phys. Jour. C **13**, 453 (2000); M. Ambrosio *et al.*, for the MACRO Collaboration, Status Report of the MACRO Experiment for the year 2001 , [arXiv:0206027(hep-ex)]; G. Giacomelli, for the MACRO Collaboration, [arXiv:0210021(hep-ex)].
- [81] A.V. Olinto *et al.* for the JEM-EUSO Collaboration, in *The 34<sup>th</sup> International Cosmic Ray Conference (ICRC)*, 2015 (will be published in Proc. Sci.)
- [82] S. Dey *et al.*, Astropart. Phys. **34**, 805 (2011).
- [83] B. Basu *et al.*, Astropart. Phys. **61**, 88 (2015).
- [84] Z.-T. Lu, R. J. Holt, P. Mueller, T. P. O'Connor, J. P. Schiffer, and L.-B. Wang, Searches for Stable Strangelets in Ordinary Matter: Overview and a Recent Example, [arXiv:0402015(nucl-ex)].
- [85] P. B. Price, Phys. Rev. Lett. **52** , 1265 (1984).
- [86] M. Brugger *et al.*, Nature **337**, 434 (1989); M. C. Perillo Isaac *et al.*, Phys. Rev. Lett. **81** 2416 (1998); *ibid.* **82** 2220 (1999) (erratum).
- [87] Brazil-Japan Emulsion Chamber Collaboration, in : *Cosmic Ray and Particle Physics* (1978), edited by T.K. Gaisser, AIP Conference Proceedings No. **49** (American Institute of Physics, New York, 1978).
- [88] Brazil-Japan Collaboration, J. A. Chinellato *et al.*, *Proc. of the 21st International Cosmic Ray Conference*, Adelaide, Australia, ed. by R. J. Protheroe (Graphic Services, Northfield, South Australia, 1990) Vol. **8**, p. 259.
- [89] M. Rybczynski, Z.Wlodarczyk, and G.Wilk, Acta Phys. Polon. B **33**, 277 (2002).
- [90] R. L. Jaffe, Phys. Lett. **38**, 195 (1977); G. Baym, E. W. Kolb, L. McLerran, T. P. Walker, and R. L. Jaffe, Phys. Lett. B **160**, 181 (1985).
- [91] D. Larousserie, *Les quarks font trembler la Terre, Sciences et Avenir*, September 2002, p. 84.

- [92] D. P. Anderson, E. T. Herrin, V. L. Teplitz, and I. M. Tibuleac, BSSA 93 No. 6 (2003) 2363 [arXiv:0205089(astro-ph)].
- [93] H. Terazawa, Jour. Phys. Soc. Japan **60**, 1848 (1991); H. Terazawa, Jour. Phys. Soc. Japan **62**, 1415 (1993); E. Gladysz-Dziadus and Z. Wlodarczyk, Jour. Phys. G: Nucl. Part. Phys. **23**, 2057 (1997); M. Rybczynski, Z. Wlodarczyk, and G. Wilk, Nuovo Cim. C **24**, 645 (2001); J. Madsen and J. M. Larsen, Phys. Rev. Lett. **90**, 121102 (2003); J. Madsen *ibid.* **92** 119002 (2004).
- [94] F. C. Michel, Phys. Rev. Lett. **60**, 677 (1988); O. G. Benvenuto, J. E. Horvath, and H. Vucetich, Int. Jour. Mod. Phys. A **4**, 257 (1989); J. E. Horvath, O. G. Benvenuto, and H. Vucetich, Phys. Rev. D **45**, 3865 (1992).
- [95] V. V. Usov, Phys. Rev. Lett. **87**, 021101 (2001); P. Haensel and J. L. Zdunik, Nature **340**, 617 (1989); C. Alcock and A. V. Olinto, Ann. Rev. Nucl. Part. Sci. **38**, 161 (1988); N. K. Glendenning and F. Weber, Astrophys. Jour. **400**, 647 (1992); Ch. Kettner, F. Weber, M. K. Weigel, and N. K. Glendenning, Phys. Rev. D **51**, 1440 (1995); *Strange Quark Matter in Physics and Astrophysics, Proc. of the International Workshop*, ed. by J. Madsen and P. Haensel, Nucl. Phys. B (Proc. Suppl.) **24** (1991).
- [96] N. K. Glendenning, Ch. Kettner, and F. Weber, Astrophys. Jour. **450**, 253 (1995); N. K. Glendenning, Ch. Kettner, and F. Weber, Phys. Rev. Lett. **74**, 3519 (1995).
- [97] N. K. Glendenning, Ch. Kettner, and F. Weber, Possible New Class of Dense White Dwarfs, *Proc. of the International Conference on Strangeness in Hadronic Matter*, ed. by J. Rafelski, AIP **340** (American Institute of Physics, New York, 1995) p. 46.
- [98] P. F. C. Romanelli, *Strange Star Crusts*, B.S. Thesis, MIT (1986).
- [99] O. G. Benvenuto and L. G. Althaus, Astrophys. Jour. **462**, 364 (1996); Phys. Rev. D **53**, 635 (1996).
- [100] F. Weber, Ch. Schaab, M. K. Weigel, and N. K. Glendenning, *From Quark Matter to Strange Machos*, in: *Frontier Objects in Astrophysics and Particle Physics*, ed. by F.

- Giovannelli and G. Mannocchi, ISBN 88-7794-096-4 (Editrice Compositori, Bologna, 1997) p. 87.
- [101] S. K. Ghosh, S. C. Phatak, and P. K. Sahu, Nucl. Phys. A **596**, 670 (1996).
- [102] A. V. Olinto, Phys. Lett. B **192**, 71 (1987); J. A. Frieman and A. V. Olinto, Nature **341**, 633 (1989); J. E. Horvath and O. G. Benvenuto, Phys. Lett. B **213**, 516 (1988).
- [103] J. E. Horvath, H. Vucetich, and O. G. Benvenuto, Mon. Not. Roy. Astron. Soc. **262**, 506 (1993); V. V. Usov, Astrophys. Jour. **550**, L179 (2001); B. Zhang, R. X. Xu, and G. J. Qiao, Astrophys. Jour. **545**, L127 (2000); V. V. Usov, Astrophys. Jour. **559**, L137 (2001); R. Ouyed, O. Elgaroy, H. Dahle, and P. Keranen, *Meissner Effect and Vortex Dynamics in Quark Stars – A Model for Soft Gamma-Ray Repeaters*, [arXiv:0308166(astro-ph)]; V. V. Usov, Phys. Rev. Lett. **80**, 230 (1998); K. S. Cheng and T. Harko, Astrophys. Jour. **596**, 451 (2003).
- [104] J. Madsen, Phys. Rev. Lett. **61**, 2909 (1988); J. Madsen, H. Heiselberg, and K. Riisager, Phys. Rev. D **34**, 2947 (1986); J. Madsen and M. L. Olesen, Phys. Rev. D **43**, 1069 (1991); *ibid.* **44**, 566 (1991) (erratum); S. J. Cho, K. S. Lee, and U. Heinz, Phys. Rev. D **50**, 4771 (1994).
- [105] G. L. Shaw, M. Shin, R. H. Dalitz, and M. Desai, Nature **337**, 436 (1989).
- [106] H.-C. Liu and G. L. Shaw, Phys. Rev. D **30**, 1137 (1984); C. Greiner, P. Koch, and H. Stoecker, Phys. Rev. Lett. **58**, 1825 (1987).
- [107] M. Kasuya *et al.*, Phys. Rev. D **47**, 2153 (1993).
- [108] J.N. Capdeville, Il Nuovo Cim. 19 **C**, 623 (1996).
- [109] N. Itoh, Prog. Theor. Phys. **44**, 291 (1970); C. Alcock, Nucl. Phys. B (Proc. Suppl.) **24**, 93 (1991).
- [110] J. P. Bondorf, A. S. Botvina, A. S. Iljinov, I. N. Mishustin, and K. Sneppen, Phys. Rep. **257**, 133 (1995).
- [111] B. S. Meyer, Annul. Rev. Astron. Astrophys. **32**, 153 (1994).

- [112] S. Pal, S. K. Samaddar, and J. N. De, Nucl. Phys. **A** 608, 49 (1996).
- [113] H. Stöcker and W. Greiner, Phys. Rep. **137**, 277 (1986).
- [114] S. K. Ma, Statistical Mechanics, World Scientific, Singapore, 1993.
- [115] S. Biswas, J.N. De, P.S. Joarder, S. Raha, and D. Syam, Phys. Lett. B **715**, 30 (2012).
- [116] A. S. Botvina and I. N. Mishustin, Eur. Phys. Jour. A **30**, 121 (2006).
- [117] S. Biswas, J.N. De, P.S. Joarder, S. Raha, and D. Syam, Proc. Indian Natn. Sci. Acad. **81**, 277 (2015).
- [118] T. Chmaj and W. Slominski, Phys. Rev. D **40**, 165 (1989).
- [119] L. Paulucci and J.E. Horvath, Phys. Lett. B **733**, 164 (2014).

## Chapter 2

# A preliminary calculation for fragmentation of astrophysical SQM

In a paper written in the year 2005, J. Madsen [1] first attempted to arrive at a theoretical estimate for the possible flux of strangelets in GCR at the top of the Earth's atmosphere. There, J. Madsen considered the strange matter, released in the tidal disruptions of SSs in compact binary stellar systems of the Galaxy, and the subsequent fragmentations of that matter to be the principal source of possible galactic strangelets in the neighborhood of the solar system. In that paper, J. Madsen assumed that the strange matter, tidally released in the merger between two SSs, would possibly fragment into strangelets of roughly equal baryon numbers (or, sizes). From thermodynamic considerations, it is, however, more natural to think that a dilute warm matter, such as the tidally released warm SQM in this particular case, would reduce its free energy by cooling and condensing into fragments of wide range of sizes [2, 3] than to disintegrate into approximately equal sized fragments. Such a plausible size (or, baryon number) distribution, ie., the mass spectrum, of astrophysical strangelets has not been satisfactorily treated in the literature so far. The principal aim of this chapter is, therefore, to find a suitable approach to calculate a tentative size distribution of strangelets that might fragment out of the hot strange matter possibly released in the tidal interactions between two SSs in a compact binary stellar system of the Galaxy. For such a purpose, we here adopt the SMM, as discussed in Sec.

## 2. A preliminary calculation for fragmentation of astrophysical SQM

---

1.9 in the previous chapter, that is often used in the analysis of disassembly of hot nuclear matter both in laboratory nuclear physics and in the astrophysical contexts [4, 5, 6]. The calculated size distribution is then used as an input in rather simple a galactic propagation model of charged CR to arrive at least at an initial estimate of the flux of those strangelets in GCR in the vicinity of the solar system.

For the purpose of such a calculation, we are required to begin from the SMH. If SQM is absolutely stable in accordance with the claim made by this hypothesis, then all the compact stars are likely to convert into SSs [7, 8] within a very short time-scale of the order of not more than a few seconds to a few minutes [9, 10]. A majority of the so-called NSs in our Galaxy may thus actually be the already converted SSs. A potentially important source for the possible production of strangelets in our Galaxy is, therefore, the merger of those SSs in the compact binary stellar systems [1, 11, 12, 13]. Recent numerical simulations [12, 13] show that at least many of such merger events are likely to produce tidal arms and the strange matter ejected from the tips of those arms may become gravitationally unbound to propagate in the ISM. Such simulations also show the formation of small condensations (or, lumps) in the ejected SQM that may be a signature of the initial formation of strangelet-clusters. It is perhaps reasonable to assume that further fragmentations and separations of those lumps, as the ejected material approaches its thermodynamic equilibrium, would ultimately develop into a strangelet-mass distribution that contributes to GCR [14]. By combining the plausible population-averaged ejected mass of  $10^{-4}M_{\odot}$  per binary interaction [12] found in their simulations and a possible SS merger rate of about  $10^{-6} - 10^{-4} \text{ yr}^{-1}$  [15], that is suggested from modern observations, we arrived at a tentative production rate  $\sim 10^{-10} - 10^{-8}M_{\odot} \text{ yr}^{-1}$  for the SQM mass in our Galaxy. Here, we note that, in a recent communication, L. Paulucci *et al.* [16] provided a somewhat different scenario for the galactic production of strangelets from the fragmentation of SQM ejected by shock waves during the SN-II explosions. Fragmentation of SQM is a common feature in both the above scenarios and, therefore, the present treatment of fragmentation would possibly be valid for the SN-II scenario as well. In this chapter, we would simply consider the bulk SQM, initially ejected by stellar mergers, as given and calculate the size distribution of strangelets resulting from the fragmentation of that initial bulk SQM. In Sec. 2.1, we invoke the formalism of SMM to find the size distribution of strangelets. Discussion

of the numerically obtained mass spectra or the size distribution of the strangelets and their observational relevance are presented in Sec. 2.2.

## 2.1. Mass-spectrum of strangelets

We would use Eq. (1.9) ie. [14, 17],

$$\omega^i = \frac{\mathcal{V}}{(\mathcal{L}^i)^3} e^{(\mu^i - F^i)/T} = \frac{\mathcal{V}}{(\mathcal{L}^i)^3} e^{(-\Omega^i/T)}, \quad (2.1)$$

to find the size (ie., the baryon number) distribution of the strangelets that arise from the fragmentation of the SQM in thermodynamic equilibrium at the freeze-out volume at a certain temperature  $T$ . The parametric form of the mass ( $m^i$ ) of a strangelet of the  $i^{\text{th}}$  species was given in Ref. [18] for various values of the bag constant ( $B$ ) and the mass ( $m_s$ ) of the strange quarks at  $T = 0$ . In this initial treatment of the fragment-size distribution of astrophysical strangelets, we consider the simplifying assumption that the quarks are massless, ie.,  $m_s = 0$ . As a consequence, each of the strangelets now contains exactly equal numbers of  $u$ ,  $d$  and  $s$  quarks, each having the same quark chemical potential  $\mu_q$  at freeze-out. It also follows from the above assumption that the strangelets are chargeless so that the Coulomb interactions among strangelets are absent in this particular situation. Following SMM, the strangelets are assumed to have no strong interactions among themselves at freeze-out [4]. For thermodynamic equilibrium of the fragmenting system, we further require that each strangelet is in mechanical equilibrium ie., its internal quark pressure exactly balances the bag pressure. Such a condition demands that each of the  $i^{\text{th}}$  species of the strangelets satisfies a condition [14, 18, 19] (see Eq. (A.5) of Sec. A.1 in Appendix A)

$$BV^i = [(19\pi^2/36)T^4 + (3/2)\mu_q^2 T^2 + (3/4\pi^2)\mu_q^4]V^i - [(41/216)T^2 + (1/8\pi^2)\mu_q^2]C^i, \quad (2.2)$$

where,  $C^i = 8(3\pi^2 V^i/4)^{1/3}$  and  $V^i = 4\pi r_o^3 A^i/3$  [14] are respectively the curvature and the

---

## 2. A preliminary calculation for fragmentation of astrophysical SQM

---

volume of a strangelet of the  $i^{\text{th}}$  species with  $r_o$  being its radius parameter, the value of which is calculated (using Eqs. (2.2) and (2.4) (see below)) to be 0.96 fm [14] for the entire range of parameter values considered in this chapter.

For three massless quark flavors having equal chemical potentials, the expressions for the thermodynamic potential  $\Omega^i$  and the baryon number  $A^i$  of a strangelet of the  $i^{\text{th}}$  species in the thermodynamically equilibrated strangelet-cluster may be written as [14, 18, 19]

$$\Omega^i = [(41/108)T^2 + (1/4\pi^2)\mu_q^2]C^i, \quad (2.3)$$

and

$$A^i = [\mu_q T^2 + (1/\pi^2)\mu_q^3]V^i - (1/4\pi^2)\mu_q C^i, \quad (2.4)$$

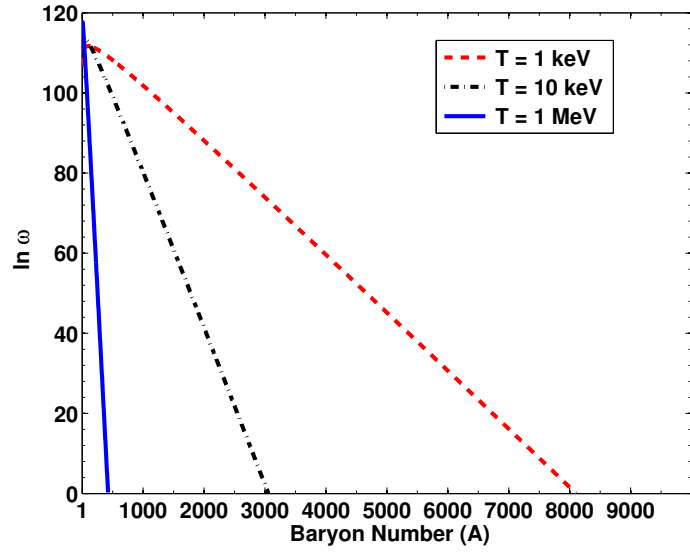
respectively (see Eqs. (A.2) and (A.6) of Sec. A.1 in Appendix A).

By using Eqs. (2.1-2.4) and also by imposing the condition for the conservation of baryon number  $A_b$  of the initial bulk SQM, namely [14]

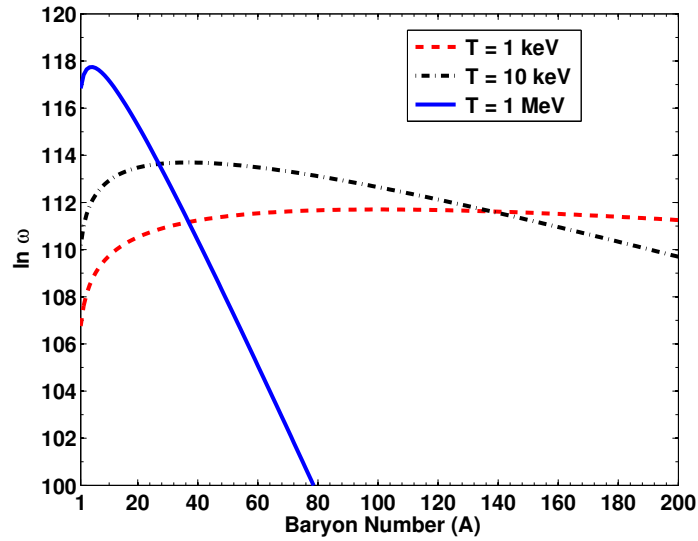
$$A_b = \sum_i A^i \omega^i(A^i), \quad (2.5)$$

we may calculate the mass-spectrum of the strangelets for the values of temperature (T) in the range  $\sim 0.001 - 1$  MeV (ie., 1 keV - 1 MeV). The lower limit ( $\sim 1$  keV) is approximately the lower bound of temperatures of the accretion disks of X-ray binary systems [20] and the upper limit of the temperature ( $\sim 1$  MeV) corresponds to the typical temperatures of the tidally released material found in the simulations of mergers between two NSs [21], although the temperature of the material ejected in SS mergers is not explicitly mentioned in the published simulation results [12, 13]. In our calculations,  $A_b = 1 \times 10^{53}$  corresponds to the average mass of about  $10^{-4} M_\odot$  ejected during each merger-event between two SSs [12, 13, 14] for a typical value of the bag constant that corresponds to  $B^{1/4} = 145$  MeV. The range of values for the available volume  $\mathcal{V}$  is taken to be  $2V_b - 9V_b$  [14] in agreement with its standard value considered in the calculations of nuclear fragmentation. Here,  $V_b = 4\pi r_b^3 A_b / 3$  is the volume of the bulk SQM before fragmentation, where  $r_b^3 = 3 / (4\pi n_B)$ ;  $n_B = 0.7 B^{3/4}$  being the typical baryon number density of that initial SQM [18]. In this

2. A preliminary calculation for fragmentation of astrophysical SQM



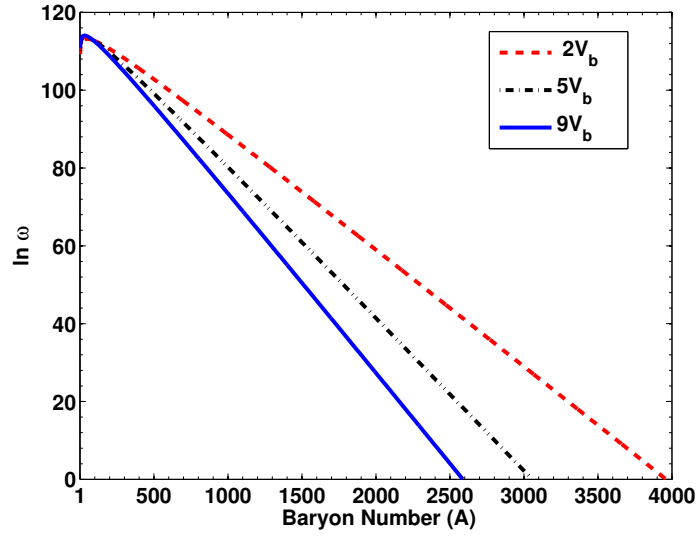
(a)



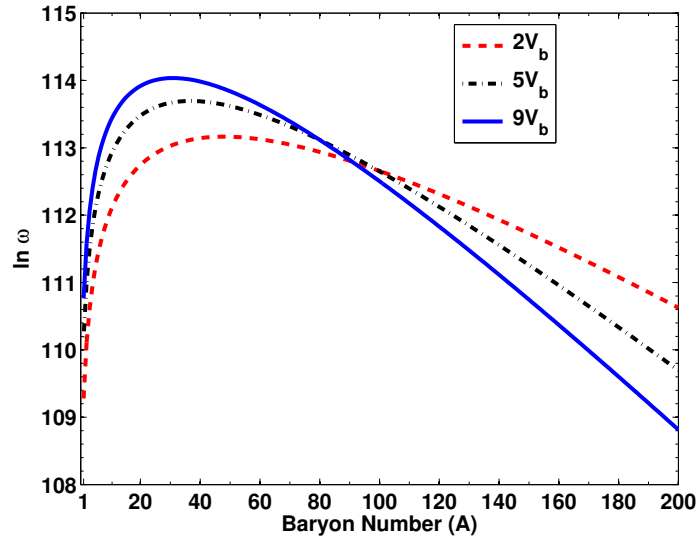
(b)

Figure 2.1.: Variation of  $\ln \omega(A)$  with the variation in  $A$  for the strangelets at different temperatures for a fixed value of the available volume  $\mathcal{V} = 5V_b$  are displayed for (a) the full range of the available baryon numbers and (b) for a limited range of baryon numbers of the strangelets. Here,  $A_b = 1 \times 10^{53}$ .

2. A preliminary calculation for fragmentation of astrophysical SQM



(a)



(b)

Figure 2.2.:  $\ln \omega$  vs.  $A$  for different values of the available volumes  $\mathcal{V}$  are shown for (a) the full range of the available baryon numbers and (b) for a limited range of baryon numbers of the strangelet-fragments. Temperature is taken as 10 keV. Here,  $A_b = 1 \times 10^{53}$ .

## 2. A preliminary calculation for fragmentation of astrophysical SQM

---

chapter, we have considered all available positive integer values for  $A^i$  of the fragment of  $i^{\text{th}}$  species to obtain the multiplicity (ie., the number of the fragments) belonging to each such species.

Figs. 2.1(a,b) display the size distribution of strangelets at  $\mathcal{V} = 5V_b$  and at three different temperatures at freeze-out, namely  $T = 1$  keV, 10 keV and 1 MeV, respectively. Enhanced production of lighter (ie., lower baryon number) fragments and a suppression of heavier (ie., higher baryon number) fragments is found at an increased temperature. An enhancement in the multiplicity of smaller fragments and a reduction in the case of larger fragments is also observed in Figs. 2.2 (a,b) as the available volume  $\mathcal{V}$  is enhanced at a fixed temperature ( $T = 10$  keV). Such patterns of fragmentation [14] is well-known in nuclear multifragmentation models; eg., [5].

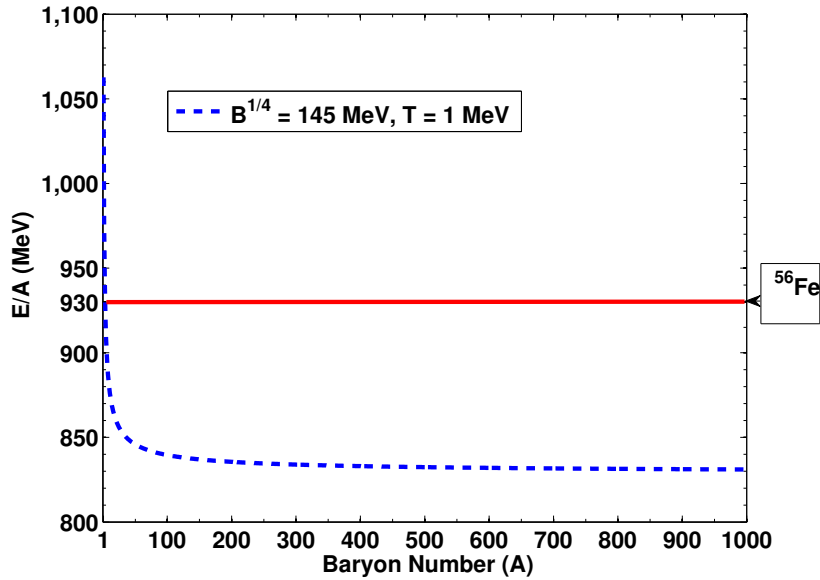


Figure 2.3.: Energy per baryon ( $E/A$ ) vs. baryon number ( $A$ ) of the strangelets at  $T = 1$  MeV but for a fixed value of the available volume  $\mathcal{V} = 5V_b$ . The solid horizontal line indicates the  $E/A$  of  $^{56}\text{Fe}$  (ie., 930 MeV). The strangelets having  $E/A \lesssim 930$  MeV are considered to be absolutely stable.

To address the question of stability of the produced strangelets, we plot the energy per baryon ( $E^i/A^i$  with  $E^i = 4BV^i$  [14, 18]) of the strangelets against their baryon number  $A^i$

at  $T = 1$  MeV and at  $\mathcal{V} = 5V_b$ ; stability of the strangelets is known to increase at lower temperatures [14, 22]. In Fig. 2.3, we find that the strangelets with  $A^i < 4$  tend to have larger energies per baryon than that (930 MeV) of the  $^{56}\text{Fe}$  nuclei. Such strangelets are possibly the metastable or the unstable ones that are likely to decay into the normal nuclei [14]. Similar problems with the stability of light ( $A \leq 6$ ) strangelets was mentioned in Ref. [23].

## 2.2. Discussion

In this chapter, our purpose was to find a trend in the baryon number distribution of a simplified model of strangelets with massless quarks that may fragment out of the warm strange matter produced in the merger between SSs in the compact binary stellar systems of the Galaxy. The following observations are, however, relevant to the fragmentation model presented above.

An important observation relating to the value of the quark chemical potential  $\mu_q$  must be mentioned in this context. An analytical calculation at  $T = 0$  by considering the condition of the strict positivity for the number of quarks in a strangelet necessitates  $(4\pi^2 B/3)^{1/4} < \mu_q < (4\pi^2 B)^{1/4}$  [14] (see Eqs. (A.10) and (A.11) in Sec. A.2 of Appendix A). By substituting  $B^{1/4} = 145$  MeV, we ultimately obtain  $275.5$  MeV  $< \mu_q < 362.5$  MeV (see Eq. (A.12) in Sec. A.2 of Appendix A) [14]. Earlier, several authors have pointed out that the value of  $\mu_q$  should be around 300 MeV [23, 24]. Thus, the magnitude of chemical potential, that we obtain in our self-consistent calculations at finite temperature, is in consonance with the above estimates.

The assumption of thermodynamic equilibrium for the fragmenting SQM plays a crucial role in the theory of fragmentation. A preliminary investigation of the recent simulations on SS merger [12, 13] suggests that the relative velocity between the end points of the tidal arm of an average length  $\sim 100$  km, that is found to be produced during a binary SS merger [13], may be  $v \sim 2\pi \times 20$  km (ms) $^{-1} \sim 10^5$  km s $^{-1}$  [14]. Also, the distance between the centers of the SSs in a binary stellar system of orbital period  $\sim 1$  ms, appears to be about 20 km at about the moment of triggering of the tidal interactions [13, 14] between the SSs. We now consider the relative motion between any two neighboring elements of the

tidal arm [14]. By ‘neighboring elements’, we mean the elements separated by distances of about 10 – 100 times the approximate collisional mean free-path of the fragmenting strangelets that is possibly just about a few fm [14]. On the other hand the relative rate of separation between such neighboring regions of the ejected matter thus seems to be  $\lesssim (10^5/100) \times 10^{-16} \sim 10^{-13} \text{ km s}^{-1}$  [14] that is orders of magnitude smaller than the thermal velocity  $\sim 5 \times 10^3 \text{ km s}^{-1}$  for the strangelets of an assumed average size  $A^i \sim 10$  at a temperature  $T \sim 1 \text{ MeV}$  [14]. In view of the above arguments, the assumption of quasi-static evolution of the tidally released SQM towards its thermodynamic equilibrium considered in the above calculations seems to be justified.

In case of finite temperature ( $T > 0$ ), the quarks are statistically distributed over energy levels and so the color singlet condition becomes applicable. Such condition increases the energy (per baryon) of a strangelet with a fixed entropy and thus the number of stable configurations of the strangelet are reduced [18, 19, 25]. In this chapter, we, however, do not take the color singlet condition into consideration as it may not produce appreciable effect at temperatures  $\lesssim 10 \text{ MeV}$  [14, 18, 19].

Finally, the assumption of massless quarks, as a consequence of which we get electrically neutral strangelets, does not allow us to directly use the size distribution obtained in this chapter in a realistic galactic propagation model. We can, nevertheless, obtain a very rough estimate for the possible galactic flux of the strangelets of a certain baryon number if we assume that the strangelets with massless quarks are only a limiting case of the strangelets having a small charge due to minute differences in their numbers of u, d and s quarks. For the purpose of the present article, we further assume that such minute difference between the numbers of quark-flavors does not appreciably change the derived size distribution of strangelets. The slightly charged strangelets may then be assumed to propagate in the inhomogeneous magnetic field of the ISM of the Galaxy so that we can perhaps use a diffusion approximation [26, 27] to describe their random motion in the ISM. In this diffusion approximation, we assume that apart from certain specific aspects, such as their unusually high mass to charge ( $A/Z$ ) ratio compared to the normal nuclei, the strangelets would in many ways behave like the ordinary cosmic ray nuclei [1] that are considered to be formed predominantly near the galactic plane and the galactic center and then they diffuse towards the boundaries of the galactic halo [26]. An order of magnitude estimate

---

## 2. A preliminary calculation for fragmentation of astrophysical SQM

---

for the total flux  $\mathcal{F}(A^i)$  of the strangelets with baryon number  $A^i$  at the solar distance  $R_s \approx 8$  kpc from the galactic center is then given by [14, 26]

$$\begin{aligned} \mathcal{F}(A^i) &= D \cdot \frac{dn(A^i, r_d)}{dr_d} \cdot 4\pi R_s^2 \\ &\sim \frac{L^2 \mathcal{R}_m \omega^i(A^i)}{2V_G R_s} \cdot 4\pi R_s^2 \text{ particles s}^{-1}. \end{aligned} \quad (2.6)$$

Here,  $n(A^i, r_d)$  is the number density of strangelets of size  $A^i$  at a distance  $r_d$  from the galactic center, an average value of which may be given by  $n_{\text{avg}}(A^i) \approx \mathcal{R}_m \tau \omega^i(A^i) / V_G$  with  $\mathcal{R}_m$  being the rate of merger between the SSs in the binary stellar systems,  $\tau$  the confinement time and  $V_G$  the effective confining volume of strangelets in the Galaxy. In Eq. (2.6),  $D$  is the diffusion coefficient of the strangelets and  $L = (2D\tau)^{1/2}$  is the root mean square distance travelled by the strangelets within their confinement time ( $\tau$ ) [26]. After the substitution of  $L \sim 10$  kpc ( $1 \text{ kpc} = 3.08 \times 10^{19} \text{ m}$ ) [18],  $V_G \sim 1000 \text{ kpc}^3$  [1] and  $\mathcal{R}_m \approx 10^{-5} \text{ yr}^{-1}$  [12, 13, 15], we finally obtain an estimate for the intensity of strangelets of size  $A^i$  in the neighborhood of the Sun. This intensity is given by [14]

$$I(A^i) \sim 5 \times 10^{-48} \omega^i(A^i) \text{ particles m}^{-2} \text{ sr}^{-1} \text{ yr}^{-1} \quad (2.7)$$

with  $\omega^i(A^i)$  given in Eq. (2.1) above and ‘sr’ denotes the unit of solid angle. Considering all the stable strangelets with  $A^i \geq 4$ , the range of values for the integrated strangelet intensity turns out to be  $\sim (10^3 - 10^5) \text{ m}^{-2} \text{ sr}^{-1} \text{ yr}^{-1}$  for the entire range of temperatures considered in this chapter. Here, the order of magnitude of the upper limit of the integrated intensity is comparable with the intensity obtained by J. Madsen [1]. We, however, note that the detailed processes, such as the ionization energy loss, decay, spallation and the re-acceleration mechanisms [1] for the strangelets in the Galaxy are absent in this simplified treatment of intensity presented above. Also, the effect of solar modulation as well as the effect of the geomagnetic rigidity cut-off on the strangelets [1] have not been taken into account in this simplified treatment of the galactic propagation of strangelets. In Chap. 4, we plan to incorporate the effect of the finite mass of strange quarks to examine the effect of finite charge on the size distribution of strangelets. It would be seen there

## *2. A preliminary calculation for fragmentation of astrophysical SQM*

---

that the simple model of SQM-fragmentation and the resulting trend in size distribution of strangelet-fragments, that we present in this chapter, would essentially provide useful guidance in the correct direction for such more involved calculations.

## Bibliography

- [1] J. Madsen, Phys. Rev. D **71**, 014026 (2005).
- [2] K. Huang, *Introduction to Statistical Physics*, Taylor and Francis, New York, USA (2002).
- [3] J. N. De and S. K. Samaddar, Phys. Rev. C **76**, 044607 (2007).
- [4] J. P. Bondorf, A. S. Botvina, A. S. Iljinov, I. N. Mishustin, and K. Sneppen, Phys. Rep. **257**, 133 (1995).
- [5] S. Pal, S. K. Samaddar, and J. N. De, Nucl. Phys. A **608**, 49 (1996).
- [6] B. S. Meyer, Annul. Rev. Astron. Astrophys. **32**, 153 (1994).
- [7] J. Madsen, Phys. Rev. Lett. **61**, 2909 (1988).
- [8] J. L. Friedman and R. R. Caldwell, Phys. Lett. B **264**, 143 (1991).
- [9] A. Bhattacharyya, S. K. Ghosh, P.S. Joarder, R. Mallick, and S. Raha, Phys. Rev. C **74**, 065804 (2006).
- [10] I. Bombaci and B. Datta, Astrophys. Jour. **530**, L69 (2000); G. Pagliara, M. Herzog, and F. K. Roepke, Phys. Rev. D **87**, 103007 (2013).
- [11] J. Madsen, Jour. Phys. G **28**, 1737 (2002).
- [12] A. Bauswein *et al.*, Phys. Rev. Lett. **103**, 011101 (2009).
- [13] A. Bauswein, R. Oechslin, and H.-T. Janka, Phys. Rev. D **81**, 024012 (2010).
- [14] S. Biswas, J.N. De, P.S. Joarder, S. Raha, and D. Syam, Phys. Lett. B **715**, 30 (2012).
- [15] V. Kalogera *et al.*, Phys. Rep. **442**, 75 (2007); K. Belczynski *et al.*, Astrophys. Jour. Lett. **680**, L129 (2008).

- [16] L. Paulucci, J. E. Horvath, and F. Grassi, Proc. Sci. International Symposium on Nuclear Astrophysics - Nuclei in the Cosmos - IX 159 (2006).
- [17] A. S. Botvina and I. N. Mishustin, Eur. Phys. Jour. A **30**, 121 (2006).
- [18] J. Madsen, in: J. Cleymens (Ed.), *Lecture Notes in Physics: Physics and Astrophysics of Strange Quark Matter*, vol. **516**, Springer Verlag, Heidelberg, 1999, p. 162, arXiv: 9809032v1(astro-ph), (1998).
- [19] D. M. Jensen and J. Madsen, Phys. Rev. D **53**, R4719 (1996).
- [20] S. Rosswog and M. Bruggen, *Introduction to High Energy Astrophysics* (Cambridge, England, 2007).
- [21] R. Oechslin, H.-T. Janka, and A. Marek, Astron. Astrophys. **467**, 395 (2007).
- [22] Y. B. He, C. S. Gao, X. Q. Li, and W. Q. Chao, Phys. Rev. C **53**, 1903 (1996).
- [23] E. Farhi and R. L. Jaffe, Phys. Rev. D **30**, 2379 (1984).
- [24] J. Madsen, Phys. Rev. Lett. **70**, 391 (1993).
- [25] M. G. Mustafa and A. Ansari, Phys. Rev. C **55**, 2005 (1997).
- [26] V. L. Ginzburg and S. I. Syrovatskii, *The origin of Cosmic Rays*, Pergamon Press, Oxford, England (1964).
- [27] T. K. Gaisser, *Cosmic Rays and Particle Physics*, Cambridge University Press, Cambridge, England (1990).

## Chapter 3

### A trend in fragmentation pattern in CFL SQM

In Sec. 1.6.3, we already mentioned that the quark matter at high density may be in its color-flavor-locked (CFL) phase, in which the quarks of three different flavors and three different color quantum numbers (see Sec. 1.4) may form CFL condensates [1, 2, 3, 4, 5, 6, 7], that are somewhat analogous to the electrons forming BCS-pairings in the laboratory condensed matter physics [8]. Considering the potentially novel properties of the hypothesized CFL strange matter, we would examine the possible fragmentation of CFL SQM into CFL strangelets in this chapter. Here, we would also examine whether it would be at all possible to obtain such particular variety of strangelets in GCR. The CFL strange matter is supposed to have excess binding energy in comparison with the ordinary (ie., unpaired) SQM for the same values of their temperatures, baryon numbers and their associated bag constants, although the range of possible values for the uncertain bag parameter is somewhat different in the case of stable CFL SQM (see Sec. 1.6.3), still having considerable overlap with the ones allowed for stable unpaired SQM. In the context of SMH, such additional binding energy signifies that the CFL SQM, rather than the unpaired SQM, perhaps constitute the true ground state of hadronic matter [1, 4]. A somewhat naive interpretation of SMH would then imply that all compact stars, including the so-called NSs and pulsars, are either CFL stars (CFLSs) or they are likely to convert into their stable CFLS ground states within a short time-scale, perhaps within seconds

to hours. A rigorous study of the phase transition of unpaired SQM into CFL matter is, however, yet to be performed. If we accept the above interpretation of SMH, an argument similar to the one presented in Chap. 2 for unpaired strangelets would then suggest that the fragmentation of the CFL material, possibly ejected in the tidal disruptions of two CFLSs, might produce CFL strangelets. It would thus be of some interest to see how the fragmentation pattern of the CFL strange matter depends on various physical parameters and the possible influence of that fragmentation pattern on the predicted flux of CFL strangelets at the location of the solar system. This chapter is aimed at such findings.

The present work is also necessitated by the recent claim in Ref. [9] that, it might be hard to obtain stable strangelets with small baryon numbers (with  $A^i \sim 100$ , say) in the vicinity of the solar system unless the enhanced stability property of CFL matter is taken into consideration. The authors of Ref. [9] further suggest that, the incorporation of color-flavor locking in the calculations of fragmentation may drastically alter that fragmentation pattern in a manner quite dissimilar to the one obtained in Chap. 2 for the unpaired SQM. As for an example, the effect of color flavor locking might result in a temperature dependence of the fragmentation pattern that is opposite to the one shown in Chap. 2, so that, heavier fragments, as opposed to the lighter ones (as in Fig. 2.1), might prevail at an enhanced temperature. A detailed examination of the dependence of the fragmentation pattern of CFL SQM on various parameters, therefore, is in order. Here, we would also like to compare the possible flux of CFL strangelets with the ones for unpaired strangelets predicted in the previous chapter, both being determined under the same assumption of massless quarks inside strangelets by using a simple diffusion model for the propagation of those strangelets in the ISM.

The chapter is organized as follows. In the next section, we will add a few comments on the possible production scenario of CFL strangelets. In Sec. 3.2, we present an outline of the disassembly model used by us to describe the fragmentation of the initial CFL matter thus leading to the formation of CFL strangelets. Sec. 3.3 is related to the equilibrium properties of a single CFL strangelet in the fragmenting complex in equilibrium at freeze-out. Numerical results for the mass distribution of strangelet fragments and its dependence on various physical parameters are described in Sec. 3.4. In Sec. 3.5, we provide an order of magnitude estimate for the possible galactic flux of CFL strangelets in the neighborhood

of the Sun by using the derived mass distribution of those strangelets. Summary of main results presented in this chapter and our conclusive comments regarding the feasibility of obtaining CFL strangelets in GCR in view of the relevant theoretical and numerical studies performed, so far, have been presented in Sec. 3.6.

### **3.1. Possible production scenario of CFL strangelets**

The above scenario for the production of astrophysical CFL strangelets from the merger between two CFLSs (in the line of the one presented in Chap. 2 for unpaired strangelets) may appear to be oversimplified in the light of the recent proposition [10, 11, 12] that bare CFLSs, with their interior temperatures being less than about 10 keV, may rapidly spin down by losing their angular momentum and rotational kinetic energy due to instabilities coupled with gravitational radiation from those stars. This, in turn, seems to suggest that at least some classes of the compact stars, such as the rapidly rotating old millisecond pulsars observed in the low mass X-ray binaries (LMXBs) with their internal temperatures in the above range, may not possibly be pure CFLSs [11, 12]. This is in contradiction with the naive interpretation of SMH mentioned in the introduction of this chapter. The issue, however, seems to be yet unsettled in view of the complexities in determining non-linear instabilities in the presence of dissipation in CFLSs and other high density compact stars, that is an area of active research till this date; eg., [13, 14, 15]. In this chapter, we therefore retain the scenario of strangelet production through binary collisions of pure CFLSs with their companion stars, at least as a simplified representation of a possibly more complex reality. We further note that several authors [13, 14, 16] are of the opinion that, even if cold CFLSs are inconsistent with certain pulsar observations, fast rotating CFLSs are likely to possess a window of stability at temperatures of about tens of MeV, typically obtained by the newly formed young pulsars. Possible mechanism for the formation of such a hot CFLS from the phase conversion of the dense core of a sufficiently massive ( $M_{\text{NS}} > 1.5M_{\odot}$ ) NS under certain favorable conditions has been discussed in Ref. [17]. In this scenario, an unconverted NS may coexist to form a compact binary system with a rapidly rotating hot CFLS if the mass of the NS is insufficient for its core to achieve nuclear deconfinement density or if the initial seeding of SQM is not available to its core [18]. Possible existence

of those particular compact binary stellar systems in the Galaxy allows one to consider an alternative production scenario for the CFL strangelets *via*. fragmentation of the CFL material tidally released during the coalescence between a CFLS and an NS [17]. The condition for such tidal disruption of a CFLS due to the force exerted by its NS companion was given in Ref. [19]. In this chapter, we adopt the above scenario to compare an approximate magnitude of the possible galactic strangelet flux obtained by us with an earlier estimation of such flux given in Appendix A of Ref. [17], the detailed analytical calculation and numerical simulation in support of which are, however, unavailable. The possible fate of a hot CFLS, as it cools down to temperatures below 0.01 MeV, is also not commented upon in Ref. [17].

### 3.2. Quantum statistical multifragmentation model for CFL strangelets

In similarity with the assumptions considered in the previous chapter in the case of unpaired strangelets, we here assume the quarks to be massless and consider every strangelet in the fragmenting assembly to contain equal numbers of up, down and strange quarks, each having the same quark number chemical potential  $\mu_q$ . To obtain the multiplicity  $\omega^i$  of the CFL strangelets of a particular species ‘ $i$ ’ with a specific baryon number  $A^i$  in the fragmenting complex, that is in thermodynamic equilibrium at temperature  $T$ , we further assume that the strangelet assembly is in chemical equilibrium with the value of  $\mu_q$  being the same throughout the (freeze-out) volume of the complex [20]. The multiplicities obtained by adopting nuclear multifragmentation models [20, 21, 22, 23, 24] are then given by (see Eqs. (B.1) and (B.2) of Sec. B.1 in Appendix B)

$$\omega^i = \frac{2\mathcal{V}}{\sqrt{\pi}(\mathcal{L}^i)^3} J_{1/2}^+(\eta_0^i) \phi^i(T), \text{ for odd } A^i \quad (3.1a)$$

and

$$\omega^i = g_0^i \frac{1}{(e^{-\eta_0^i} - 1)} + \frac{2\mathcal{V}}{\sqrt{\pi}(\mathcal{L}^i)^3} J_{1/2}^-(\eta_0^i) \phi^i(T), \text{ for even } A^i. \quad (3.1b)$$

### 3. A trend in fragmentation pattern in CFL SQM

---

The CFL strangelets with odd  $A^i$  are considered to obey Fermi statistics; those with even  $A^i$  obey Bose-Einstein statistics. In Eqs. (3.1a) and (3.1b),  $\phi^i(T)$  is the internal partition function of the fragments of the  $i^{\text{th}}$  species that are excited but particle stable [23], ie.,

$$\phi^i(T) = \sum_j g_j^i e^{-E_j^{*i}/T} = e^{-F^{*i}/T}, \quad (3.1c)$$

where,  $F^{*i}$  is the internal free energy that pertains to the excited states of the  $i^{\text{th}}$  species. In Eq. (3.1c),  $g_j^i$  and  $E_j^{*i}$  are, respectively, the degeneracy and excitation energy of the  $j^{\text{th}}$  state pertaining to the  $i^{\text{th}}$  species relative to the ground state. The ground state is represented by  $j = 0$  and  $E_0^{*i} = 0$ . The mass of the species of baryon number  $A^i$  is (assumed to be)  $m^i = 930A^i$  MeV [25] and their thermal de Broglie wavelength is  $\mathcal{L}^i = h/\sqrt{2\pi m^i T}$ . Here,  $\mathcal{V}$  is the available volume, ie., the freeze-out volume minus the volume of the produced fragments and  $J_{1/2}^\pm(\eta_0^i)$  designate the Fermi or the Bose integral [20] (see Secs. B.2 and B.3 in Appendix B for the estimation of the Bose and the Fermi integrals). In the absence of observational or theoretical models for the spin states of the strangelets, we assume, although somewhat arbitrarily, for the sake of simplicity  $g_j^i = 1$  for bosons and  $g_j^i = 2$  for fermions. In Eqs. (3.1a, b), the quantity  $\eta_0^i$  is the fugacity of the ground state, ie.,  $\eta_0^i = (\mu^i + \mathcal{B}^i)/T$ , where  $\mathcal{B}^i \equiv -E_0^i$  is the binding energy of the ground state. The excitation spectrum of strangelets is still an ill-known entity; furthermore, since we would be dealing with temperatures  $T \sim (0.001- 1)$  MeV, after some algebra, we write the multiplicities as [26](see Eqs. (B.1), (B.2), and (B.3) in Sec. B.1 of Appendix B)

$$\omega^i = \frac{2\mathcal{V}}{\sqrt{\pi}(\mathcal{L}^i)^3} J_{1/2}^+(\eta^i), \text{ for odd } A^i \quad (3.2a)$$

and

$$\omega^i = \frac{1}{(e^{-\eta_0^i} - 1)} + \frac{2\mathcal{V}}{\sqrt{\pi}(\mathcal{L}^i)^3} J_{1/2}^-(\eta^i), \text{ for even } A^i, \quad (3.2b)$$

where, the total fugacity  $\eta^i$  may now be written as

$$\eta^i = (\mu^i - F^i)/T = -\Omega^i/T, \quad (3.2c)$$

$F^i$  being the total (ie., including the ground state energy  $E_0^i$ ) free energy of the  $i^{\text{th}}$  species. Here,  $\mu^i = 3\mu_q A^i$  is the chemical potential and  $\Omega^i$  is the thermodynamic potential of the  $i^{\text{th}}$  species. The first term on the right of Eq. (3.2b) represents the Bose-Einstein condensation. The relative magnitude of this term in comparison with the second term on the right of Eq. (3.2b), representing the non-Bose-condensate fragments, is  $\sim \mathcal{V}^{-1}T^{-3/2}$ . In view of the enormously large value of  $\mathcal{V}$  in the specific astrophysical situation considered in this chapter, we may ignore the contribution from the Bose-Einstein condensation term to the multiplicities of strangelet fragments even in the case of appreciably low temperature of the SQM ejecta undergoing disassembly at freeze-out. We further note that the terms containing  $T^2$  and  $T^4$  begin to dominate the expression of  $\Omega^i$  [27] at increasing temperature such that  $|\eta^i| \gg 1$ ,  $J_{1/2}^\pm \simeq (\sqrt{\pi}/2)e^{\eta^i}$  ( $\eta^i < 0$ ) at large  $T$ . Eqs. (3.2) then attain their classical limit [24]

$$\omega^i = \frac{\mathcal{V}}{(\mathcal{L}^i)^3} e^{(-\Omega^i/T)}, \quad (3.3)$$

which is the same as Eq. (2.1), that we used in Sec. 2.1 of the previous chapter to determine the size distribution of unpaired strangelets. For the purpose of the present chapter, we, however, use Eqs. (3.2), that are derived directly from quantum statistics, to evaluate the multiplicities of CFL strangelets. As in Chap. 2, we consider the freeze-out temperatures in the range 1 keV to 1 MeV here also.

### 3.3. Equilibrium equations for a CFL strangelet

To find the equilibrium equations for a CFL strangelet of arbitrary size, we confine ourselves to the multiple reflection expansion [28] as applied to the MIT bag model supplemented by a condensating interaction [3]. The thermodynamic potential of the CFL strangelets with baryon number  $A^i$  may then be written as [3, 4, 5, 6, 7]

$$\Omega^i = \Omega_f^i + \Omega_{\text{pair}}^i + BV^i, \quad (3.4)$$

where,  $\Omega_f^i$  is the thermodynamic potential (minus the contribution from the bag) of non-CFL strangelet,  $\Omega_{\text{pair}}^i$  is the binding energy from the color superconducting condensates

and  $B$  is the bag constant. In zero quark-mass assumption, the expression for  $\Omega_f^i$  is given (for  $\Omega_{\text{pair}}^i = 0$  and without the  $BV^i$  term, Eq. (A.1) in Appendix A is same as  $\Omega_f^i$  in Eq. (3.4)) as [26, 27, 29]

$$\Omega_f^i = - \left[ \frac{19\pi^2}{36} T^4 + \frac{3}{2} \mu_q^2 T^2 + \frac{3}{4\pi^2} \mu_q^4 \right] V^i + \left[ \frac{41}{72} T^2 + \frac{3}{8\pi^2} \mu_q^2 \right] C^i. \quad (3.5)$$

As in Chap. 2 (see the discussion following Eq. (2.2)), the quantities  $V^i$  and  $C^i$  are respectively the volume and the curvature coefficient of the (assumed) spherical strangelet with  $r_o$  being its radius parameter. We here note that, in Eq. (3.5), the thermodynamic potential of the unpaired strangelet does not have any contribution from the surface  $S^i = 4\pi r_o^2 (A^i)^{2/3}$  of the  $i^{\text{th}}$  species. Absence of such surface effects (represented by the term  $\propto (\text{bag radius})^2$ ) and the important role of curvature (represented by the term  $\propto (\text{bag radius})$ ) for a confined gas of massless, non-interacting quarks, described within the framework of the MIT bag model, was noted earlier by numerous authors for both the vanishingly small and finite values of the temperature of the system; eg., Refs. [27, 30, 31, 32]. The question of “intrinsic surface tension” of strangelets has been recently re-examined in Ref. [33] without considering the curvature term but by taking the effect of Debye screening (see Chap. 4) into account. A model independent theoretical framework has been considered by those authors to determine the detailed equilibrium structure and stability of a single, large strangelet. There, it has been claimed that a large strangelet would be unstable with respect to fission instability to ultimately fragment into smaller strangelets if the value of the surface tension between the quark matter and the vacuum is less than a certain critical value that depends on the charge density and the electric charge susceptibility of quark matter on the surface of the strangelet. We, however, note that this critical value of surface tension approaches zero in the limit of massless strange quarks; cf. Ref. [33]. The authors of Ref. [33] further observed that the Cooper-like condensates between quarks of all the three colors and flavors in CFL strangelets make them electromagnetic insulators, ie., a relatively large CFL strangelet may be considered to be nearly neutral in comparison with the slightly positively charged large unpaired strangelets. As a consequence, a finite-sized

### 3. A trend in fragmentation pattern in CFL SQM

---

CFL matter may, perhaps be considered as stable against fission instability even in the case of an arbitrarily small value of the surface tension of those strangelets. It is, however, interesting to note that several authors [34, 35, 36], working either with lattice QCD or with theoretical models such as the NJL model or the Linear Sigma Model (LSMq) model, have predicted non-vanishing surface tension at the vacuum-SQM interface. Being motivated by such results, Bjerrum-Bohr et al. [35] have recently considered an arbitrary but appreciable surface energy term in the energy expression of finite-sized quark-gluon plasma droplets with massless quarks to describe the deconfinement-hadronization transition process in the early universe or in a large hadron collider, while still working within the framework of the MIT bag model. In this work, we, however, confine ourselves entirely to the standard bag model in the multiple reflection expansion framework in which we do not consider such additional surface tension in our analysis for the sake of the internal consistency of the MIT bag model. We further note that, Refs. [35] have associated their additional surface energy of the QGP droplet to the gradients in the number of diquark condensates that may set themselves up between the regions internal and external to the droplet. In the context of the CFL strangelets, the effects of such conventional diquark condensates are, however, expected to be much less than the effect of the dominant CFL condensates [8].

The (color superconducting) pairing (ie., the color condensate) energy term in Eq. (3.4) is written as [3, 4, 5, 6, 7]

$$\Omega_{\text{pair}}^i \approx -\frac{3}{\pi^2} \Delta^2(T) \bar{\mu}^2 V^i = -\frac{3}{\pi^2} \Delta^2(T) \mu_q^2 V^i \quad (3.6)$$

with  $\bar{\mu} = \mu_q$  being the average chemical potential of the quarks over their three flavors and  $\Delta(T)$  being the (color superconducting) pairing energy gap. The above expression for pairing energy is true for a bulk system [1, 4]; for a finite strangelet, it is an approximation. For strangelets with finite baryon number, the mass-dependent higher order terms (such as the curvature) in the pairing energy have been ignored. This approximation is only valid as long as  $\Omega_{\text{pair}}^i$  is itself a perturbation to  $\Omega_f^i$  [1, 4]. In Eq. (3.6) [26],

$$\Delta(T) = 2^{-1/3} \Delta_o \left[ 1 - \left( \frac{T}{T_c} \right)^2 \right]^{1/2} \quad (3.7)$$

with  $\Delta_o$  being a constant parameter and  $T_c = 2^{1/3} \times 0.57 \Delta_o$  being the critical temperature

### 3. A trend in fragmentation pattern in CFL SQM

---

above which the system can no longer support pairing between quarks [7, 8, 37]. For strongly interacting quark system, the value of the gap parameter  $\Delta_o$  is usually suggested to be in the range  $10 \text{ MeV} \lesssim \Delta_o \lesssim 100 \text{ MeV}$  [1, 4, 5, 38], but much higher values, about 200 MeV or even larger, have sometimes been considered in the literature [6, 39, 40, 41, 42]. With the choice  $\Delta_o = 100 \text{ MeV}$ , for example, we get  $T_c \approx 72 \text{ MeV}$ . For the values of temperature within the range 1 keV to 1 MeV, so that  $T/T_c \ll 1$ , Eq. (3.7) yields  $\Delta(T) \approx \Delta = 2^{-1/3} \Delta_o \approx 79 \text{ MeV}$ .

Using Eqs. (3.4), (3.5) and (3.6), the total thermodynamic potential of CFL-strangelets of the  $i^{\text{th}}$  species is then written as [26]

$$\begin{aligned} \Omega^i = & - \left[ \frac{19\pi^2}{36} T^4 + \frac{3}{2} \mu_q^2 T^2 + \frac{3}{4\pi^2} \mu_q^4 + \frac{3}{\pi^2} \Delta^2(T) \mu_q^2 \right. \\ & \left. - B \right] V^i + \left[ \frac{41}{72} T^2 + \frac{3}{8\pi^2} \mu_q^2 \right] C^i. \end{aligned} \quad (3.8)$$

For thermodynamic equilibrium, the strangelet fragments, in addition to being in chemical equilibrium are in mechanical equilibrium; their internal quark pressure thus exactly balances the external bag pressure, ie.,  $-\left(\frac{\partial \Omega^i}{\partial V^i}\right)_{T, \mu_q} = 0$ . From Eq. (3.8), one then gets [26]

$$\begin{aligned} BV^i = & \left[ \frac{19\pi^2}{36} T^4 + \frac{3}{2} \mu_q^2 T^2 + \frac{3}{4\pi^2} \mu_q^4 + \frac{3}{\pi^2} \Delta^2(T) \mu_q^2 \right] V^i \\ & - \left[ \frac{41}{216} T^2 + \frac{1}{8\pi^2} \mu_q^2 \right] C^i. \end{aligned} \quad (3.9)$$

In the particular case of bulk ( $A^i \rightarrow \infty$ ,  $C^i = 0$ ) CFL SQM, Eq. (3.9) reduces to a quadratic equation in  $\mu_q^2$  that agrees (at  $T = 0$ ) with the equilibrium criterion in Ref. [5] after we ignore the terms involving finite mass of strange quarks and an additional external pressure on the SQM. The approximate solutions of the quadratic equation are given by

$$\mu_q \approx (\pi T) \left[ -1 + \left\{ 1 + \left( \frac{4B}{3\pi^2 T^4} \right) \right\}^{1/2} \right]^{1/2}, \text{ if } \Delta_o = 0, T \neq 0 \quad (3.10a)$$

and

$$\begin{aligned} \mu_q &\approx \sqrt{2}\Delta \left\{ 1 + \left( \frac{\pi^2 T^2}{2\Delta^2} \right) \right\}^{1/2} \left\{ -1 + \left[ 1 + \left( \frac{\pi^2 B}{3\Delta^4} \right) \right. \right. \\ &\times \left. \left. \left\{ 1 - \left( \frac{\pi^2 T^2}{\Delta^2} \right) \right\} \right]^{1/2} \right\}^{1/2}, \text{ if } \Delta_o \neq 0, T \neq 0, \end{aligned} \quad (3.10b)$$

provided that  $\left(\frac{\pi^2 T^2}{2\Delta^2}\right) \ll 1$ . At  $T = 0$  and for  $\left(\frac{\pi^2 B}{3\Delta^4}\right) \ll 1$ , Eq. (3.10b) reduces to  $\mu_q \approx \frac{\pi\sqrt{B}}{\sqrt{3}\Delta}$  that agrees with Ref. [6] in the case of the so-called ‘slet-3’ (ie., a solution of chemical potential, obtained from the mechanical equilibrium of CFL strangelet, is related to the nearly charge-neutral CFL strangelet [6]) CFL strangelets, a detailed discussion of which is beyond the scope of the present discussion. We will use Eqs. (3.10) for an approximate estimates of the quark chemical potential in the fragmenting complex at freeze-out.

Using Eq. (3.8), we may also obtain an expression for the baryon number  $-\frac{1}{3}\left(\frac{\partial\Omega^i}{\partial\mu_q}\right)_{T,V^i}$  of a CFL strangelet at equilibrium. This expression reads [26]

$$A^i = \left[ \mu_q T^2 + \frac{1}{\pi^2} \mu_q^3 + \frac{2}{\pi^2} \Delta^2(T) \mu_q \right] V^i - \frac{1}{4\pi^2} \mu_q C^i. \quad (3.11)$$

Eqs. (3.8), (3.9) and (3.11) further allow us to determine the total energy of a CFL strangelet in mechanical equilibrium with the help of the thermodynamic relations  $E^i = \Omega^i + 3\mu_q A^i + T S^i$ , where the entropy is  $S^i = -\left(\frac{\partial\Omega^i}{\partial T}\right)_{V^i, \mu_q}$ . We thus obtain [26]

$$\begin{aligned} E^i &= \left( \frac{19\pi^2}{12} T^4 + \frac{9}{4\pi^2} \mu_q^4 + \frac{3}{\pi^2} \Delta^2(T) \mu_q^2 \right. \\ &+ \left. \frac{9}{2} \mu_q^2 T^2 - \frac{3}{0.41\pi^2} \mu_q^2 T^2 + B \right) V^i \\ &- \left( \frac{41}{72} T^2 + \frac{3}{8\pi^2} \mu_q^2 \right) C^i \\ &= 4B V^i - \frac{6}{\pi^2} \Delta^2(T) \mu_q^2 V^i - \frac{3}{0.41\pi^2} \mu_q^2 T^2 V^i. \end{aligned} \quad (3.12)$$

Here, the term  $-\frac{3}{0.41\pi^2} \mu_q^2 T^2 V^i$  arises from the quantity  $\frac{3}{\pi^2} \mu_q^2 V^i \left(\frac{\partial\Delta^2(T)}{\partial T}\right)_{\mu_q, V^i}$  in the volume entropy of the strangelet [7]. The contribution from this additional stabilizing term in

energy is, however, expected to be rather small for the range of temperatures considered in this article. Eq. (3.12) agrees with the expression for the energy of CFL SQM (at  $T = 0$ ) given in Ref. [5] provided that the external pressure considered there is set equal to zero. We would use Eq. (3.12) to examine the stability of strangelet fragments in the following section. We also note that, from Eqs. (3.9) and (3.11), it is straightforward to derive an algebraic expression for the radius parameter  $r_o$  that in general depends on  $\mu_q$ ,  $B$ ,  $T$  and  $\Delta_o$  but does not have an explicit dependence on the baryon number  $A^i$ . An approximate estimate for the radius parameter is obtained by retaining only the bulk term (ie., ignoring the contribution of curvature) in the above expression and by setting  $T \approx 0$ . Thus [26]

$$r_b^3 \approx \frac{3\pi}{4} \left( \mu_q^3 + 2\Delta^2 \mu_q \right)^{-1}, \quad (3.13)$$

where  $r_b$  is the bulk radius parameter. Upon appropriate substitutions of  $\mu_q$  from Eqs. (3.10), Eq. (3.13) provides us with an approximate value  $V_b = \frac{4\pi}{3} r_b^3 A_b$  for the volume of the initial bulk CFL SQM with  $A_b$  being the baryon number of such SQM. It is also to be noted that, at  $T = 0$  and under the assumption  $\frac{\pi^2 B}{3\Delta^4} \ll 1$ , Eq. (3.13) simplifies to  $r_b \approx \left( \frac{3\sqrt{3}}{8\Delta\sqrt{B}} \right)^{1/3}$  obtained in Ref. [6] for the radius parameter of the ‘slet-3’ CFL strangelets. We further add that, from Eqs. (3.8), (3.9), (3.11) and (3.12), the equilibrium properties of ordinary strangelets, described in Chap. 2, are assured in the case  $\Delta_o = 0$  provided that we ignore the additional contribution from entropy in Eq. (3.12).

### 3.4. Mass spectra of CFL strangelets

In this section, our purpose is to examine the influence of variations of the bag and the gap parameters as well that of the temperature at freeze-out on the size distribution and stability of CFL strangelets.

Eqs. (3.2), (3.8), (3.9), (3.11), (3.13), with the added condition for the conservation of the baryon number  $A_b$ , given already in Eq. (2.5) of the previous chapter, allow us to evaluate the mass spectra of CFL strangelets for the values of temperature in the range  $(0.001 - 1)$  MeV at freeze-out. The available volume  $\mathcal{V}$ , which is a free parameter in the problem, is chosen as  $5V_b$ . This is consistent with the range  $(2 - 9)V_b$  usually considered in nuclear fragmentation models; eg., Ref. [22], see also the discussion following

Eq. (2.5) in Chap. 2. For the baryon number of the initial bulk CFL matter, we choose  $A_b = 1 \times 10^{52}$  for the purpose of demonstration; this corresponds to the lowest value in the range  $(10^{-5} - 10^{-2}) M_\odot$  of tidally ejected mass noted earlier in the simulations of NS merger [25]. Such ejected mass is also at the limit of mass-resolution of the recent simulations of SS merger [18, 43]. In this context, it is also important to note that, we have chosen the values of the bag parameter satisfying  $B^{1/4} > 156$  MeV (for  $\Delta_o \approx 100$  MeV,  $T \ll \mu_q$ ) in this chapter for modelling CFL SQM unlike in the case of the unpaired SQM (discussed in Chap. 2), for which we chose  $B^{1/4} \geq 145$  MeV. This is to avoid the spontaneous decay of the ordinary nuclei into two-flavored color superconducting states. Such requirement of a higher bag value, as the color superconductivity is taken into account in the calculations of SQM, was discussed in detail in Ref. [4].

Fig. 3.1(a) compares the mass distributions of the ( $\Delta_o = 100$  MeV) CFL fragments for two different values of the bag parameter at the same temperature  $T = 10$  keV. Here, we find that an increasing bag value leads to the suppression of lighter fragments along with an enhanced production of heavier fragments from the disintegrating CFL SQM. For example, the multiplicity ( $\omega^i$ ) for the fragments of size  $A^i = 3000$  is enhanced by about 100%, whereas, such multiplicity for  $A^i = 10$  is suppressed by about 27% as the value of  $B^{1/4}$  is increased from 160 MeV to 180 MeV. The reason for such change in fragmentation lies in a complex interplay of several factors. Eq. (3.10b) predicts an increase in the quark chemical potential  $\mu_q$  with an increase in the bag value. For  $T \ll \mu_q$ , the curvature energy of strangelets at mechanical equilibrium varies as  $\mu_q^2$  [44], as a consequence of which more energy is required to produce smaller fragments out of the initial bulk CFL SQM at a higher bag value. This tendency to produce larger fragments is further facilitated by a reduction in  $r_b$  (see Eq. (3.13)) thus causing almost 30% reduction in the available volume  $\mathcal{V}$  ( $= 5V_b$ ) of the fragmenting strangelets. We here note that the association of fragment sizes with the volume available for fragmentation was discussed earlier in Fig. 2.2 (a, b), Chap. 2 (see also Ref. [20]) of this thesis in the context of the fragmentation of ordinary SQM.

Fig. 3.1(b) demonstrates the influence of the variation of  $\Delta_o$  on the fragmentation of strange matter for a fixed value of the bag parameter  $B^{1/4} = 160$  MeV at a specific temperature  $T = 10$  keV at freeze-out. In this figure, we find that an increment in the

### 3. A trend in fragmentation pattern in CFL SQM

value of  $\Delta_o$  from 10 MeV to 140 MeV is associated with about 96% suppression of  $\omega^i$  for strangelets of size  $A^i = 3000$  and the corresponding  $\sim 9\%$  enhancement of  $\omega^i$  for the fragments of size  $A^i = 10$ . A reduction in the value of  $\mu_q$  due to an enhanced value of the gap parameter  $\Delta_o$ , in accordance with Eq. (3.10b), with corresponding reduction in the curvature energy favors the production of lighter fragments in this particular case. This tendency is further supported by slight increase in  $r_b$ , in accordance with Eq. (3.13), with corresponding increase in the available volume of the strangelets.

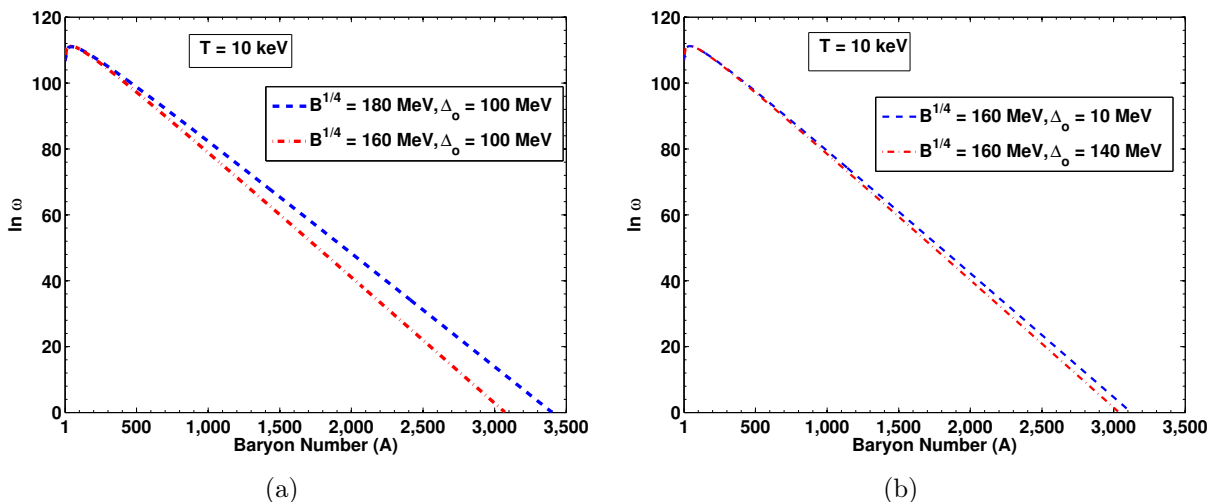


Figure 3.1.: Variation of  $(\ln \omega)$  of CFL strangelets with the variation in their baryon number ( $A$ ) for (a) fixed value of the gap parameter  $\Delta_o$  but two different values of the MIT bag parameter  $B$  and for (b) fixed value of the bag parameter but two different values of the gap parameter as indicated in the diagrams. The available volume is chosen to be  $\mathcal{V} = 5V_b$  in both the figures at  $T = 10$  keV at freeze-out. Here,  $A_b = 1 \times 10^{52}$ .

Fig. 3.2(a) displays the size distributions for the ( $B^{1/4} = 160$  MeV,  $\Delta_o = 100$  MeV) CFL strangelets at three different temperatures, namely  $T = 1$  keV, 10 keV and 1 MeV, respectively. The figure shows a clear tendency towards the suppression of heavier fragments and enhanced production of lighter fragments with increasing temperature. Average fragment size decreases from  $\bar{A} \approx 170$  at 1 keV through  $\bar{A} \approx 65$  at 10 keV to  $\bar{A} \approx 10$  at 1 MeV. The changes in the fragmentation pattern, that are demonstrated in this figure, are due to the consequent reduction in the curvature free energy of strangelets at higher temperatures

### 3. A trend in fragmentation pattern in CFL SQM

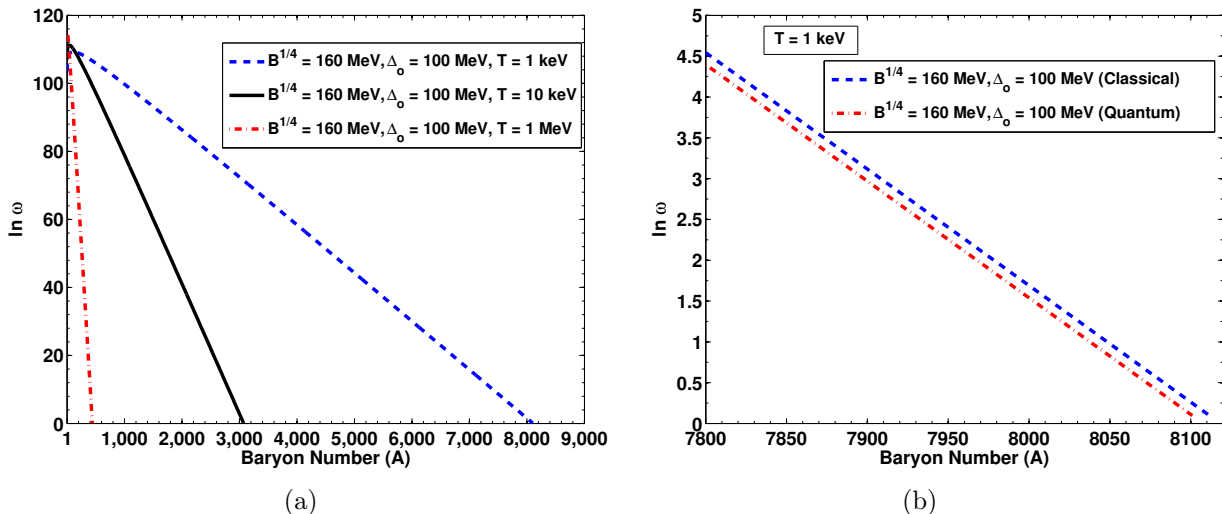


Figure 3.2.: (a) Variations of  $\ln \omega$  vs. baryon number ( $A$ ) of CFL strangelets for the available volume  $\mathcal{V} = 5V_b$  at three different temperatures at freeze-out are indicated in the diagram. (b) Difference between the logarithm of multiplicities of CFL strangelets, determined separately from quantum and classical formulae, is shown for a limited range of values of the baryon number of strangelets and only for the lowest temperature  $T = 1 \text{ keV}$  at freeze-out considered in (a). Available volume and the remaining parameters, considered to draw this diagram, are the same as in (a). In both the figures,  $A_b = 1 \times 10^{52}$ .

[7]. Here, it is important to note that the variation in fragmentation pattern of the CFL SQM with changing temperature, that we find in this chapter, seems to contradict the results obtained recently in [9] that predicts heavier fragments to prevail at an enhanced temperature at freeze-out. Our results, presented here, are however in perfect consonance with the changing fragmentation pattern found by us in the case of unpaired strangelets in Fig. 2.1, Chap. 2 of this thesis. As was mentioned in Chap. 2, this behavior of the fragmentation pattern, that we find consistently in the present thesis, is also in agreement with the well-known results in nuclear fragmentations.

In our numerical results displayed in Fig. 3.2(b), we find a decreasing deviation between the multiplicities determined by using classical (ie., by using Eq. 3.3) and quantum (ie., by using Eqs. 3.2) distributions with increasing temperature that is not included in Fig. 3.2(a) for the sake of clarity. Such deviations are expected from similar discrepancies

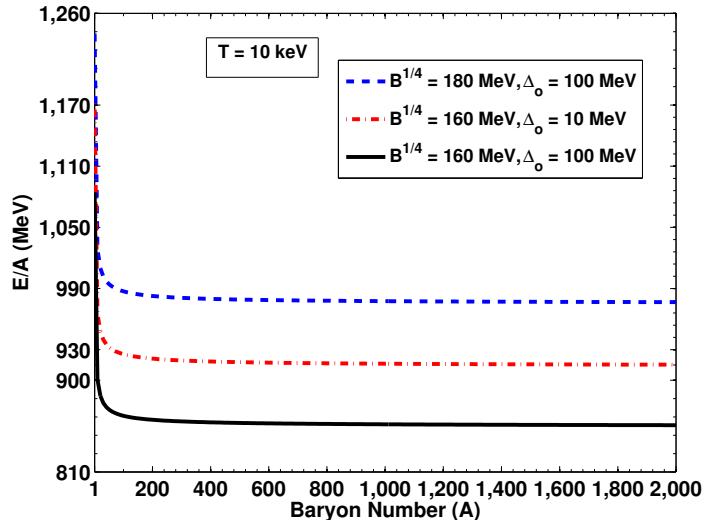


Figure 3.3.: Energy per baryon ( $E/A$ ) vs. baryon number ( $A$ ) of strangelets with their parameter values being indicated in the diagram. Here, the available volume is taken as  $\mathcal{V} = 5V_b$  at  $T = 10$  keV at freeze-out. Also,  $A_b = 1 \times 10^{52}$ .

between classical and quantum results found earlier [45] in nuclear systems. In Fig. 3.2(b), we display these deviations between classical and quantum systems for limited range of values of the baryon number only at temperature  $T = 1$  keV for the sake of demonstration. We have checked that the said discrepancy is not more than about 26% even for such low temperature and for the largest available values of the baryon number of the fragments. Having very small multiplicities, such large fragments are, however, found to have insignificant contribution to the possible galactic strangelet flux in the neighborhood of the Sun. Significant contribution to this strangelet flux is expected to come from much lighter fragments, for which the discrepancies between fragment multiplicities arising from quantum and classical distributions are found to be much less than 1%. Due to such small deviation between the results obtained from the Maxwell-Boltzmann (MB) and the Fermi-Dirac (FD)/ Bose Einstein (BE) distributions in the regions of practical interest in the fragmentation pattern, we hereafter use only the classical (MB) distribution to obtain results in the rest of this thesis.

To probe the stability of the produced fragments, we examine the energy per baryon

$(E^i/A^i)$  of each species of those fragments against its baryon number  $A^i$ . Here,  $E^i$  is determined from Eq. (3.12). Fig. 3.3 shows an example of such investigation at a particular temperature of the strangelet assembly, namely  $T = 10$  keV. An examination of Fig. 3.3 shows that a reasonable approximation for the energy per baryon of CFL fragments with large baryon numbers at sufficiently low ( $T \ll \mu_q$ ) temperatures may be given by their bulk limit (at  $T \approx 0$ )  $E^i/A^i \approx 3\mu_q$  [5, 6],  $\mu_q$  being approximately given in Eq. (3.10b). For small  $A^i$ , on the other hand, curvature of the fragments introduces a minimum baryon number  $A_{\min}$  for their absolute ( $E^i/A^i < 930$  MeV) stability [4, 7, 27, 29, 46]. The value of  $A_{\min}$  depends on  $B$  and  $\Delta_o$  of the initial bulk CFL matter but does not change appreciably with temperature (at freeze-out) that lies within the range of values considered in this work. We here note that similar variation of  $A_{\min}$  with temperature was obtained by us in Fig. 2.3 in the case of normal strangelets.

In Fig. 3.3, we find that the ( $B^{1/4} = 180$  MeV,  $\Delta_o = 100$  MeV) strangelets of arbitrary size are metastable (ie.,  $930 \text{ MeV} < E^i/A^i < 1116 \text{ MeV}$ ) [29];  $\mu_q$  is about 325 MeV in that case. Strangelets with so large a bag value are absolutely stable for  $\Delta_o \gtrsim 150$  MeV. We also note that extremely large values of the gap parameter, such as  $\Delta_o \gtrsim 230$  MeV, are required for the stability of CFL strangelets with  $B^{1/4} \approx 200$  MeV. We do not consider such extreme values of the pairing energy gap in this chapter. Fig. 3.3 further shows that, while the ( $B^{1/4} = 160$  MeV,  $\Delta_o = 10$  MeV) strangelets of sizes  $A^i \gtrsim 63$  are marginally stable (ie.,  $E^i/A^i \lesssim 930$  MeV) with  $\mu_q \approx 305$  MeV, the ( $B^{1/4} = 160$  MeV,  $\Delta_o = 100$  MeV) strangelets, having  $A_{\min} < 10$ , are absolutely stable with  $\mu_q \approx 285$  MeV. It is thus apparent from Fig. 3.3 that, at low temperatures, an enhanced bag value of the initial bulk CFL matter with fixed  $\Delta_o$  tends to yield comparatively less stable CFL strangelets; whereas, an enhanced value of the (color superconducting) gap parameter of the bulk SQM with its bag value remaining the same, tends to yield more stable fragments. Together with Figs. 3.1-3.3, the results presented in this section would suggest that absolutely stable CFL strangelets of wide array of sizes, in the range  $10 \lesssim A^i \lesssim 10^4$ , might have some possibilities to form as a consequence of tidal disruption and consequent mass-shedding of a CFLS during its merger with either another CFLS or an NS provided that the CFLS is not too compact to compel the entire merger-product to promptly collapse into BH before the tidal forces have sufficient time to spew appreciable CFL matter out of the gravitational

influence of the coalescing system. Preliminary simulations [18, 43] of SS mergers have, in fact, indicated the possibility of such collapse with little or no mass-shedding in the case of large bag values that, in turn, imply highly compact nature of the colliding stars. We here note that, due to their additional binding energy as well as the requirement of larger bag values for their absolute stability [4] than the ones that would have pertained to the normal SSs, the CFLSs may be particularly vulnerable to rapid collapse. In this chapter, we, therefore, considered a conservative estimate  $\sim 10^{-5}M_{\odot}$  for the average CFL mass ejected per binary collision in comparison with a population-averaged mass  $\sim 10^{-4}M_{\odot}$  ejected per simulated SS collision [18, 43] in the particular case of  $B^{1/4} \approx 145$  MeV. Further high-resolution simulations of compact binary stellar mergers, by incorporating the effect of color superconductivity in the equations of state of their constituent SQM and also by considering full effects of general relativity as well as the differential rotation of the stars are, however, necessary to arrive at definite conclusions regarding the amount of CFL mass ejected due to tidal disruption of a CFLS during binary stellar collisions.

### **3.5. An approximate estimate for the flux of CFL strangelets in the vicinity of the solar system**

To obtain a rough estimate for the possible flux of CFL strangelets in solar neighborhood within the framework of the simplified model with massless quarks considered in this chapter, we are required to take resort to the approximate formula for such flux as adapted in Eq. (2.6), Sec. 2.2 of Chap. 2. To use Eq. (2.6) for our present purpose, we require to substitute  $\mathcal{R}_m$  by a suitable merger rate for the compact binary companion stars in the Galaxy. Considering the appreciable uncertainty (see, Sec. 3.1) regarding the production scenario of CFL strangelets through binary stellar collisions, we may choose a conservative estimate, namely,  $\mathcal{R}_m \sim 10^{-7}\text{yr}^{-1} \text{ Galaxy}^{-1}$  which is the lower limit of a possible range of values of the galactic CFLS-NS merger rate estimated in Ref. [17]. As was mentioned in Sec. 3.1, the model provided in Ref. [17] has been claimed to be free from the controversy regarding the r-mode instability in cold CFLSs. With the above value of  $\mathcal{R}_m$ , the substitution of  $L \approx 10$  kpc for the root mean square distance travelled by the CFL strangelets

### 3. A trend in fragmentation pattern in CFL SQM

---

within their typical confinement volume  $V_G \approx 1000 \text{ kpc}^3$  in the Galaxy ultimately yields an approximate estimate for the intensity of the CFL strangelets of a particular species  $i$  with multiplicity  $\omega^i$  and baryon number  $A^i$ . This estimate reads [20]

$$I(A^i) \sim 5 \times 10^{-50} \omega^i \text{ particles m}^{-2} \text{ sr}^{-1} \text{ yr}^{-1} \quad (3.14)$$

with  $\omega^i$  given in Eqs. (3.2). While applying Eq. (3.14) to the particular case of absolutely stable CFL strangelets, we find that, in the absence of experimental results, the values of the characteristic parameters  $B$  and  $\Delta_o$  of those strangelets are still unsettled. Despite such uncertainty, we prefer a “not-unreasonable” [3] value  $\Delta_o = 100 \text{ MeV}$  for the gap parameter of a typical CFL strangelet. Values of the remaining parameter may then be chosen as  $B^{1/4} \approx 160 \text{ MeV}$  from the requirement of the absolute stability (see Fig. 3.3) of CFL fragments. We further checked that, for an assumed fixed amount of tidally released CFL mass, a consideration of larger values, such as  $B^{1/4} = 180 \text{ MeV}$  and  $\Delta_o = 150 \text{ MeV}$  for example, does not appreciably change the order of magnitude of the total (for all sizes) strangelet flux calculated in the following except that the strangelet fragments with their masses ranging from  $A^i \approx 10$  to about 50 are now metastable due to higher bag values.

Consider then the ( $B^{1/4} = 160 \text{ MeV}$ ,  $\Delta_o = 100 \text{ MeV}$ ) stable strangelets of size  $A^i \approx 10$ . Those strangelets have multiplicities  $\omega^i$  ( $A^i = 10$ )  $\approx 6.1 \times 10^{46}$ ,  $1.3 \times 10^{48}$  and  $8.2 \times 10^{49}$  at temperatures  $T = 1 \text{ keV}$ ,  $10 \text{ keV}$  and  $1 \text{ MeV}$ , respectively. We here assumed an average tidally released CFL mass  $\lesssim 10^{-5} M_\odot$  per stellar merger as in Figs. 3.1 and 3.2; this amount of mass-loss has been reported to be at the limit of resolution of the recent numerical simulations of the SS merger events [18, 43]. Corresponding intensities of the  $i^{\text{th}}$  species of CFL strangelets with  $A^i = 10$  in the neighborhood of the Sun, that were originally formed at the above three temperatures at freeze-out, are derived from Eq. (3.14) as  $I(A^i = 10) \lesssim 3 \times 10^{-3}$ ,  $6.3 \times 10^{-2}$  and  $4.1 \text{ particles m}^{-2} \text{ sr}^{-1} \text{ yr}^{-1}$ , respectively. Similarly,  $I(A^i = 100) \lesssim 1.7 \times 10^{-2}$ ,  $4.3 \times 10^{-2}$  and  $1.5 \times 10^{-9} \text{ particles m}^{-2} \text{ sr}^{-1} \text{ yr}^{-1}$  at the above three temperatures at freeze-out. Fragment sizes as large as  $A^i = 10^3$  are not available at a freeze-out temperature  $1 \text{ MeV}$  (see Fig. 3.2(a) above). Intensities of those large strangelets at temperatures  $T = 1 \text{ keV}$  and  $10 \text{ keV}$  (at freeze-out) are also small, being  $I(A^i = 10^3) \lesssim 10^{-6}$  and  $10^{-15} \text{ particles m}^{-2} \text{ sr}^{-1} \text{ yr}^{-1}$ , respectively. It is important to note that, all but one of the intensities determined above are orders of magnitude

smaller than the typical threshold sensitivity  $\sim 1$  particle  $\text{m}^{-2} \text{sr}^{-1}\text{yr}^{-1}$  of the modern detector-systems employed in recent space-based strangelet-search experiments, such as the one used in the AMS-02 experiment. The above estimates for the intensities of CFL strangelets of different sizes, determined from a preliminary model of those strangelets with massless quarks, seem to suggest that we may obtain low ( $A^i \sim 10$ ) mass, stable CFL strangelets in the vicinity of our solar system only for rather narrow ranges of values of the three important model parameters, namely the bag constant, the pairing energy gap and the formation temperature of those strangelets. Considering all the stable CFL strangelets with  $A^i \gtrsim 10$ , the integrated intensity for those strangelets in the neighborhood of the Sun may be determined by integrating Eq. (3.14) over the strangelets of relevant sizes. Such intensity turns out to be about 10 particles  $\text{m}^{-2} \text{sr}^{-1}\text{yr}^{-1}$ , that is applicable for the entire range of their formation temperatures considered in this chapter. This possible integrated intensity of stable CFL strangelets in the vicinity of the Sun is only about an order of magnitude larger than the above threshold sensitivity of the modern detector systems but depends sensitively on the uncertain values of the average mass-loss in a single CFLS-NS merger event. An assumption of an average mass-loss  $\sim 10^{-7} M_\odot$  per stellar merger, for example, would reduce all the above intensity estimates roughly by two orders of magnitude. Detailed high resolution simulations of the mergers between the rapidly rotating hot CFLSs with their NS companions in the compact binary stellar systems in the galaxy are, therefore, required to settle this particular issue of the population averaged amount of tidally released CFL mass, that might be actually be ejected outside the gravitational influence of such a merging stellar system.

### 3.6. Discussion

In this chapter, we have extended the work presented in Chap. 2 to the case of multi-fragmentation of CFL SQM to examine the possible size-distribution of the resulting CFL strangelets. This study was motivated by the recent work in Ref. [9], that applied a slightly different version of the nuclear multifragmentation models to the case of CFL SQM. The authors of Ref. [9] could not find substantial fragmentation out of the initial bulk CFL matter that led them to conclude that the incorporation of color-superconductivity in the

equation of state of the strange matter might substantially alter the basic fragmentation pattern from the one obtained in Chap. 2, for example, in the case of unpaired SQM. Those authors have claimed that the variations of the size-distribution of CFL fragments with changing temperature (at freeze-out) would exhibit a tendency, that is opposite to the one obtained in the case of normal strangelets in Chap. 2. They have further commented that one cannot expect substantial strangelet flux above the atmosphere of the Earth unless one considers the additional binding energy of the color superconducting strangelets. In the present chapter, we have carefully examined those important conclusions drawn by the authors of Ref. [9] in their study. In our present calculations, we, however, confine ourselves to the simplifying assumption of massless quarks in the CFL SQM. The results of this study show that, in contradiction to the claims made in Ref. [9], the incorporation of color superconductivity in the equation of state of the initial SQM before fragmentation does not qualitatively change the nature of the fragmentation pattern of that SQM from the one shown in Chap. 2 in the case of ordinary SQM. Here, the nature of variation of the size-distribution of CFL strangelets with increasing temperature (at freeze-out) is also found to be similar to the one obtained in the previous chapter that has already been reported to be in consonance with the well-known results in nuclear disassembly models. By employing a simple diffusion model for the propagation of CFL strangelets in the galactic magnetic field, we, however, find that the approximate estimates of the possible fluxes of stable CFL strangelets in the neighborhood of the Sun are orders of magnitude smaller than the ones found in Chap. 2 in the case of unpaired strangelets. Such lower fluxes of the CFL strangelets, as opposed to the normal ones, are mainly the consequence of the requirement of slightly higher bag values for the stability of those strangelets as was mentioned earlier in Sec. 3.4 of this chapter. In the preceding section, we have also found that, depending on the uncertain values of the tidally released strange matter in a CFLS-NS merger event, such flux estimates may even be several orders of magnitude lower than the threshold sensitivity of the modern detector systems designed to search for the astrophysical strangelets. Recent simulations [18, 43] of the merger between two normal SSs have further suggested that the amount of such tidally released mass, that may eventually become gravitationally unbound from the merged stellar system, is expected to altogether vanish in cases in which the SSs are so massive and compact so that the time taken by the

merged system to collapse to a BH is much shorter than the time required for the tidal arms to form during the merger process. Moreover, in the context of the coalescence between a CFLS and its NS companion, the possibility of the NS turning into another CFLS, that is supposed to be more compact than a normal SS, may not be altogether ruled out. In the case of such a conversion, two hot and rapidly rotating CFLSs are likely to collapse to a BH without spewing any mass in the ISM. We may expect little or no mixture of CFL strangelets in GCR in that particular case. Considering such uncertainties regarding the availability of CFL strangelets in GCR, we do not further discuss the possible formation of CFL strangelets and their tentative flux in the neighborhood of the Sun in this thesis. In the rest of this thesis, we, therefore, confine our attention only to the plausible formation of the normal strangelets and to the estimation of their possible fluxes in the vicinity of the solar system.

## Bibliography

- [1] J. Madsen, Jour. Phys. G **28**, 1737 (2002).
- [2] M. Alford, K. Rajagopal, and F. Wilczek, Nucl. Phys. B **537**, 433 (1999); R. Rapp, T. Schaefer, E.V. Shuryak, and M. Velkovsky, Ann. Phys. (NY) **280**, 35 (2000).
- [3] K. Rajagopal and F. Wilczek, Phys. Rev. Lett. **86**, 3492 (2001).
- [4] J. Madsen, Phys. Rev. Lett. **87**, 172003 (2001).
- [5] G. Lugones and J.E. Horvath, Phys. Rev. D **66**, 074017 (2002).
- [6] G.X. Peng, X.J. Wen, and Y.D. Chen, Phys. Letts. B **633**, 314 (2006).
- [7] L. Paulucci and J.E. Horvath, Phys. Rev. C **78**, 064907 (2008).
- [8] M.G. Alford, A. Schmitt, K. Rajagopal, and T. Schäfer, Rev. Mod. Phys. **80**, 1455 (2008).
- [9] L. Paulucci and J.E. Horvath, Phys. Lett. B **733**, 164 (2014).
- [10] N. Andersson, Astrophys. Jour. **502**, 708 (1998).
- [11] J. Madsen, Phys. Rev. Lett. **85**, 10-13 (2000).
- [12] C. Manuel, A. Dobado, and F.J. Llanes-Estrada, Jour. High Energy Phys. **09**, 076 (2005); C. Manuel and F.J. Llanes-Estrada, Jour. Cosm. Astropart. Phys., **0708**, 001 (2007); M. Mannarelli, C. Manuel, and B.A. Sa'd, Phys. Rev. Lett. **101**, 241101 (2008); C. Manuel, 'Hydrodynamics of the superfluid CFL phase and r-mode instabilities' in: Electronic Proc. Hirscheegg'09 - Nuclear Matter at High Density: International workshop on gross properties of nuclei and nuclear excitations, Hirscheegg, Austria, 2009, Edited by M. Buballa, B. Friman, K. Langanke, and J. Wambach, available online at: <http://theory.gsi.de/hirscheegg/2009/Proceedings/>.
- [13] M.G. Alford and A. Schmitt, AIP Conf. Proc. **964**, 256 (2007); doi: 10.1063/1.2823860.

- [14] P. Jaikumar, G. Rupak, and A.W. Steiner, Phys. Rev. D **78**, 123007 (2008); G. Rupak and P. Jaikumar, Phys. Rev. C **82**, 055806 (2010).
- [15] N. Andersson, B. Haskell, and G.L. Comer, Phys. Rev. D **82**, 023007 (2010); M. Mannarelli and C. Manuel, Phys. Rev. D **81**, 043002 (2010); M.G. Alford, S. Mahmoodifar, and K. Schwenzer, Jour. Phys. G **37**, 125202 (2010); M.G. Alford, S. Mahmoodifar, and K. Schwenzer, Phys. Rev. D **85**, 024007 (2012); G. Colucci, M. Mannarelli, and C. Manuel, Astrophys. **56**, 88 (2013); G. Colucci, M. Mannarelli, and C. Manuel, Astrophys. **56**, 104 (2013); M.G. Alford, S.K. Mallavarapu, A. Schmitt, and S. Stetina, Phys. Rev. D **87**, 065001 (2013).
- [16] B.A. Sa'd, [arXiv:0806.3359v1 (astro-ph)] (2008).
- [17] R. Ouyed, R.E. Pudritz, and P. Jaikumar, Astrophys. Jour. **702**, 1575 (2009).
- [18] A. Bauswein *et al.*, Phys. Rev. Lett. **103**, 011101 (2009).
- [19] S. Koshy, *Coalescence of compact binary stars with a quark star component*, M.Sc. Thesis, Department of Physics and Astronomy, California State University, Long Beach, USA, 2012.
- [20] S. Biswas, J.N. De, P.S. Joarder, S. Raha, and D. Syam, Phys. Lett. B **715**, 30 (2012).
- [21] J. Randrup, and S.E. Koonin, Nucl. Phys. A **471**, 355c (1987); B.S. Meyer, Annul. Rev. Astron. Astrophys. **32**, 153 (1994); J.N. De and S.K. Samaddar, Phys. Rev. C **76**, 044607 (2007).
- [22] A.S. Botvina and I.N. Mishustin, Eur. Phys. Jour. A **30**, 121 (2006).
- [23] S. Pal, S.K. Samaddar, and J.N. De, Nucl. Phys. A **608**, 49 (1996).
- [24] J.P. Bondorf, A. S. Botvina, A.S. Iljinov, I. N. Mishustin, and K. Sneppen, Phys. Rep. **257**, 133 (1995).
- [25] J. Madsen, Phys. Rev. D **71**, 014026 (2005).

- [26] S. Biswas, J.N. De, P.S. Joarder, S. Raha, and D. Syam, Proceedings of the 33rd International Cosmic Rays Conference (2013) [ISBN: 978-85-89064-29-3].
- [27] J. Madsen, in *Lecture Notes in Physics: Physics and Astrophysics of Strange Quark Matter*, edited by J. Cleymens, Vol. **516** (Springer Verlag, Heidelberg, 1999), p. 162, arXiv: astro-ph/9809032v1, (1998).
- [28] R. Balian and C. Bloch, Ann. Phys. (N.Y.) **60**, 401 (1970).
- [29] D.M. Jensen and J. Madsen, Phys. Rev. D **53**, R4719 (1996).
- [30] E. Farhi and R.L. Jaffe, Phys. Rev. D **30**, 2379 (1984).
- [31] C.M. Bender and P. Hays, Phys. Rev. D **14**, 2622 (1976); K.A. Milton, Phys. Rev. D **22**, 1444 (1980), B.K. Jennings and R.K. Bhaduri, Phys. Rev. D **26**, 1750 (1982); J. Baacke and Y. Igarashi, Phys. Rev. D **27**, 460 (1983); R.K. Bhaduri, J. Dey, and M.K. Srivastava, Phys. Rev. D **31**, 1765 (1985); H.-Th. Elze and W. Greiner, Phys. Lett. B **179**, 385 (1986); M. Berger, Phys. Rev. D **40**, 2128 (1989); I. Mardor and B. Svetitsky, Phys. Rev. D. **44**, 878 (1991); J. Madsen, Phys. Rev. Lett. **70**, 391 (1993); L. Paria, M.G. Mustafa, and A. Abbas, Int. Jour. Mod. Phys. E **99**, 149 (2000); M. Oertel and M. Urban, Phys. Rev. D **77**, 074015 (2008).
- [32] M.S. Berger and R.L. Jaffe, Phys. Rev. C **35**, 213 (1987).
- [33] M.G. Alford, K. Rajagopal, S. Reddy, and A.W. Steiner, Phys. Rev. D **73**, 114016 (2006).
- [34] L.F. Palhares and E.S. Fraga, Phys. Rev. D **82**, 125018 (2010); K.A. Bugaev and G.M. Zinovjev, Nucl. Phys. A **848**, 443 (2010); A. Dumitru, Y. Guo, Y. Hadaka, C.P.K. Altes, and R.D. Pisarski, Phys. Rev. D **83**, 034022 (2011); M.B. Pinto, V. Koch, and J. Randrup, Phys. Rev. C **86**, 025203 (2012).
- [35] J.J. Bjerrum-Bohr, I. Mishustin, and T. Dossing, Nucl. Phys. A, **882**, 90 (2012).
- [36] J.J. Bjerrum-Bohr, I. Mishustin, and T. Dossing, Nucl. Phys. A, **923**, 19 (2014).
- [37] A. Schmitt, Q. Wang, and D.H. Rischke, Phys. Rev. D **66**, 114010 (2002).

- [38] K. Rajagopal and F. Wilczek, in *At the Frontier of Particle Physics: Handbook of QCD, Boris loffe-Festschrift*, edited by M. Shifman (World Scientific, Singapore, 2001), Vol. **3**, Chapter 35, p. 2061.
- [39] M. Alford, K. Rajagopal, and F. Wilczek, *Phys. Lett. B* **422**, 247 (1998).
- [40] J. Berges and K. Rajagopal, *Nucl. Phys. B* **538**, 215 (1999).
- [41] G.W. Carter and D. Diakonov, *Phys. Rev. D* **60**, 016004 (1999).
- [42] R. Rapp, E. Shuryak, and I. Zahed, *Phys. Rev. D* **63**, 034008 (2001).
- [43] A. Bauswein, R. Oechslin, and H.-T. Janka, *Phys. Rev. D* **81**, 024012 (2010).
- [44] J. Madsen, *Phys. Rev. Lett.* **70**, 391 (1993).
- [45] Z. Majka *et al.*, *Phys. Rev. C* **55**, 2991 (1997).
- [46] Y.B. He, C. S. Gao, X.Q. Li, and W.Q. Chao, *Phys. Rev. C* **53**, 1903 (1996).

## Chapter 4

# An improved fragment distribution for unpaired SQM

In an exploratory analysis in Chap. 2, we obtained the basic nature of the size distribution of normal strangelets and the variations of that size distribution with changing parameter values by assuming the quarks to be massless for the sake of simplicity. In this chapter, we retain the assumption of massless  $u$  and  $d$  quarks, but assume the  $s$  quarks to be massive (see the footnote in Sec. 1.5, Chap. 1, for a justification) to obtain an improved fragmentation pattern of those strangelets. For quite long a time, the value of the current quark-mass ( $m_s$ ) of the  $s$  quarks used to be believed to lie somewhere within a wide range  $\sim (100 - 300)$  MeV [1, 2, 3]. After a number of sophisticated experiments followed by several high precision estimates [4, 5], the scientists have now agreed upon a value of  $m_s$  lying within a much narrower interval of  $\sim (82 - 100)$  MeV with the mostly accepted value being  $m_s = 95 \pm 5$  MeV [5].

As mentioned in Sec. 1.6, a finite  $m_s$  allows each of the strangelets to possess a small but finite electric charge that depends on the baryon number of that strangelet. This finite electric charge would, in turn, influence the binding energy of the strangelet through the destabilizing effect of the internal Coulomb repulsion of that strangelet. According to the standard MIT bag model [6, 7, 8, 9], a non-zero value for  $m_s$  would further make the  $s$  quarks “less relativistic” in comparison with the lighter ( $u$  and  $d$ ) quarks, so that, the heavier  $s$  quarks would tend to confine themselves to the interior of the strangelets - away from the

surface of those strangelets [8]. The resulting depletion of the surface density of states of the massive  $s$  quarks within the strangelets would contribute a “quark mode surface tension” to those strangelets. This quark-mass dependent surface tension, that is often referred to as the “dynamical surface tension” [6, 7, 8, 9] in the literature, did not appear in the expression of the thermodynamic potential of a strangelet with massless quarks obtained earlier in Eq. (2.3) of Chap. 2 or in Eq. (3.5) of Chap. 3. The absence of such dynamical surface tension in the case of strangelets with massless quarks was also pointed out in the discussion following Eq. (3.5). If we assume a chemical potential  $\mu_s \sim 300$  MeV for the  $s$  quarks, the magnitude of such dynamical surface tension turns out to be  $\sim 9$  MeV fm<sup>-2</sup> at zero temperature and for  $m_s \sim 95$  MeV as mentioned in the previous paragraph. This value of the dynamical surface tension of the strangelets, as determined from the MIT bag model, is consistent with the surface tension  $\sigma_s \sim (5 - 20)$  MeV fm<sup>-2</sup> calculated recently in Refs. [10] by adapting sophisticated QCD models, such as the linear sigma model (coupled with constituent quarks; LSMq) [11] or the NJL model [12], of strangelets although the origin of the surface tension is different in the MIT bag model from the ones appearing in those latter models. Apart from the speculated [13] fundamental change in the nature of the fragmentation pattern from the ones found earlier in Chaps. 2 and 3 of this thesis, a consideration of the finite charge and the dynamical surface tension, arising from a non-zero current-mass of the  $s$  quarks within the strangelets, would also tend to make those strangelets unstable by increasing their energies per baryon above the one for the <sup>56</sup>Fe nuclei or even above the ones for the nucleons, so that, very few or no strangelets may be available in GCR in the vicinity of the Sun - far away from the regions in which the strangelets are formed by fragmentation of the bulk SQMs ejected due to the SS merger events. It is, therefore, important to investigate the effect of such dynamical surface tension and the electric charge, associated with  $m_s \neq 0$ , on the fragmentation pattern and the stability of strangelets. Such an investigation has been undertaken in the present chapter, in which we also provide a revised order of magnitude estimate for the integrated (over baryon numbers) flux of stable strangelets of various possibly available sizes in the solar neighborhood.

The chapter is organized along the following line. In Sec. 4.1, we briefly review the SMM, originally presented in Sec. 1.9, Chap. 1. Sec. 4.2 contains the equations representing the thermodynamic equilibrium of a single strangelet. In Sec. 4.3, we apply the formalism of

SMM to find the fragment-size distribution of strangelets. The stability of the produced fragments, that may be available in GCR in the solar neighborhood, is studied in Sec. 4.4. In Sec. 4.5, we will discuss the results and their observational implications.

## 4.1. The multifragmentation model

In Chap. 2, we have used a classical (MB) version of SMM to predict the size distribution of normal strangelets. In Chap. 3, on the other hand, we found that the calculated multiplicities of strangelet-fragments, that are obtained by using a quantum statistical version of the SMM, do not differ substantially from the ones obtained by using MB statistics, even at considerably low temperatures at freeze-out except for the multiplicities of the fragments with very large baryon numbers, the contributions from which to the integrated fluxes of strangelets were found to be insignificant. In this chapter, we therefore confine ourselves only to the classical version of the SMM to find the mass spectrum of the strangelet-fragments in equilibrium at freeze-out.

While applying SMM to the bulk SQM before fragmentation, that is supposed to be tidally released in the merger between two SSs, we assume that original SQM to have rather large (but finite) a volume such that the finite-size effects, like the surface and the curvature effects, of that bulk matter could be ignored. Similar assumption was also considered in Chaps. 2 and 3 in the case of the SQM with vanishingly small quark-masses. As discussed in Secs. 1.5 and 1.6, the bulk SQM, mentioned above, is also considered to be globally charge-neutral due to the presence of electrons inside that SQM. We further assume that the initial average temperature of the tidally released SQM might have exceeded the value corresponding to its binding energy (about 10 MeV [14]) per nucleon during the coalescence phase of the stellar merger, so that, considerable degree of density fluctuations (or, fractures) could be developed in that warm and excited SQM. After the ejected matter becomes gravitationally unbound from its parent system of the merged SSs [15], the initially fractured SQM undergoes quasi-static evolution, during which it tries to minimize its free energy by cooling and expanding while the initial fractures develop into more or less well-defined lumps of different baryon numbers (or sizes) still interacting among themselves. The globally charge-neutral and beta-equilibrated lumpy matter

---

#### 4. *An improved fragment distribution for unpaired SQM*

---

eventually occupies a freeze-out volume at thermodynamic equilibrium at a certain temperature  $T$ . This freeze-out volume is assumed to be much larger than the original volume of the initially ejected and gravitationally unbound SQM. It is further assumed that, at this freeze-out volume, both the strong and the electromagnetic interactions between the eventually well-developed, locally charge-neutral lumps, each consisting of a strangelet within its own electron environment, cease to exist. The equilibrium temperature  $T$  at freeze-out is also considered to be lower than the initial temperature of the original SQM at the time of its ejection by the tidal forces arising from the merger process.

In the following, we adopt SMM to find a plausible mass (or, the baryon number) distribution of strangelets in the fragmenting system (at freeze-out), that is often referred to as the "strangelet-complex" in this chapter. This strangelet-complex is supposed to be a globally charge-neutral blob of highly inhomogeneous quark matter accompanied by electrons, the volume of which is sufficiently large so that the finite-size effects of this strangelet-complex can be ignored. The blob with a constant total baryon number  $A_b$  consists of finite domains that are going to be permanently segregated into numerous sparsely distributed, positively charged, finite-sized strangelets. Each of those strangelets is embedded in a charge-neutralizing cloud of degenerate electrons having a volume that is much larger than the volume of the strangelet. At freeze-out, the average distance between the strangelets is assumed to be so large so that the residual strong interactions between those strangelets may be taken to be insignificant. The globally charge-neutral strangelet-complex, consisting of the positively charged strangelets being immersed in an electron gas, is in thermodynamic and chemical equilibrium (including the beta-equilibrium) at freeze-out. For thermodynamic equilibrium, the temperature ( $T$ ) must be constant throughout the volume of the strangelet-complex. The number density ( $n_e^i(r)$ ) of electrons in this complex has spatial variations with their typical length scale being comparable to (or even shorter) than the Debye screening length  $\lambda_D = (\frac{\pi}{8\alpha})^{1/2} \frac{1}{\mu_q} \approx \frac{7.33}{\mu_q} \sim 5$  fm [16, 17, 18, 19, 20, 21] (see Sec. C.1 of Appendix C) inside each individual strangelet-fragment, where,  $r$  is the radial distance from the centre of the (assumed spherical) strangelet of the  $i^{\text{th}}$  species characterized by its baryon number  $A^i$ . Here,  $\mu_q (\gg T)$  is the quark number chemical potential [22] of the strangelet-complex at thermodynamic and chemical equilibrium at freeze-out and  $\alpha (= \frac{1}{137})$  is the fine structure constant. By definition, the quark number chemical potential

---

#### 4. An improved fragment distribution for unpaired SQM

---

$\mu_q$  is equal to one third of the baryon number chemical potential [22] of the strangelet-complex. A constant baryon number at thermodynamic equilibrium demands that  $\mu_q$  is constant over the volume of the strangelet-complex [21]. Except its small-scale spatial variations as stated above, the distribution of electrons (as viewed over length scales that are orders of magnitude longer than  $\lambda_D$ ) in the strangelet-complex should otherwise be uniform, as demanded by the condition of the global equilibrium, with constant number density  $n_e$  [21]. As a consequence of the above condition, the electron chemical potential  $\mu_e \approx (3\pi^2 n_e)^{1/3}$  is also a global constant, satisfying  $\mu_e \lesssim \frac{m_s^2}{4\mu_q}$ , over the entire volume of the strangelet-complex [21]. The above upper limit of  $\mu_e$  corresponds to the electron chemical potential in a globally charge-neutral, cold ( $T = 0$ ) and uniform bulk SQM at zero pressure [18, 19, 20, 22, 23]. This limit of  $\mu_e$  is derived by considering the lowest non-trivial order of  $m_s$  and assuming  $\mu_q^2 \gg m_s^2$ , that may be justified for  $m_s \approx 95$  MeV and  $\mu_q \sim 300$  MeV. In view of a number of uncertain physical parameters used for the purpose of modelling in the particular problem discussed in this thesis, we have to be satisfied here only with the order of magnitude estimates for the possible sizes of the strangelets and their plausible approximate flux in the neighborhood of the solar system. For the purpose of such rough estimations, it is perhaps sufficient to consider  $\mu_e \approx \frac{m_s^2}{4\mu_q}$  in the calculations presented in this chapter for the sake of simplicity.

The weak interaction processes, as shown in Eqs. (1.1) of Sec. 1.6.1, Chap. 1, maintain the chemical equilibrium of the strangelet-complex. These processes demand that the chemical potential  $\mu_f$  of the quarks of the  $f^{\text{th}}$  flavor ( $f = u, d, s$ ) in the strangelet-complex should satisfy the relations [22]:

$$\left. \begin{aligned} \mu_u &= \mu_q - \frac{2}{3}\mu_e \\ \mu_d &= \mu_q + \frac{1}{3}\mu_e \\ \mu_s &= \mu_q + \frac{1}{3}\mu_e \end{aligned} \right\} \quad (4.1)$$

thus implying the fact that, except for the small scale local variations of  $\mu_f^i(r)$  with a typical length scale  $\lesssim \lambda_D$  inside each individual strangelet, the value of  $\mu_f$  of an arbitrary quark-flavor ‘ $f$ ’ should be uniform throughout the volume of the strangelet-complex.

In Eqs. (4.1), the chemical potential of the neutrinos is ignored as they are likely to

contribute very little to the energy density and pressure of the strangelet-complex in equilibrium at freeze-out [6] (see Sec. 1.6 of Chap. 1). It is also to be noted that, over length scale  $\lesssim \lambda_D$  inside a strangelet of the  $i^{\text{th}}$  species, the equilibrium conditions, as stated in Eq. (4.1), transform into a relation between the local (ie., position dependent) chemical potentials, ie.,

$$\mu_f^i(r) + q_f \mu_e^i(r) = \mu_q. \quad (4.2)$$

In Eq. (4.2),  $q_f$  is the charge of a quark of the  $f^{\text{th}}$  flavor, ie.,  $(q_u, q_d, q_s) = (\frac{2}{3}, \frac{-1}{3}, \frac{-1}{3})$  in the unit of  $e$ ,  $e$  being the magnitude of the electronic charge. Eq. (4.2) couples the equilibrium distribution of quarks inside a particular strangelet to the charge-neutralizing electron cloud surrounding that strangelet through the non-zero values of the local electrostatic potentials  $\mu_e^i(r)/e$  [18, 19, 20] at different positions inside that same strangelet. This coupling gives rise to the phenomenon of Debye screening [16, 17, 18, 19, 20] inside a strangelet in thermodynamic, electrostatic and chemical equilibrium with its electron environment. In Sec. 4.2 of this chapter, we will discuss Debye screening in somewhat more detail. There, we will also use the formulae (ie., Eqs. (4.7) and (4.8)), obtained by earlier authors [16, 17, 18], for the expressions of two integrated (over the radial coordinate  $r$ ) quantities, namely, the total electric charge and the Coulomb energy of an individual fragment in the strangelet-complex. Those formulae are derived by making use of the concept of Debye-screening inside an individual fragment. It is, however, important to note that, in this chapter, our sole purpose is to obtain the equilibrium size-distribution of numerous newly-born strangelets (with their associated charge-neutralizing electron clouds) located randomly within the freeze-out volume of the strangelet-complex in equilibrium at freeze-out. For such a purpose, we would use the position independent and uniform values of  $\mu_e$ ,  $\mu_f$  and  $\mu_q$ , that are the chemical potentials characterizing the global equilibrium configuration of the strangelet-complex (at freeze-out), instead of the position-dependent local chemical potentials of the quarks and electrons pertaining to each individual strangelet-fragment. Those local potentials enter in our analysis only indirectly, ie., through the integrated properties of each individual strangelet as mentioned above. In principle, such local and global chemical potentials should be connected through the appropriate boundary conditions on the surface of each individual strangelet. Examples of such boundary

---

#### 4. An improved fragment distribution for unpaired SQM

---

conditions have been provided in Refs. [18, 19, 20], in which substantially rigorous calculations (by using the solutions of two separate Poisson's equations inside and outside the strangelet that match on its surface) have been considered to numerically determine the equilibrium radial distributions of the charge density and other physical properties inside and outside an individual strangelet embedded in an inhomogeneous but spherically symmetric electron cloud. From those calculations, we obtain some physical insight into the phenomenon of Debye screening. Such rigorous calculations to find the detailed radial structure of each of the almost innumerable strangelets of various sizes in equilibrium with its charge-neutralizing electron environment are, however, not attempted in this chapter.

As mentioned above, the strangelet-complex is considered here to be in thermodynamic equilibrium at a certain temperature ( $T$ ) at freeze-out. In the absence of any clue regarding the actual values of the temperature at which the strangelets may be formed, we here choose a plausible range of such values, namely ( $0.001 \leq T \leq 1.0$ ) MeV, somewhat arbitrarily. The justification of choosing such a particular range of values for the temperature of the strangelet-complex in thermodynamic equilibrium at freeze-out was given earlier in the Sec. 2.1, Chap. 2 of this thesis.

At freeze-out, the multiplicity ( $\omega^i$ ) of the strangelets of the ' $i^{\text{th}}$ ' species can be written as (see Eq. (1.9) in Chap. 1) [21, 24, 25, 26, 27, 28]

$$\omega^i = \frac{\mathcal{V}}{(\mathcal{L}^i)^3} e^{(\mu^i - F^i)/T}. \quad (4.3)$$

In Eq. (4.3),  $\mathcal{V}$  is the available volume of the strangelet-complex in thermodynamic equilibrium at freeze-out as was defined earlier in Sec. 1.9 of Chap. 1 of this thesis. In this particular case of the disassembly of SQM with massive  $s$  quarks, the value of  $\mathcal{V}$  is to be determined self-consistently from the condition of the global charge-neutrality of the fragmenting system as opposed to the case considered earlier in Chaps. 2 and 3, in which the value of  $\mathcal{V}$  was simply taken to be a free parameter of the problem. In Eq. (4.3),  $\mu^i (= \sum_f \mu_f N_f^i + \mu_e N_e^i)$  is the chemical potential of a strangelet of the  $i^{\text{th}}$  species with a volume  $\mathcal{V}^i$  and  $N_{(f,e)}^i = \left( - \frac{\partial \Omega_{(f,e)}^i}{\partial \mu_{(f,e)}} \right)_{\mathcal{V}^i, T}$  being either the number of quarks of the  $f^{\text{th}}$  flavor ( $f = u, d, s$ ) or the number of electrons constituting that strangelet; their corresponding thermodynamic potentials are  $\Omega_{(f,e)}^i$ . The thermal de Broglie wavelength of a strangelet of

the  $i^{\text{th}}$  species can be defined as  $\mathcal{L}^i = h/\sqrt{2\pi m^i T}$  where  $m^i$  is the mass of the strangelet. For an approximate value of  $m^i$ , we use the mass-formulae as derived in Refs. [9, 29] by taking into account a bulk approximation to the baryon number chemical potential of the strangelet-fragment at  $T = 0$ . The mass of a strangelet with  $m_s = 95$  MeV is obtained by means of an interpolation between the masses derived in Ref. [29] for different values of  $m_s$ . Moreover, the masses of strangelets corresponding to various bag values can be obtained by using a scaling law derived in Ref. [9]. Here,  $F^i (= \Omega^i + \mu^i + E_C^i)$  denotes the Helmholtz free energy of the  $i^{\text{th}}$  species while  $\Omega^i$  is its thermodynamic potential and  $E_C^i$  is its Coulomb energy.  $F^i$  may be rewritten as  $F^i = \Omega_{\text{tot}}^i + \mu^i$ , where,  $\Omega_{\text{tot}}^i = \Omega^i + E_C^i$ . Thus, Eq. (4.3) can be reframed as [21, 24, 27]

$$\omega^i = \frac{\mathcal{V}}{(\mathcal{L}^i)^3} e^{-\Omega_{\text{tot}}^i/T}. \quad (4.4)$$

We will use Eq. (4.4) to determine the multiplicities of various strangelet-fragments in the strangelet-complex after specifying the thermodynamic quantities that represent the overall behavior of an individual strangelet in that complex in equilibrium at freeze-out.

## 4.2. Thermodynamics of a strangelet

For the calculation of the thermodynamic potential of the strangelet of a particular species, we shall use the multiple reflection expansion method [30] with smoothed density of states as applied to the standard MIT bag model [6, 9, 29]. The approach, that we here consider in modelling a strangelet, is analogous to the ‘‘liquid drop model’’ in the context of theoretical nuclear physics [9]. This approach has earlier been found to satisfactorily reproduce the average properties of the strangelets obtained from the mode-filling calculations of the shell model [2, 31]. Here, the strangelets are assumed to be spherical for the sake of simplicity. Radius of such a spherical strangelet of the  $i^{\text{th}}$  species is  $R^i = r_o^i (A^i)^{1/3}$ , where,  $r_o^i$  is its radius parameter. Volume, surface and curvature of a strangelet are denoted as  $\mathcal{V}^i = \frac{4}{3}\pi(R^i)^3$ ,  $\mathcal{S}^i = 4\pi(R^i)^2$  and  $\mathcal{C}^i = 8\pi R^i$ , respectively. Thermodynamic potential of a strangelet of the  $i^{\text{th}}$  species is written as [21, 24, 27]

---

#### 4. An improved fragment distribution for unpaired SQM

---

$$\Omega^i = \sum_f \Omega_f^i + \Omega_e^i + \Omega_{\text{gluon}}^i + BV^i = \Omega_V^o V^i + \Omega_S^o S^i + \Omega_C^o C^i + BV^i, \quad (4.5)$$

where, the contribution  $\Omega_{\text{gluon}}^i$  (thermodynamic potential for gluons) is obtained from Ref. [9]. In Eq. (4.5) [21, 24] (see Sec. C.2 of Appendix C for the approach used for the calculations),

$$\begin{aligned} \Omega_V^o = & -\frac{37}{90}\pi^2 T^4 - \left(\frac{\mu_u^2 + \mu_d^2}{2}\right) T^2 - \left(\frac{\mu_u^4 + \mu_d^4}{4\pi^2}\right) - \frac{\mu_s^4}{4\pi^2} \left[ \left(1 - \frac{5}{2}\lambda_s^2\right) \sqrt{1 - \lambda_s^2} \right. \\ & \left. + \frac{3}{2}\lambda_s^4 \ln\left(\frac{1 + \sqrt{1 - \lambda_s^2}}{\lambda_s}\right) + 2\pi^2 \left(\frac{T}{\mu_s}\right)^2 \sqrt{1 - \lambda_s^2} + \frac{7\pi^4}{15} \left(\frac{T}{\mu_s}\right)^4 \frac{(1 - \frac{3}{2}\lambda_s^2)}{(1 - \lambda_s^2)^{3/2}} \right] \\ & - \frac{\mu_e^4}{12\pi^2}, \end{aligned} \quad (4.6a)$$

$$\begin{aligned} \Omega_S^o = & \frac{3}{4\pi}\mu_s^3 \left[ \frac{(1 - \lambda_s^2)}{6} - \frac{\lambda_s^2}{3}(1 - \lambda_s) - \frac{1}{3\pi} \left\{ \tan^{-1}\left(\frac{\sqrt{1 - \lambda_s^2}}{\lambda_s}\right) + \lambda_s^3 \ln\left(\frac{1 + \sqrt{1 - \lambda_s^2}}{\lambda_s}\right) \right. \right. \\ & \left. \left. - 2\lambda_s \sqrt{1 - \lambda_s^2} \right\} + \frac{\pi}{3} \left(\frac{T}{\mu_s}\right)^2 \left\{ \frac{\pi}{2} - \tan^{-1}\left(\frac{\sqrt{1 - \lambda_s^2}}{\lambda_s}\right) \right\} + \frac{7\pi^3}{180} \left(\frac{T}{\mu_s}\right)^4 \frac{\lambda_s^3}{(1 - \lambda_s^2)^{3/2}} \right] \end{aligned} \quad (4.6b)$$

and

$$\begin{aligned} \Omega_C^o = & \frac{19}{36}T^2 + \left(\frac{\mu_u^2 + \mu_d^2}{8\pi^2}\right) + \frac{\mu_s^2}{8\pi^2} \left[ \frac{1}{\lambda_s} \left\{ \frac{\pi}{2} - \tan^{-1}\left(\frac{\sqrt{1 - \lambda_s^2}}{\lambda_s}\right) \right\} + \left(\frac{\pi^2}{\lambda_s}\right) \left(\frac{T}{\mu_s}\right)^2 \right. \\ & \left. \times \left\{ \frac{\pi}{2} - \tan^{-1}\left(\frac{\sqrt{1 - \lambda_s^2}}{\lambda_s}\right) \right\} + \lambda_s^2 \left\{ \pi + \ln\left(\frac{1 + \sqrt{1 - \lambda_s^2}}{\lambda_s}\right) \right\} \right. \\ & \left. - \frac{3\pi}{2}\lambda_s - \left(\frac{2\pi^2}{3}\right) \left(\frac{T}{\mu_s}\right)^2 \frac{1}{\sqrt{1 - \lambda_s^2}} - \frac{7\pi^4}{60} \left(\frac{T}{\mu_s}\right)^4 \frac{\lambda_s^2(1 + \lambda_s^2)}{(1 - \lambda_s^2)^{5/2}} \right] \end{aligned} \quad (4.6c)$$

with  $\Omega_V^o$ ,  $\Omega_S^o$  and  $\Omega_C^o$  being the thermodynamic potential densities connected with the

---

#### 4. An improved fragment distribution for unpaired SQM

---

volume, surface and the curvature of the strangelets. The quantity  $\Omega_s^0$  can be denoted as the quark mode surface tension while the quantity  $\Omega_C^0$  is defined as the curvature coefficient of the strangelet. In Eqs. (4.6),  $\lambda_s = \frac{m_s}{\mu_s}$  and  $B$  is the bag pressure. For  $m_s \rightarrow 0$ , we obtain  $\lambda_s \rightarrow 0$  and  $\mu_u = \mu_d = \mu_s = \mu_q$ . In this limit  $m_s \rightarrow 0$ , charge-neutrality of the strangelet-complex no longer requires the presence of electrons in that complex so that  $\mu_e \rightarrow 0$  as  $m_s \rightarrow 0$ . We have checked that Eqs. (4.5) and (4.6) reduce to the thermodynamic potential of an isolated (ie., not embedded in an electron cloud) strangelet, as described in Chap. 2 (see Eq. A.1 in Sec. A.1 of Appendix A), in this limit of massless quarks inside the strangelet. For  $T = 0$ , on the other hand, the thermodynamic potential of cold strangelets with finite  $m_s$  [9] is restored from Eqs. (4.5) and (4.6) except for an additional term involving  $\mu_e^4$  in Eq. (4.6a). This term was ignored in Ref. [9] while discussing the thermodynamics of a small, isolated strangelet (not embedded in a charge-neutralizing background of electrons) so that  $\mu_e = 0$  for that strangelet. In this chapter, we, however, take the presence of those charge-neutralizing electrons surrounding the strangelet into account.

It is apparent from Eqs. (4.5) and (4.6b) that, in the limit  $m_s \rightarrow 0$ , the quark mode surface energy, proportional to  $(R^i)^2$ , vanishes in the traditional MIT bag model of strangelets [6, 7]. Advanced QCD models, such as the LSMq and the NJL models, of SQM, however, predict non-vanishing surface tension (at the vacuum-quark matter phase boundary) even in this case of massless quarks constituting the SQM [10]. Such absence of a surface tension in the traditional MIT bag model in the limit  $m_s \rightarrow 0$  seems to be a direct consequence of ignoring the effects of the dynamical (or explicit) chiral symmetry breakdown in the QCD vacuum in that model. According to the Nambu-Goldstone theory of chiral symmetry, such a breakdown would essentially lead to a qualitative re-arrangement of the QCD vacuum by enabling it to host strong condensates of quark-antiquark pairs [32, 33, 34]. A strong quark-mass independent surface tension is supposed to arise due to the discontinuities of such condensates across the bag surface which may be determined from the sum of those quark condensates [32]. Despite the above inability of the MIT bag model in taking the dynamical (or the explicit) breaking of QCD chiral symmetry into consideration, we still use this model in the present thesis for its mathematical and conceptual simplicity in modelling the consequences of selected features in QCD, namely the short distance ( $< 0.1$  fm)

asymptotic freedom as well as a perfect spatial and color confinement of the quarks at long ( $> 1$  fm) distance scales by the bag pressure ( $B$ ), which is assumed in this model to include all the non-perturbative effects from the QCD vacuum on the quarks inside the bag [34]. As we have discussed in Secs. 1.4 and 1.5, the above simplicity of the standard MIT bag model proves to be convenient for a preliminary investigation of the multifragmentation of the original bulk SQM into myriads of strangelets. The mathematically harder tasks of describing multifragmentation within the framework of more sophisticated theoretical models of SQM, such as the LSMq and the NJL models, or the chirally invariant bag models (eg., [32, 35]), will be a major step forward beyond the basic analysis presented in this thesis.

While the traditional MIT bag model of strangelets with massless quarks yields a vanishing surface tension at the vacuum-quark matter boundary, it nevertheless provides for a positive curvature coefficient (Eq. (4.6c))  $\sigma_c = \Omega_c^0 = (3/8\pi^2)\mu_q^2 \sim 17 \text{ MeV fm}^{-1}$  (at zero temperature and for  $\mu_q \sim 300 \text{ MeV}$ ) [9, 36] of the strangelets. This curvature coefficient arises from finite-size corrections to the quark density of states that are required to match the quark wave functions to the bag boundary conditions [36]. In analogy with the quark mode surface tension, we may refer to this (curvature) coefficient as the “quark mode curvature coefficient” of the strangelets. In spite of the important distinction between the energies associated with them (which scale differently with the baryon number  $A^i$ ; see Eq. (4.5)), the surface tension and the curvature coefficient play somewhat similar roles in the multifragmentation of SQM. Both these quantities require additional energy to produce a large number of smaller fragments at the expense of a few large fragments as we will find in Sec. 4.3. Apart from that, both the surface tension and the curvature coefficient tend to destabilize finite-sized fragments by increasing their energies per baryon; see Sec. 4.4. In view of the above, we may like to investigate into the relative magnitude of the quark mode curvature energy (in the limit of massless quarks in the MIT bag model) of the strangelets *vis-a-vis* their surface energy determined in Refs. [10] from the LSMq and the NJL models. For a strangelet having  $A^i \sim 10$ , the value of the curvature energy (per baryon) turns out to be  $\sigma_c C^i/A^i \sim 100 \text{ MeV}$ , whereas, the value of the surface energy (per baryon) determined in Refs. [10] lies in the range  $\sigma_s S^i/A^i \sim (30 - 120) \text{ MeV}$ . For  $A^i \sim 100$ , the values of these energies are  $\sim 20 \text{ MeV}$  and  $\sim (10 - 50) \text{ MeV}$ , respectively. Similarly,

these quantities take on values  $\sim 4$  MeV and  $\sim (6 - 25)$  MeV for  $A^i \sim 10^3$ . In the above, we have considered  $m_s = 0$ ,  $r_o^i \sim 1$  fm [37],  $T = 0$  and  $\mu_q \approx 300$  MeV to calculate the curvature energies of strangelets by using the MIT bag model. Above comparisons reveal that, for an approximate range of most of the fragment-sizes ( $10 \lesssim A^i \lesssim 10^3$ ) obtained (in Sec. 4.3) in this chapter, the magnitude of curvature energy of strangelets (with massless quarks in the MIT bag model) is more-or-less compatible at least with the lower bound of the surface energy determined in Refs. [10] by using various QCD models of strangelets that are supposed to be more sophisticated than the MIT bag model. Numerical examples presented above seem to suggest that, notwithstanding the absence of a surface energy for massless quarks in the MIT bag model, it is perhaps not unreasonable to use this model (having a positive curvature coefficient) for the sake of a rudimentary analysis of multifragmentation of SQM. Such an analysis, undertaken originally in Chaps. 2 and 3 of this thesis, provides us with some basic idea regarding the trend in the fragment-size distribution of the strange matter that, in fact, serves as an useful guidance in the calculations presented in this chapter. Hopefully, the same analysis would even be useful in guiding the computations of multifragmentation in other sophisticated models of SQM as well. We further add that the present chapter, that employs MIT bag with  $m_s \neq 0$ , is relatively less vulnerable to the afore said drawback of the traditional MIT bag model with massless quarks as, along with a positive curvature coefficient, the model presented in this chapter also predicts a positive dynamical surface tension whose magnitude is found to be compatible with the ones in Refs. [10] in the introductory section of this chapter.

In Eqs. (4.5) and (4.6), we have considered the fact that  $\mu_e \ll \mu_f$ ;  $f = (u, d, s)$ . We, therefore, take into account only the leading order contribution from the electron chemical potential in  $\Omega_V^Q$  in Eq. (4.6a). We also assume that, even though the electron chemical potential is non-zero inside strangelets, the sizes of those strangelets are too small to have electrons physically localized inside them, so that, the contribution of those electrons to the thermodynamic potentials associated with the surface and the curvature of a strangelet (Eqs. (4.6b) and (4.6c)) need not be taken into account. The electric charge of a strangelet is given by that of the quark matter alone in the case of such small strangelets [18]. Moreover, as the  $s$  quarks are massive, the number of those quarks is less than the numbers of quarks of other (viz.  $u$  and  $d$ ) flavors inside the strangelet. A strangelet of the  $i^{\text{th}}$  species

---

#### 4. An improved fragment distribution for unpaired SQM

---

possesses a positive charge number  $Z^i$  in this situation [6, 16, 18]. It was pointed out in Refs. [6, 7, 16] that the approximation of no localized electrons inside strangelets may be justified when  $A^i \lesssim 10^5$ , so that, the radius of a strangelet satisfies the condition  $R^i \lesssim 46 \text{ fm} < a_B/Z^i \sim 253 \text{ fm} < 2\pi/m_e \sim 2.4 \times 10^3 \text{ fm}$ . Here,  $a_B = 1/(\alpha m_e)$  is the Bohr radius;  $m_e$  is the mass of the electron and  $2\pi/m_e$  is the electron Compton wavelength in the units considered in this chapter. In the above,  $\mu_u \sim \mu_d \sim \mu_s \sim \mu_q \sim 300 \text{ MeV}$  [6, 16] and  $Z^i \leq 214$  (see Eq. (4.7) below). We have checked that the above condition for the absence of localized electrons inside strangelets is satisfied by all the fragments in the strangelet-complex that we finally obtain in Sec. 4.3. The charge-neutralizing electron cloud surrounding such a strangelet has been treated here within the framework of the Wigner-Seitz approximation as described in a later paragraph of this section.

In this chapter, we take the effect of Debye screening [16, 17, 18, 19, 20] on the charge distribution inside relatively larger ( $a_B/Z^i > R^i > \lambda_D$ ) strangelets into account. Equilibrium of the quarks in the electrostatic field inside such a strangelet, that is given by the solution of Eq. (4.2) in Sec. 4.1 above [16, 18], bar its core from having a positive electric charge density, ie. the deep interior of that strangelet is charge neutral. The positive charge density inside that strangelet is confined within a layer of thickness  $\sim \lambda_D$  from its surface. In this situation, the total charge and the Coulomb energy of the strangelet are obtained by integrating over the radial coordinate ( $r$ ) measured from its centre. The expressions of these integrated quantities are given as [16, 17, 18]

$$Z^i \approx \frac{m_s^2}{4\alpha\mu_q} R^i \left[ 1 - \frac{\tanh(R^i/\lambda_D)}{(R^i/\lambda_D)} \right] \quad (4.7)$$

and

$$E_C^i \approx \frac{m_s^4}{32\alpha\mu_q^2} R^i \left[ 1 - \frac{3 \tanh(R^i/\lambda_D)}{2 (R^i/\lambda_D)} + \frac{1}{2} \left\{ \cosh(R^i/\lambda_D) \right\}^{-2} \right]. \quad (4.8)$$

In reality, after the application of statistical multifragmentation model to the initial bulk SQM, we would have rather large an array of strangelets of various sizes. Many of those

---

#### 4. An improved fragment distribution for unpaired SQM

---

strangelets may not be large enough to satisfy the condition of charge-screening. Whatever may be the case, Eqs. (4.7) and (4.8) are generalized enough to equally account for the large ( $R^i > \lambda_D$ ) as well as the small ( $R^i \lesssim \lambda_D$ ) strangelets. In the following, we, therefore, adopt those two equations to proceed with the calculations.

The entropy of a strangelet of the  $i^{\text{th}}$  species is  $\mathcal{S}^i = -\left(\frac{\partial \Omega^i}{\partial T}\right)_{V^i, \mu^i}$ . Thus, the total energy of a strangelet may be written as

$$\begin{aligned} E^i &= T\mathcal{S}^i + \mu^i + \Omega_{\text{tot}}^i \\ &= T\mathcal{S}^i + \mu^i + \Omega^i + E_C^i. \end{aligned} \quad (4.9)$$

For thermodynamic equilibrium, the strangelet-fragments, in addition to being in electrostatic and chemical equilibrium (including beta-equilibrium) are also in mechanical equilibrium, ie.,  $P_{\text{ext}}^i = -\left(\frac{\partial \Omega_{\text{tot}}^i}{\partial V^i}\right)_{T, \mu^i}$ ;  $P_{\text{ext}}^i$  being the external pressure (as distinct from the bag pressure) on a strangelet of the  $i^{\text{th}}$  species. This pressure is assumed to be exerted by  $Z^i$  charge-neutralizing relativistic electrons residing outside the  $i^{\text{th}}$  fragment but within the Wigner-Seitz cell \* surrounding that particular fragment. Following Ref. [39], a strangelet-fragment of the  $i^{\text{th}}$  species is approximated to be a point-like (ie.,  $V^i \ll V_{\text{cell}}^i$ ;  $V_{\text{cell}}^i$  being the volume of the  $i^{\text{th}}$  Wigner-Seitz cell) positive charge ( $Z^i$ ) surrounded by the spherical Wigner-Seitz cell containing electrons of uniform number density  $\frac{Z^i}{V_{\text{cell}}^i} = \frac{N_e^{\text{total}}}{\mathcal{V}} = n_e \approx \frac{m_s^6}{192\pi^2 \mu_q^3}$ ;  $N_e^{\text{total}}$  being the total number of electrons in the strangelet-complex. We choose  $V_{\text{cell}}^i = \frac{Z^i}{\sum_i Z^i \omega^i} \mathcal{V}$  so that it satisfies the condition  $\sum_i \omega^i V_{\text{cell}}^i = \mathcal{V}$ . The expression for the pressure of relativistic electrons on the strangelet may then be written as [21, 39]

---

\*Wigner-Seitz cell is a special type of primitive-cell which contains one lattice point, and volume of the cell encloses all neighboring points in space which are closer to this particular lattice point [38].

$$\begin{aligned}
 P_{\text{ext}}^i &\approx (3\pi^2)^{1/3} \left[ \frac{(n_e)^{4/3}}{4} \right] + \left( \frac{\pi^2}{2} \right) \left[ \frac{T^2}{(3\pi^2)^{1/3}} \right] (n_e)^{2/3} \\
 &- \left( \frac{3}{10} \right) \left( \frac{4\pi}{3} \right)^{1/3} \alpha (Z^i)^{2/3} (n_e)^{4/3} \\
 &- \left( \frac{1}{6} \right) \left( \frac{324}{175} \right) \left( \frac{4}{9\pi} \right)^{2/3} (3\pi^2)^{1/3} (Z^i)^{4/3} \alpha^2 (n_e)^{4/3} \\
 &+ \left( \frac{1}{8\pi} \right) \alpha (3\pi^2)^{1/3} (n_e)^{4/3} - \frac{0.062}{6} \alpha^2 m_e n_e.
 \end{aligned} \tag{4.10}$$

In Eq. (4.10), the first two terms on the right hand side represent the pressure of a degenerate Fermi gas of non-interacting, relativistic electrons at temperature  $T$ . The third term stands for the Coulomb interactions between the point-like strangelet and the uniformly distributed electrons as well as the electron-electron interactions. The fourth term in Eq. (4.10) represents the Thomas-Fermi correction that results from first order deviation of the electron distribution from uniformity. This deviation is obtained by expanding the relativistic electron kinetic energy about its value given by the uniform approximation and then assuming that the ratio of the Coulomb potential energy of the electron to the electron Fermi energy to be of the same order as the deviation in the electron distribution. The fifth term arises due to the interactions between the relativistic electrons *via*. transverse electromagnetic field while the sixth term represents the influence of the electric field of ions on the above interactions between electrons. Here, it is important to note that an analytical expression for the electron pressure, that is similar to the one in Eq. (4.10), has also been derived in Ref. [20] by using a ‘‘low pressure approximation’’, in which the electrons may be assumed to have an uniform number density inside the Wigner-Seitz cell pertaining to a strangelet. In Ref. [20], the said approximation was found to be justified in the case  $a_B/Z^i > R_{\text{cell}}^i \gg R^i$  with  $R_{\text{cell}}^i = (\frac{3}{4\pi} V_{\text{cell}}^i)^{1/3}$  being the radius of the spherical Wigner-Seitz cell. We have verified that the above criterion is satisfied by all the Wigner-Seitz cells associated with the charged fragments in the strangelet-complex, that are obtained numerically in Sec. 4.3 by using the relations  $\mu_e \approx \frac{m_s^2}{4\mu_q}$  and  $n_e \approx \frac{\mu_e^3}{3\pi^2}$  mentioned in Sec. 4.1 above. The authors of Ref. [20] determined the pressure of the charge-neutralizing electrons on a strangelet by considering the contributions from the degeneracy pressure (at

zero-temperature) of electrons along with that from the Coulomb interactions between the strangelet and the electrons as well as a contribution from the finite electron-mass ( $m_e$ ) within the framework of the low pressure approximation described above. We have checked that the discrepancy between the numerical values of multiplicities of strangelets, obtained (in Sec. 4.3) by using Eq. (4.10) and then by using the expression in Ref. [20], is not more than about 0.01% for the ranges of values of temperature, bag parameter and fragment-size considered in this chapter.

With the definitions given in Eqs. (4.5), (4.6), (4.7), (4.8) and (4.10), the condition for mechanical equilibrium mentioned above ultimately yields an expression for the total thermodynamic potential  $\Omega_{\text{tot}}^i$  of the strangelet at thermodynamic equilibrium at freeze-out. This expression is [21]

$$\Omega_{\text{tot}}^i = (-\Omega_{\text{V}}^0 - B)\mathbf{V}^i \left( \frac{\Omega_{\text{S}}^0 \mathbf{S}^i + 2\Omega_{\text{C}}^0 \mathbf{C}^i + 3E_{\text{C}}^i - \Delta E_{\text{C}}^i - 3P_{\text{ext}}^i \mathbf{V}^i}{2\Omega_{\text{S}}^0 \mathbf{S}^i + \Omega_{\text{C}}^0 \mathbf{C}^i + \Delta E_{\text{C}}^i + 3P_{\text{ext}}^i \mathbf{V}^i} \right), \quad (4.11)$$

where,

$$\Delta E_{\text{C}}^i \approx \frac{m_s^4}{32\alpha\mu_q^2} R^i \left[ 1 - \cosh^{-2} \left( \frac{R^i}{\lambda_D} \right) \left\{ 1 + \left( \frac{R^i}{\lambda_D} \right) \tanh \left( \frac{R^i}{\lambda_D} \right) \right\} \right]. \quad (4.12)$$

In the following, we will use Eqs. (4.11) and (4.12) to evaluate the multiplicities of strangelets of the  $i^{\text{th}}$  species as defined in Eq. (4.4). For doing this, we require an additional relation

$$N_u^i = A^i + Z^i, \quad (4.13)$$

that is obtained from the definitions of the baryon number and the charge of a strangelet with  $N_u^i$  being the number of the  $u$  quarks in that strangelet. In Eq. (4.13), we have assumed that no electrons are localized inside strangelets. This equation may be rewritten in the form of a transcendental equation, by using the definition  $N_u^i = \left( -\frac{\partial \Omega_u^i}{\partial \mu_u} \right)_{T, \mathbf{V}^i}$  along with Eq. (4.7) for  $Z^i$ , that involves the radius parameter  $r_0^i$  as defined in the discussion preceding Eq. (4.5). This transcendental equation is solved iteratively to obtain the radius parameter of a particular species of strangelets corresponding to each trial value of the quark number chemical potential ( $\mu_q$ ) of the strangelet-complex in equilibrium at freeze-out.

### 4.3. Mass spectra of strangelets

In this section, we will explain the procedure adopted by us for the numerical determination of multiplicities of various species of strangelets in the strangelet-complex in thermodynamic equilibrium at freeze-out. For that purpose, we first examine the condition of global charge-neutrality in the strangelet-complex. This condition can be written as [21, 24]

$$\sum_i \frac{\omega^i}{\mathcal{V}} Z^i = \sum_i n^i Z^i = n_e \approx \frac{m_s^6}{192\pi^2 \mu_q^3}, \quad (4.14)$$

where,  $n^i = \frac{\omega^i}{\mathcal{V}}$  is the multiplicity density of strangelet-fragments of the  $i^{\text{th}}$  species. For the derivation of Eq. (4.14), we have used the approximation for the electron chemical potential, ie.,  $\mu_e \approx \frac{m_s^2}{4\mu_q}$  (see the third paragraph of Sec. 4.1), in the strangelet-complex. The values of  $n^i$  for arbitrary positive integer values of  $A^i$  are determined after we self-consistently solve the system of equations, ie., Eq. (4.4), along with Eqs. (4.6)-(4.8) and (4.10)-(4.14), for  $\mu_q$  in the strangelet-complex in thermodynamic equilibrium at freeze-out.

The next step is to determine the value of the available volume ( $\mathcal{V}$ ) of the strangelet-complex. This can be achieved by using the condition for the conservation of the initial baryon number  $A_b$  [25] of the SQM that is released in a SS merger event. This condition is written in the following form [21, 24]

$$\mathcal{V} = \frac{A_b}{\sum_i A^i n^i}. \quad (4.15)$$

The value of  $\omega^i$  of strangelets of the  $i^{\text{th}}$  species can now be easily determined from the known values of  $n^i$  and  $\mathcal{V}$ . We choose  $A_b = 1 \times 10^{53}$ , that corresponds to the population averaged tidally released mass  $M_{\text{ejected}} \approx 10^{-4} M_{\odot}$  [15] per binary SS merger obtained in the simulations with the model SSs having a bag value  $B^{1/4} \approx 145$  MeV. Keeping in mind the limited accuracy of the MIT bag model, we may, consider  $B^{1/4} = 145$  MeV as the most favourable choice of the bag constant for which the ordinary nuclei can decay into their strange quark phases only on a time-scale longer than the age of the universe [40]. In Chap. 2, we considered only this value of the bag constant to find the basic size distribution

#### 4. An improved fragment distribution for unpaired SQM

---

of the strangelets. For the calculations in this chapter, we, however, consider the fact that the value of the bag constant for unpaired SQM lies within the range  $145 \text{ MeV} \leq B^{1/4} \leq 158 \text{ MeV}$ ; see the subsection 1.6.1 and the inequality relation (1.2) for a justification of considering the above limiting values for the bag constants in the standard MIT bag model.

It is also important to note that, in Chaps. 2 and 3, the condition of the global charge-neutrality (Eq. (4.14)) of the strangelet-complex was not required to obtain the size distribution of strangelets with  $m_s = 0$ . We, therefore, took  $\mathcal{V}$  as a free parameter in Chap. 2. In that particular case, we chose  $\mathcal{V} = (2 - 9)V_b = (2 - 9) \times (\frac{4\pi}{3}r_b^3 A_b)$  by following the standard practice in the computations in nuclear fragmentation models [26, 41, 42, 43], where,  $V_b$  is the initial volume of the ejecta with  $r_b$  as its bulk radius parameter. For an approximate estimate of  $V_b$ , we there considered  $r_b \approx (\frac{3}{4\pi n_b})^{1/3}$  [9] at zero temperature and zero pressure with  $n_b$  being the baryon number density in the bulk SQM before fragmentation. Following Ref. [9], baryon number density of the bulk SQM corresponding to  $m_s \rightarrow 0$  and  $T = 0$  was denoted as  $n_b = 0.7B^{3/4}$ [25]. In this chapter, it is possible to self-consistently determine a unique numerical value of  $\mathcal{V}$  by considering the condition of global charge-neutrality (Eq. (4.14)) along with the condition of the baryon number conservation (Eq. (4.15)) in the strangelet-complex with massive  $s$  quarks. Here,  $n_b$  is approximated as  $n_b \approx \frac{1}{3} \left[ \frac{2\mu_b^3}{\pi^2} + \frac{\mu_b^3}{\pi^2} (1 - \lambda_{sb}^2)^{3/2} \right]$  [9], where  $\lambda_{sb} = \frac{m_s}{\mu_b}$ . Approximately,  $\mu_b$  (ie., the value of the quark number chemical potential of the initial bulk SQM) can be taken as one third of the parametrized form of its energy ( $E_b$ ) per baryon at  $P_{\text{ext}}^i = 0$  and  $T = 0$ , ie.,  $\mu_b = \frac{1}{3}(E_b/A_b)$  [9, 29]. The procedure for the calculation of  $E_b$  has been outlined in the discussion preceding Eq. (4.4) in Sec. 4.1. Following the above prescription, an approximate value of  $V_b$  of the initial bulk SQM with  $m_s \neq 0$  may easily be determined. If  $A_b = 1 \times 10^{53}$ , the numerical value of the available volume turns out to be  $\mathcal{V} \approx 4 \times 10^{50} \text{ MeV}^{-3} \approx 8 \times 10^3 V_b$  [21]. We also find that  $\mathcal{V}$  remains nearly the same for different bag values and for different values of the temperature (at freeze-out) chosen in this chapter. The available volume is, however, found to scale linearly with the values of  $A_b$ .

Before the presentation of the numerical results, we would like to add that, similar to the case of the nuclear disassembly models, the derived size distribution of strangelet fragments is also sensitive to channel selection (ie., the selection of their baryon numbers). In this chapter, we consider all possible positive integer values of  $A^i$  of the fragment-species to

#### 4. An improved fragment distribution for unpaired SQM

obtain the number of fragments (ie., the multiplicity) pertaining to each species. During the selection of those channels, we also take the charge numbers of strangelets into account. For this, we round off the real values obtained from Eq. (4.7) to their nearest positive integers. The lower cut-off in the baryon number of a strangelet with  $m_s = 95$  MeV is chosen so that the corresponding  $Z^i = 1$  after rounding off [21].

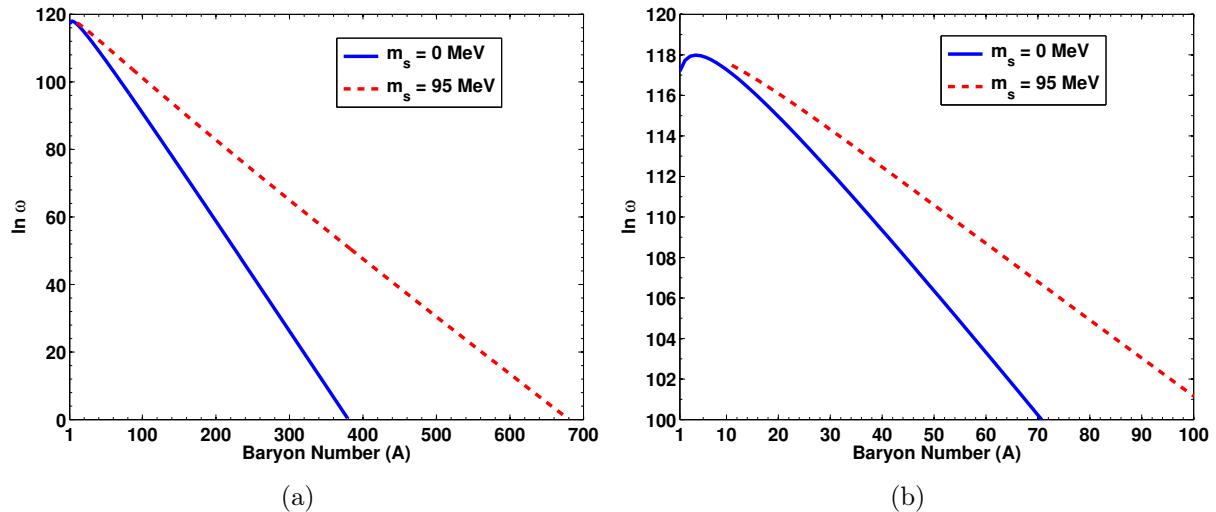


Figure 4.1.: Multiplicity ( $\ln \omega$ ) distribution of strangelets for massless ( $m_s = 0$ ) and massive ( $m_s = 95$  MeV)  $s$  quarks both for a fixed value of the bag parameter ( $B^{1/4} = 145$  MeV) at a specific temperature ( $T = 10$  keV) at freeze-out. The  $u$  and the  $d$  quarks are considered to be massless in both cases. The results are displayed for (a) the full range of the available baryon numbers and (b) for a limited range of baryon numbers of the strangelet-fragments. Fig. 4.1(b) is included to focus on the lower cut-off ( $A \approx 11$  for  $m_s = 95$  MeV) in the baryon numbers as well as the baryon number ( $A \approx 4$ ) at which the peak of the distribution (for  $m_s = 0$ ) is obtained. Available volume is determined to be  $\mathcal{V} \approx 8 \times 10^3 V_b$ ,  $A_b = 1 \times 10^{53}$ .

In Fig. 4.1(a), we have compared the multiplicities of strangelets in two cases, namely  $m_s = 0$  and  $m_s = 95$  MeV, for a fixed bag value ( $B^{1/4} = 145$  MeV) at  $T = 10$  keV at freeze-out. Fig. 4.1(b) also displays the same in truncated baryon number range (ie., a limited range of baryon numbers). These figures show that the effect of  $m_s \neq 0$  on the multiplicity distribution is not equivalent to an enhanced Boltzmann suppression as seems to have been recently suggested in Ref. [13]. The distribution for  $m_s = 0$  starts from  $A^i \approx 1$ ; the

strangelets are charge-neutral in this particular case. On the other hand, the distribution for  $m_s \neq 0$  starts from  $A^i \approx 11$  which corresponds to  $Z^i \approx 1$ . The difference in the nature of the distribution in the two cases arises from a complex interplay of several factors. The dynamical surface tension arises due to finite  $m_s$  and vanishes for massless  $s$  quarks according to the standard MIT bag model [6, 7, 9]. This surface term can be considered as the energy required for creating the surface whereas the curvature term represents the energy required for bending it [44]. Due to the presence of an additional surface term for  $m_s \neq 0$ , the total (surface + curvature) requirement of the energy is more than the energy required for curvature alone in the particular case  $m_s = 0$ . This implies that more energy is required to produce small fragments out of the bulk SQM in the case of massive  $s$  quarks. At fixed temperature, this energy has to be supplied from the limited reserve of thermal energy of the strangelet-complex. In SMM, an increment in the total (surface + curvature) requirement of energy (at a fixed temperature) to form light strangelets leads to the production of heavier fragments at the cost of lighter fragments so that the total baryon number is conserved. These features (or patterns) of multifragmentation, appears consistently in our results both in Chap. 2 and in this chapter. Such features of the disassembly model are independent of whether we consider massless or massive quarks. They are also independent of the choice of CFL or the unpaired strangelets (see Chap. 3).

The size distributions of strangelet-fragments for a fixed bag value ( $B^{1/4} = 145$  MeV) at three different temperatures, namely  $T = 1$  keV,  $T = 10$  keV and  $T = 1$  MeV, respectively, are displayed in Figs. 4.2(a,b). The variation of size distribution with changing temperature is in qualitative agreement with the one obtained in Chap. 2. Enhanced production of lighter fragments and suppression of heavier fragments with increasing temperature are noted for both  $m_s = 0$  [25] and  $m_s \neq 0$  [21, 24, 27]. Such features of the fragmentation pattern are commonplace in the case of nuclear fragmentation [26, 42, 43].

It is known that the surface free energies and the curvature free energies of both the baryonic (ie., the nuclei) and the quasi-baryonic (ie., the SQM) fragments decrease with increasing temperature [45, 46]. This fact has also been noticed in our numerical calculations. The above fact implies that the total requirement of (surface + curvature) free energy to produce small size strangelets out of the initial bulk SQM is reduced at higher temperature. This reduced requirement of free energy is easily met by a larger reserve of

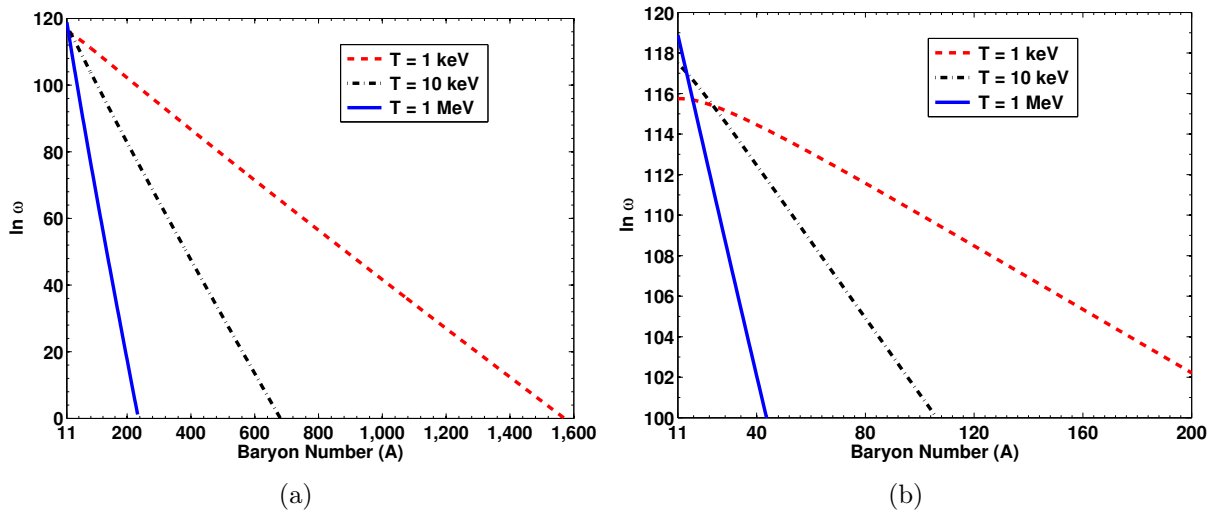


Figure 4.2.:  $\ln \omega$  vs.  $A$  for the strangelet-fragments with  $B^{1/4} = 145$  MeV and  $m_s = 95$  MeV at three different temperatures at freeze-out. Variations are displayed for (a) the full range of possible baryon numbers and for (b) a limited range of baryon numbers of the fragments.

thermal energy of the strangelet-complex at a higher temperature [21]. This, along with the condition for the conservation of baryon number, ensure an enhanced production of lighter fragments and suppressed production of heavier fragments with increasing temperature. The patterns, as shown in Figs. 4.2(a,b), are in consonance with the standard results of nuclear fragmentation models [42, 43, 47]. However, recent discussion on fragmentation in Ref. [13] obtains an opposite tendency in the variation of size distribution of CFL strangelets with changing temperature. The authors of Ref. [13] attribute this behavior of the size distribution to finite  $m_s$  combined with the color-superconductivity of the strangelets. We would like to point out that an earlier exploratory work in Chap. 3 found that the changes in the size distribution of CFL strangelets [28], having massless quarks, with changing temperature are in qualitative agreement with Figs. 4.2(a,b).

In Figs. 4.3(a,b), we study the effect of bag values on the size distribution (or, the baryon number distribution) of strangelets for  $m_s = 95$  MeV at  $T = 10$  keV (at freeze-out). If other parameters are fixed, an enhanced bag value increases the quark number chemical potential

#### 4. An improved fragment distribution for unpaired SQM

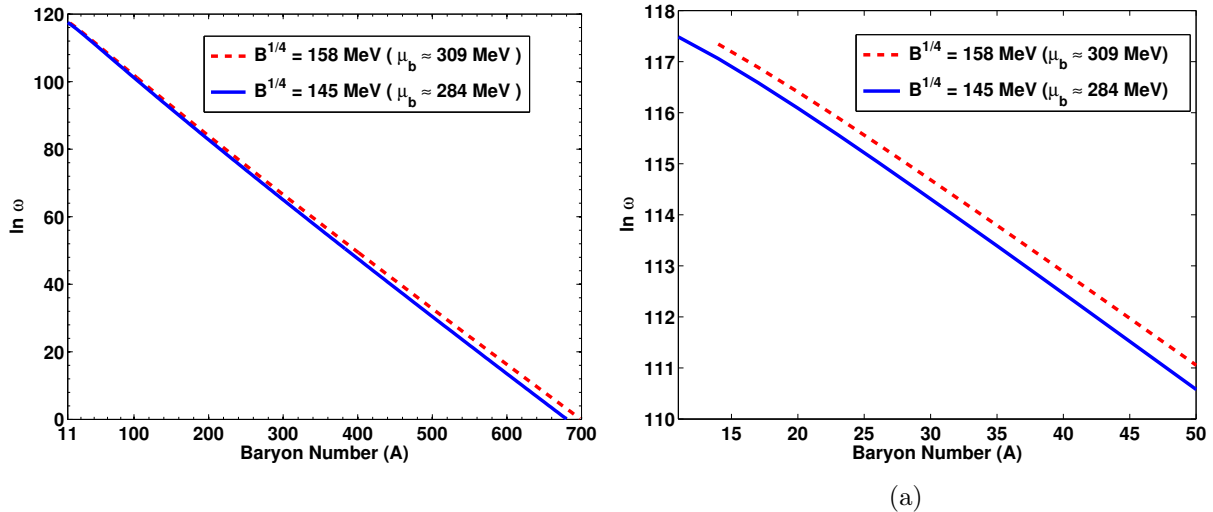


Figure 4.3.: Variations of  $\ln \omega$  vs.  $A$  for strangelets with  $m_s = 95$  MeV at a specific temperature ( $T = 10$  keV) but at two different bag values have been shown for (a) the full range of possible baryon numbers and for (b) a limited range of baryon numbers of the fragments. Approximate value of the quark number chemical potential ( $\mu_b$ ) of the initial bulk matter before fragmentation, that corresponds to each value of the bag parameter at zero external pressure and zero temperature, is also displayed.

in the strangelet-complex that, in turn, increases the surface and curvature energies of the strangelet-fragments. Due to the enhancement in the requirement of the energy for the formation of lighter fragments, the formation of heavier fragments at the cost of the lighter ones is preferred. In Figs. 4.3(a,b), the lower cut-off (corresponding to  $Z^i \approx 1$ ) in the baryon number of the strangelet-fragment distributions changes from  $A^i \approx 11$  for  $B^{1/4} = 145$  MeV (corresponding to  $\mu_b \approx 284$  MeV) to  $A^i \approx 14$  for  $B^{1/4} = 158$  MeV (corresponding to  $\mu_b \approx 309$  MeV).

In Figs. 4.3(a,b), the results are obtained (for both the bag constants) by considering the same mass ejection (ie.,  $10^{-4}M_\odot$ ) in a SS merger event. Numerical simulations [15] of SS merger, however, find no mass ejection in the case  $B^{1/4} \approx 158$  MeV due to the compactness of the merging SSs. These simulations may seem to indicate that, for  $B^{1/4} \sim 158$  MeV, the merged system collapses into a BH faster than the time required for the formation of the tidal arms. Although the actual simulations in Ref. [15] were done only

at two nearly extreme bag values in the range  $145 \text{ MeV} \lesssim B^{1/4} \lesssim 158 \text{ MeV}$ , the authors performing those simulations expected that the population averaged ejecta mass ( $M_{\text{ejected}}$ ) for any intermediate bag value within the above interval would lie somewhere in the range  $10^{-4}M_{\odot} > M_{\text{ejected}} \gtrsim 0$  with lesser amount of ejected mass corresponding to a larger bag constant. We have checked that the shape of the fragmentation pattern corresponding to a particular bag value remains almost invariant for any reduced value of the mass of the initially released bulk SQM except that all the multiplicities are now reduced by an appropriate factor from the ones obtained for  $M_{\text{ejected}} = 10^{-4}M_{\odot}$  (ie.,  $A_b = 1 \times 10^{53}$ ) [21]. Such scaling makes it convenient to estimate the possible fluxes of strangelets in GCR for different amounts of strange matter being tidally released by the merger of two SSs with different values of the bag constants being assigned in their modelling.

#### 4.4. Stability of the produced fragments

In this section, we will investigate the stability of the fragments that are produced due to the fragmentation of the initial bulk SQM. This investigation is important as our ultimate aim is to estimate the flux of absolutely stable strangelets in the vicinity of the Sun. The strangelets having energy per baryon ( $E^i/A^i$ ) less than 930 MeV belong to this category of the absolutely stable strangelets. Those strangelets are possibly the only ones to survive during the plausible confinement-time ( $\sim 10^7 \text{ yr}$  [48]) of strangelets in the Galaxy and are easily detectable in GCR in the solar neighborhood. It was, however, pointed out in Ref. [40] that, in view of the uncertainties in the accuracy of the results derived from the MIT bag model, the strangelets having their energy per baryon in the vicinity of that of the nucleons cannot be discarded. In fact, precise values of  $E^i/A^i$  of strangelets, ie., whether they lie marginally above the nucleon mass or below the energy per nucleon in  $^{56}\text{Fe}$ , is a matter that involves only  $\sim 1\%$  deviation in numerical calculations and the deviation of such magnitude may be insignificant for the results derived from the MIT bag model. Keeping this issue in mind, we study the values of  $E^i/A^i$  of strangelet fragments as a function of their baryon number  $A^i$  for three different values of the bag constant at a temperature  $T = 1 \text{ MeV}$  at freeze-out. As we know that the stability of the strangelets decreases with increasing temperature [37], we investigate the stability of strangelets at  $T =$

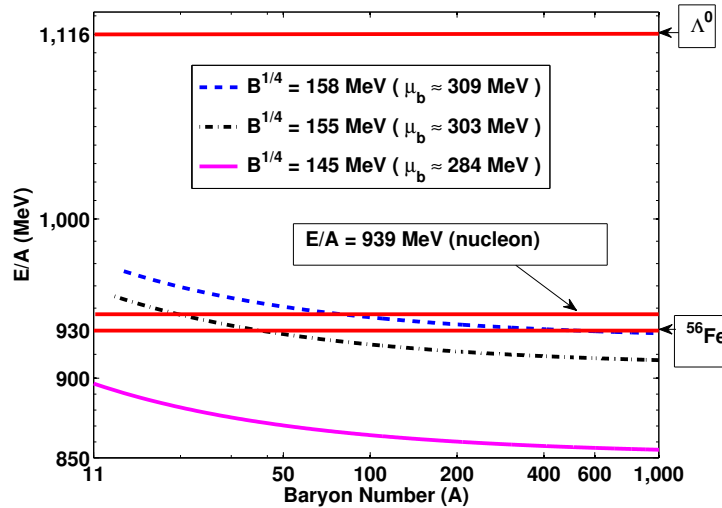


Figure 4.4.: Variation of the energy per baryon ( $E/A$ ) against changing baryon number ( $A$ ) of the strangelet-fragments (with  $m_s = 95$  MeV) for three different values of the bag parameter at a specific temperature ( $T = 1$  MeV) at freeze-out. Corresponding value of the quark number chemical potential ( $\mu_b$ ) of the initial bulk matter at zero pressure ( $P_{\text{ext}} = 0$ ) and zero temperature is displayed against each bag value for the sake of comparison. The solid (red) horizontal lines mark the energies per baryon of  $^{56}\text{Fe}$ , nucleon and  $\Lambda^0$ -hyperon, respectively, that delineate the thresholds for absolute stability, metastability and instability of the fragments.

1 MeV, the highest temperature considered in our case. The results of such investigation are shown in Fig. 4.4. In Fig. 4.4, the solid (red) horizontal lines denote the values of the energy per baryon of  $^{56}\text{Fe}$  ( $E/A = 930$  MeV) nucleus, nucleons ( $E/A = 939$  MeV) and  $\Lambda^0$ -hyperons ( $E/A = 1116$  MeV), respectively. Here, we simply look for fragment-sizes satisfying the stability criterion in Ref. [40], according to which the strangelets are stable if their energy per baryon is below the energy per baryon of nucleon (within 1% of 930 MeV) for each value of  $B^{1/4}$  (or,  $\mu_b$ ) displayed in Fig. 4.4. In the Fig. 4.4, we find that all the strangelets having  $A^i \gtrsim 11$  are stable relative to the  $^{56}\text{Fe}$  nucleus for  $B^{1/4} = 145$  MeV (ie.,  $\mu_b \approx 284$  MeV). For  $B^{1/4} = 155$  MeV (ie.,  $\mu_b \approx 303$  MeV) and  $B^{1/4} = 158$  MeV (ie.,  $\mu_b \approx 309$  MeV), the strangelets having their sizes in the respective ranges  $A^i \gtrsim 23$  and  $A^i \gtrsim 90$  are stable relative to the nucleons.

It is also relevant to take note of an altogether different scenario of fragmentation of a (positively charged) strangelet (embedded in a charge-neutralizing cloud of electrons), with its radius satisfying  $R \gg \lambda_D$ , through the “fission instability” proposed in Refs. [18, 19, 20, 23] within a model-independent theoretical framework. This instability affects even the cold ( $T = 0$ ) strangelets and this instability depends crucially on the surface tension ( $\sigma_s$ ) at the boundary of the quark matter. Instability sets in whenever  $\sigma_s < \sigma_{\text{crit}}$ , where,  $\sigma_{\text{crit}}$  is a critical surface tension whose values have been determined in Ref. [18] in the case of MIT bag model for a wide range of  $m_s$  along with different values of  $\mu_b$  of the absolutely stable, charge-neutral bulk SQM at zero external pressure and zero temperature. For  $\mu_b = 305$  MeV, for example,  $\sigma_{\text{crit}}$  takes on values in the range  $0.1 \text{ MeV fm}^{-2} \leq \sigma_{\text{crit}} \lesssim 2.7 \text{ MeV fm}^{-2}$  for the mass of the  $s$  quarks lying in the range  $100 \text{ MeV} \leq m_s \leq 240 \text{ MeV}$  [18]. The value of  $m_s$  has recently been estimated to be  $m_s \lesssim 100 \text{ MeV}$  with reasonable accuracy. Hence, the possible value of  $\sigma_{\text{crit}}$  in the MIT bag model (estimated from Fig. 3 in Ref. [18]) seems to be  $\sigma_{\text{crit}} \sim 0.1 \text{ MeV fm}^{-2}$  for values of  $\mu_b$  lying in the range (284 – 309) MeV (corresponds to the whole range of the bag constant, see Fig. 4.4). Such value of  $\sigma_{\text{crit}}$  is at least an order of magnitude smaller than the typical values of the quark mode surface tension ( $\sigma_s \sim (5 - 10) \text{ MeV fm}^{-2}$ ) in the MIT bag model of strangelets. Above comparison seems to suggest that the stable strangelets, with their sizes in the range  $R^i \sim (0.4-2.2)\lambda_D$  that we obtain in this chapter, are also stable against the fission instability proposed in Refs. [18, 19, 20, 23]. In the next section, we will use those stable strangelets to estimate the possible integrated (over baryon numbers) intensity of strangelets in the vicinity of the solar system.

## 4.5. Discussion

In this section, we mainly aim at the debris produced due to possible collisions between SSs that may be a major source of strangelets in GCR [9, 15, 48, 49]. Earlier in Chap. 2, we attempted to estimate the integrated (sum over baryon numbers) intensity of those strangelets in GCR by employing a diffusion approximation [50] and considering the limit  $m_s \rightarrow 0$ . In this section, we will use the same diffusion approximation and try to improve upon the estimate by incorporating the effects of finite  $m_s$  and a wider range of permissible

#### 4. An improved fragment distribution for unpaired SQM

---

values of bag constant. We assume strangelets, possibly produced in merger of binary SS having a merger rate  $\sim 10^{-5} \text{ yr}^{-1}$  [15, 51] in each Galaxy, spread homogeneously in a galactic halo of radius  $\sim 10 \text{ kpc}$  [9] within their galactic confinement time. Therefore, an approximate intensity of strangelets of the  $i^{\text{th}}$  species in the solar neighborhood can be written, as in Ref. [25] (see also Eq. (2.7)),

$$I(A^i) \sim 5 \times 10^{-48} \omega^i \text{ particles m}^{-2} \text{ sr}^{-1} \text{ yr}^{-1}. \quad (4.16)$$

Here, numerical values of  $\omega^i$  have been determined in Sec. 4.3 using the thermodynamic properties of strangelets and satisfying the conditions of charge-neutrality and the baryon number conservation in the strangelet-complex.

Table 4.1.: Expected ranges of the integrated (over baryon number) intensity of stable strangelets in the solar neighborhood for different intervals of plausible bag values and for the corresponding ranges of the (tentatively) estimated tidally released mass per SS merger. The estimations of ejected masses are inspired by the recent simulations [15] of SS mergers in binary systems in which the limit of mass-resolution was  $\sim 10^{-5} M_{\odot}$  [21].

$B^{1/4}$ (MeV)	$\mu_b$ (MeV)	Mass of strange matter released per SS merger ( $M_{\odot}$ )	Estimated integrated intensity of stable strangelets (particles $\text{m}^{-2} \text{sr}^{-1} \text{yr}^{-1}$ )
145	$\approx 284$	$\sim 10^{-4}$	$\sim (2 - 5) \times 10^4$
(146 - 150)	$\approx (286 - 294)$	$\sim (0.01 - 1.0) \times 10^{-4}$	$\sim (2 - 500) \times 10^2$
(151 - 158)	$\approx (296 - 309)$	$\sim (0.0 - 1.0) \times 10^{-6}$	$\sim (0 - 2) \times 10^2$

Approximation (4.16) provides only an order of magnitude estimate of integrated intensity of strangelets in GCR. In this section, we did not consider the important issue of the acceleration of the strangelets by the astrophysical shock waves and the dependence of diffusion coefficient on kinetic energies of the accelerated (by the shock wave) strangelets. A more rigorous estimate of flux of galactic strangelets will be provided in the next chapter by incorporating those effects. Moreover, the present estimate does not take the effects of possible interaction of strangelets with ISM (still now it is very poorly known) the ge-

omagnetic field and the solar modulation into consideration. The simulations find, for  $B^{1/4} \approx 145$  MeV, a population averaged tidally released mass  $M_{\text{ejected}} \approx 10^{-4} M_{\odot}$  per SS merger. The integrated intensity of galactic strangelets in the solar neighborhood is estimated from the approximation (4.16) by considering all the values of  $\omega^i$  for all the stable ( $A^i \gtrsim 11$ ) fragments as obtained from the results displayed in Figs. 4.2 and 4.4. The estimated values of this intensity lie within the range  $\sim (2 - 5) \times 10^4$  particles  $\text{m}^{-2} \text{sr}^{-1} \text{yr}^{-1}$ . These results depend on the formation temperature of the strangelets. Increment in the value of bag constant within the range  $145 \text{ MeV} < B^{1/4} \lesssim 158 \text{ MeV}$  has a significant effect. In that case, the results of recent numerical simulations of coalescence of SSs indicate that the average tidally released mass per SS merger would be within the range  $10^{-4} M_{\odot} > M_{\text{ejected}} \gtrsim 0$ . However, it should be noted that those simulations were performed only at two extreme ends of the aforesaid interval of the bag value. Hence, precise value of tidally ejected mass for any intermediate bag constant cannot be determined from those simulations. Such uncertainty notwithstanding, in Table 4.1 [21], we display the estimated ranges of integrated strangelet flux in the solar neighborhood for tentative ranges of values of the average mass ( $M_{\text{ejected}}$ ) released per SS merger corresponding to different intervals of bag constants with the *caveat* that the amounts of ejected mass quoted in Table 4.1 for intermediate bag values are presented only for the sake of an illustration. The actual amount of this ejected mass for an intermediate bag value can only be determined through detailed high resolution simulations of SS merger for a number of bag values lying within the range  $145 \text{ MeV} < B^{1/4} < 158 \text{ MeV}$ . Such detailed high resolution simulations are yet to be performed. In Table 4.1, large dispersions in the estimated fluxes for different bag values actually reflect the limitation of the recent simulations in scanning the parameter space as well as the limited mass-resolution of the present simulations. They also indicate the theoretical uncertainty in predicting the formation temperature of the strangelets. In the case  $B^{1/4} \sim 158$  MeV, the simulated results predict that almost no mass would be ejected in SS merger which points out the vanishing strangelet flux in the solar neighborhood. On the other hand, for an assumed tidally ejected mass  $M_{\text{ejected}} \sim 10^{-6} M_{\odot}$  per stellar merger (that is an order of magnitude smaller than the limit of mass-resolution of the existing simulations), the approximation (4.16), yields an integrated flux  $\sim 1$  particle  $\text{m}^{-2} \text{sr}^{-1} \text{yr}^{-1}$  at a sufficiently low temperature ( $T \sim 1$  keV) at freeze-out in this particular case. Such

integrated flux is, in principle, measurable in the observations with the AMS-02 experiment at the present level of its sensitivity [52].

The ultimate vindication of SMH would depend on the detection of strangelets in GCR. In this section, we have studied a plausible model of the rate of injection of strangelets in the Galaxy. A more sophisticated galactic propagation model for the strangelets is required to arrive at a definite conclusion of strangelet-flux in GCR for AMS-02 [52] and other potential experiments.

## Bibliography

- [1] C.E. DeTar and J.F. Donoghue, *Ann. Rev. Nucl. Part. Sc.* **33**, 235 (1983).
- [2] J. Madsen, *Phys. Rev. D* **50**, 3328 (1994).
- [3] R.M. Barnett *et al.* (Particle Data Group), *Phys. Rev. D* **54**, 1 (1996); J.J. Broderick *et al.*, *Astrophys. Jour.* **492**, L71 (1998); D.E. Groom *et al.* (Particle Data Group), *Eur. Phys. Jour. C* **15**, 1 (2000); A. W. Steiner, S. Reddy, and M. Prakash, *Phys. Rev. D* **66**, 094007 (2002); M. Alford and Q. Wang, *Jour. Phys. G: Nucl. Part. Phys.* **32**, 63 (2006); P. Maris and P.C. Tandy, *Nucl. Phys. B (Proc. Supp.)* **161**, 136 (2006).
- [4] B. Blossier *et al.* [ETM Collaboration], *Phys. Rev. D* **82**, 114513 (2010); A. Bazavov *et al.* POS LATTICE2010, 083 (2010); S. Durr *et al.*, *Phys. Lett. B* **701**, 265 (2011); S. Durr *et al.*, *Jour. High Energy Phys.* **1108**, 148 (2011); Y. Aoki *et al.* [RBC and UKQCD Collaboration], *Phys. Rev. D* **83**, 074508 (2011); C.T.H Davies *et al.* [HPQCD Collaboration] *Phys. Rev. Lett.* **104**, 132003 (2010); C. McNeile *et al.* *Phys. Rev. D* **82**, 034512 (2010); A.V. Manohar and C.T. Sachrajda (Particle Data Group), <http://pdg.lbl.gov/2011/reviews/rpp2011-rev-quark-masses.pdf>.
- [5] J. Beringer *et al.* (Particle Data Group), *Phys. Rev. D* **86**, 010001 (2012) and (2013), partial update for the 2014 edition (URL:<http://pdg.lbl.gov>); K.A. Olive *et al.* (Particle Data Group), *Chin. Phys. C* **38**, 090001 (2014).
- [6] E. Farhi and R.L. Jaffe, *Phys. Rev. D* **30**, 2379 (1984).
- [7] M.S. Berger and R.L. Jaffe, *Phys. Rev. C* **35**, 213 (1987); M.S. Berger, *Phys. Rev. D* **40**, 2128 (1989); L. Paria, A. Abbas, and M.G. Mustafa, *Int. Jour. Mod. Phys. E* **9**, 149 (2000).
- [8] E.P. Gilson and R.L. Jaffe, *Phys. Rev. Lett.* **71**, 332 (1993).
- [9] J. Madsen, *Physics and Astrophysics of Strange Quark Matter*, edited by J. Cleykens, *Lecture Notes in Physics Vol. 516* (Springer, Heidelberg, 1999) p. 162, arXiv:9809032v1 [astro-ph].

- [10] L.F. Palhares and E.S. Fraga, Phys. Rev. D **82**, 125018 (2010); M.B. Pinto, V. Koch, and J. Randrup, Phys. Rev. C **86**, 025203 (2012).
- [11] B. Lee, *Chiral Dynamics* (Gordon and Breach, New York, 1972).
- [12] J.K. Boomsma and D. Boer, Phys. Rev. D **80**, 034019 (2009).
- [13] L. Paulucci and J.E. Horvath, Phys. Lett. B **733**, 164 (2014).
- [14] J. Madsen, Phys. Rev. Lett. **92**, 119002-1 (2004).
- [15] A. Bauswein *et al.*, Phys. Rev. Lett. **103**, 011101 (2009); A. Bauswein, R. Oechslin, and H.-T. Janka, Phys. Rev. D **81**, 024012 (2010).
- [16] H. Heiselberg, Phys. Rev. D **48**, 1418 (1993).
- [17] R. Jensen, *Searches for Strange Quark Matter*: Masters Thesis, University of Aarhus, Denmark, 2006. <https://dcwww.fysik.dtu.dk/robertj/speciale.pdf>.
- [18] M.G. Alford, K. Rajagopal, S. Reddy, and A.W. Steiner, Phys. Rev. D **73**, 114016 (2006).
- [19] M.G. Alford and D.A. Eby, Phys. Rev. C **78**, 045802 (2008).
- [20] M.G. Alford, S. Han, and S. Reddy, Jour. Phys G: Nucl. Part. Phys. **39**, 065201 (2012).
- [21] S. Biswas, J.N. De, P. S. Joarder, S. Raha, and D. Syam, [arXiv:1409.8366v5 (2015)].
- [22] M. Alford and K. Rajagopal, Jour. High Energy Phys. **06**, 031 (2002).
- [23] P. Jaikumar, S. Reddy, and A.W. Steiner, Phys. Rev. Lett. **96**, 041101 (2006).
- [24] S. Biswas, A. Bhadra, J.N. De, P.S. Joarder, S. Raha, and D. Syam, Proc. Sci. ICRC 2015 504 (2016).
- [25] S. Biswas, J.N. De, P.S. Joarder, S. Raha, and D. Syam, Phys. Lett. B **715**, 30 (2012).

- [26] J.P. Bondorf, A.S. Botvina, A.S. Iljinov, I.N. Mishustin, and K. Sneppen, Phys. Rep. **257**, 133 (1995).
- [27] S. Biswas, J.N. De, P. S. Joarder, S. Raha, and D. Syam, Proc. Indian Natn. Sci. Acad. **81** No.1, 277 (2015).
- [28] S. Biswas, J.N. De, P.S. Joarder, S. Raha, and D. Syam, Proceedings of the 33rd International Cosmic Rays Conference (2013) [ISBN: 978-85-89064-29-3].
- [29] J. Madsen, in *Strangeness in Hadronic Matter*, AIP Conf. Proc. **340**, 32 (1995) [arXiv:9502242 (hep-ph)].
- [30] R. Balian and C. Bloch, Ann. Phys. (NY) **60**, 401 (1970).
- [31] M.G. Mustafa and A. Ansari, Phys. Rev. D **53**, 5136 (1996).
- [32] Yu.E. Pokrovsky, Sov. Jour. Nucl. Phys. **50**, 565-566 (1989), Yad. Fiz. **50**, 907-909 (1989).
- [33] W. Weise, Progress of Theoretical Physics, Supplement; (no.149); Jul 2003; p. 1-19; Chiral 02: YITP-RCNP workshop on chiral restoration in nuclear medium; Kyoto (Japan); 7-9 Oct 2002.
- [34] S. Hartmann in: M. Morgan and M. Morrison (eds.), *Models as Mediators* (Cambridge Univ. Press, Cambridge, UK), 1999, p. 326; S. Hartmann, Studies in History and Philosophy of Modern Physics B **32**, 267 (2001); S. Hartmann in: N. Shanks (ed.) *Idealization in Contemporary Physics* (Rodopy, Amsterdam, The Netherlands), 1998, p. 99.
- [35] R. Friedberg and T.D. Lee, Phys. Rev. D **18**, 2623 (1978); R. Bhaduri, *Models of the Nucleon. From Quarks to Solitons* (Levant Books, Kolkata, India, reprinted in 2002).
- [36] J. Madsen, Phys. Rev. Lett. **70**, 391 (1993).
- [37] Y.B. He, C.S. Gao, X.Q. Li, and W.Q. Chao, Phys. Rev. C **53**, 1903 (1996).

- [38] G. Ladonisi, G. Cantele, and M.L. Chiofalo, *Introduction to Solid State Physics and Crystalline Nanostructures*, Springer (2014); S.H. Simon, *Oxford Solid State Basics*, Oxford (2013).
- [39] E.E. Salpeter, *Astrophys. Jour.* **134**, 669 (1961).
- [40] N.K. Glendenning, *Compact Stars: Nuclear Physics, Particle Physics, and General Relativity*, second edition (Springer, New York, 2000).
- [41] J. Randrup and S.E. Koonin, *Nucl. Phys. A* **471**, 355c (1987); B.S. Meyer, *Ann. Rev. Astron. Astrophys.* **32**, 153 (1994); A.S. Botvina and I.N. Mishustin, *Eur. Phys. Jour. A* **30**, 121 (2006).
- [42] D.H.E. Gross, *Rep. Prog. Phys.* **53**, 605 (1990).
- [43] S. Pal, S.K. Samaddar, and J.N. De, *Nucl. Phys. A* **608**, 49 (1996); J.N. De and S.K. Samaddar, *Phys. Rev. C* **76**, 044607 (2007).
- [44] I. Mardor and B. Svetitsky, *Phys. Rev. D* **44**, 878 (1991); M.B. Christiansen and N.K. Glendenning, *Phys. Rev. C* **56**, 2858 (1997).
- [45] J.N. De, S.K. Samaddar, and B.K. Agrawal, *Phys. Lett. B* **716**, 361 (2012); B.K. Agrawal, D. Bandyopadhyay, J.N. De, and S.K. Samaddar, *Phys. Rev. C* **89**, 044320 (2014).
- [46] L. Paulucci and J.E. Horvath, *Phys. Rev. C* **78**, 064907 (2008).
- [47] S. Rosswog and M. Bruggen, *Introduction to High Energy Astrophysics* (Cambridge, England, 2007).
- [48] J. Madsen, *Jour. Phys. G: Nucl. Part. Phys.* **28**, 1737 (2002).
- [49] J. Madsen, *Phys. Rev. D* **71**, 014026-(1-9) (2005).
- [50] V.L. Ginzburg and S.I. Syrovatskii, *The Origin of Cosmic Rays* (Pargamon, England, 1964).

- [51] K. Belczynski *et al.*, *Astrophys. Jour. Lett.* **680**, L129 (2008).
- [52] A. Kounine (AMS-02 Collaboration), in *XVI International Symposium on Very High Energy Cosmic Ray Interactions* (ISVHECRI 2010), Batavia, IL, USA [[arXiv:1009.5349v1.pdf](#) (astro-ph.HE)].

## Chapter 5

# Estimation of flux of galactic strangelets in the solar neighborhood

In each of the previous chapters (ie., Chap. 2. - Chap. 4), we have estimated an order of magnitude of the integrated intensity (ie., the sum of the intensity of each stable strangelet of all possible baryon numbers) of galactic strangelets with the help of simple diffusion approximation. The diffusion coefficient in those cases does not depend on kinetic energies of the strangelets. In this chapter, our goal is to obtain a more realistic estimate of the flux (ie., the kinetic energy dependence of flux) of galactic strangelets in the solar neighborhood which would be useful for the ongoing and future experiments involved in the search of strangelets in GCR. For such estimate, we need to take into account the acceleration of the strangelets at the site of the SS merger in the binary stellar system and the propagation of those accelerated strangelets in the ISM. In Sec. 5.1 of this chapter, we will consider the first order Fermi acceleration and the standard diffusive propagation of strangelets in the ISM. Results are shown in Sec. 5.2. Sec. 5.3 contains the discussion part.

### 5.1. Acceleration and propagation of galactic strangelets

In the previous chapter (ie., Chap. 4), we have seen that strangelets carry positive charges (see Eq. (4.7)). Due to this characteristic, strangelets may be compared with CR. Being

## 5. Estimation of flux of galactic strangelets in the solar neighborhood

---

charged particles, CR move along the randomly oriented magnetic field lines in the ISM which would re-enter in the vicinity of the accelerating site of CR due to which CR interact with the SN shock front and they are accelerated by the SN shock following first order Fermi acceleration mechanism [1, 2] (see also the brief discussion in Sec. 1.3 of Chap. 1). Finally, such accelerated CR propagate far away from their site of acceleration following the randomly oriented magnetic field lines in the ISM. Similar to CR, the strangelet-fragments, after originating from the SS merger events, are expected to undergo first-order Fermi acceleration mechanism by interacting with shock wave produced either directly from the SS collisions or from the collision of the tidally ejected mass with its surrounding ISM [3]. Shock waves, thus generated, are likely to be relativistic as indicated by the observations of the gamma ray bursts (GRBs) \* [4] that are believed to occur in the mergers of two compact stellar objects. Typically, 1 – 10% of the shock energy is considered to be used for CR acceleration [7, 8] in SNe shocks. Since strangelets are heavier (ie., more massive) than protons, we will consider lower (ie., 1%) conversion efficiency (ie., 1% of the shock energy is used for acceleration) for our calculation. Due to lack of observations and simulations of coalescence of SSs, we have considered that 1% of the shock energy  $\sim 10^{49}$  ergs (lower limit of the ejected kinetic energy as obtained in the simulations of binary NS mergers) [9] is used for the acceleration purpose of the strangelets produced in each binary SS merger. The resultant energy spectrum of all the strangelets, summed over their species, is expected to be a power law  $d\mathcal{N}(\mathcal{E})/d\mathcal{E} = \mathcal{N}_o\mathcal{E}^{-\alpha}$  [3]. Here,  $\mathcal{N}(\mathcal{E})d\mathcal{E}$  is the (assumed) number of strangelets with their kinetic energies being in the range  $[\mathcal{E}, \mathcal{E} + d\mathcal{E}]$  with  $\mathcal{N}_o$  being a normalization constant. The spectral index, for lower kinetic energies (ie., the kinetic energy range of GCR; see Sec. 1.3 of Chap. 1), is assumed to have a value around  $\alpha \approx 2.2$  [3, 10] in this chapter. We, further, consider the propagation of these accelerated strangelets through the ISM by taking into account a standard diffusive propagation model.

In the standard diffusive propagation model, we need to consider the diffusive transport of the strangelets from a source (ie., SSs in a binary stellar system), located at a position  $\vec{r}_{so} = (x_{so}, y_{so}, z_{so})$  (ie., the position coordinate of the site of the merger event or simply the position coordinate of the compact remnant existing after the merger event and it is

---

\*GRBs are considered as the extremely energetic explosions and possibly the brightest electromagnetic events which are known to occur in the universe [5]. These events can last from ten milliseconds to several hours [6].

## 5. Estimation of flux of galactic strangelets in the solar neighborhood

---

assumed to be a point-like source for the sake of simplification), that injects strangelet spectrum (ie., the spectrum is assumed to follow a power-law distribution after shock acceleration), at a time  $t_{so}$ . Hence, the diffusive transport equation for  $i^{\text{th}}$  species can be written as [8]

$$\frac{\partial n_{st}^i}{\partial t} = \nabla^i \left[ D^i \nabla^i n_{st}^i \right] - \Gamma_{sp}^i n_{st}^i + \mathcal{N}_{st}^i \delta(t - t_{so}) \delta^3(\vec{r}^i - \vec{r}_{so}), \quad (5.1)$$

where,  $t$ ,  $n_{st}^i$ ,  $\vec{r}^i$  and  $\Gamma_{sp}^i$  are any arbitrary time, the number density and the position vector of accelerated strangelets and the rate of spallation <sup>†</sup> of  $i^{\text{th}}$  species respectively. The injection spectrum of  $i^{\text{th}}$  species is denoted as  $\mathcal{N}_{st}^i = \frac{dN^i}{d\mathcal{E}^i} = \frac{\mathcal{E}_0 \omega^i}{6 \sum_i \epsilon_{\min}^i \omega^i} (\mathcal{E}^i)^{-2.2}$  (see Eq. (D.8) in Appendix D). Here,  $\epsilon_{\min}^i = \frac{1}{2} m_0^i \beta_{\min}^2$  [3] with  $\beta_{\min} = v_{\min}/c = 0.15$  ( $c$  is the speed of light) [3, 9], for the minimum initial speed ( $v_{\min}$ ) at which the strangelets are injected in the Galaxy.  $m_0^i$  denotes the rest mass energy (here it is taken in GeV unit) of the strangelet of  $i^{\text{th}}$  species which is same as  $E^i$  in Eq. (4.9), Chap. 4. Along with this,  $\mathcal{E}^i$  and  $\omega^i$  are the kinetic energy and multiplicity (see Eq. (4.4) in Chap. 4) of  $i^{\text{th}}$  species respectively.  $\mathcal{E}_0$  is considered as the effective kinetic energy used by the shock waves to accelerate the strangelets. For our calculation, we have considered  $\mathcal{E}_0 = 6.25 \times 10^{49}$  GeV (ie., 1% of the  $10^{49}$  erg [9]; 1 erg = 625 GeV). In Eq. (5.1), we have used the energy dependent diffusion coefficient,  $D^i = 3 \times 10^{28} \left( \frac{\mathcal{E}^i}{1 \text{ GeV } Z^i} \right)^{0.5}$  cm<sup>2</sup>/s [11] which is assumed to be spatially constant and  $\mathcal{E}^i = \sqrt{(\mathcal{R}^i)^2 (Z^i e)^2 + (m_0^i)^2} - m_0^i$ , where, rigidity ( $\mathcal{R}^i$ , in unit of GV) for a particular charged species ( $Z^i$ ) is  $\mathcal{R}^i = \frac{m_0^i}{Z^i e} \frac{\beta^i}{\sqrt{1 - (\beta^i)^2}}$  ( $e$  is the magnitude of the electronic charge) with  $v^i (= \beta^i c)$  being their (assumed) speed in the vicinity of the Sun.

Our Galaxy can roughly be described as a cylindrical disc with a thickness of about  $\sim 600$  pc which is much shorter than its radius  $R_d \sim 15$  kpc (1 kpc = 1000 pc =  $3.08 \times 10^{21}$  cm). For the diffusive transport of strangelets, we may also assume a cylindrical diffusion region (including the galactic plane) of radius  $R_d$  and half-height  $H$  [12] (see Fig. 5.1 [12]). We further assume that the diffusion coefficient is constant in that cylindrical region [8]. We have also considered that strangelets can escape only through the upper and lower boundaries of the cylindrical region which can be modelled by assuming  $n_{st}^i = 0$  at  $z^i =$

---

<sup>†</sup>A process in which CR interact with the matter of ISM or with other CR and light elements such as lithium, boron etc. are produced. For strangelets, spallation process is poorly known.

## 5. Estimation of flux of galactic strangelets in the solar neighborhood

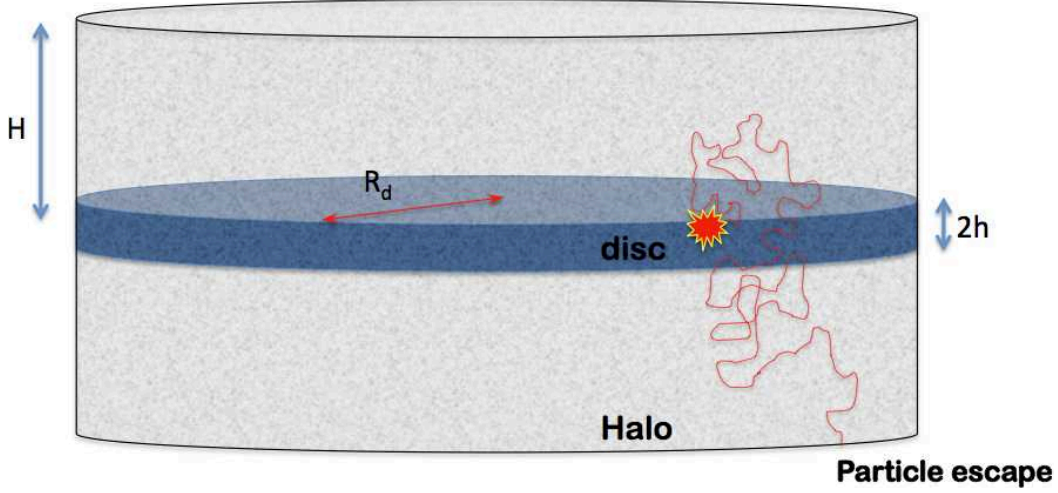


Figure 5.1.: A model to study the propagation of strangelets in the Milky Way Galaxy [12]. In the schematic diagram,  $H$  and  $h$  are half-height of the cylinder and half-thickness of the central plane respectively.

$\pm H$  [8] and the escape flux of strangelets through the surfaces  $z^i = \pm H$  is denoted by  $D^i \frac{\partial n_{st}^i}{\partial z^i} |_{z^i = \pm H}$  [8].

The free Green function (ie., without considering any boundary conditions) of Eq. (5.1) can be written as [8]

$$\mathcal{G}_{free}^i(\vec{r}^i, t; \vec{r}_{so}, t_{so}) = \frac{\mathcal{N}_{st}^i}{[4\pi D^i \tau]^{3/2}} \exp(-\Gamma_{sp}^i \tau) \exp\left[-\frac{(\vec{r}^i - \vec{r}_{so})^2}{4D^i \tau}\right], \quad (5.2)$$

where,  $\tau = t - t_{so}$ . The actual Green function, ie., the Green function that satisfies the correct boundary condition at  $z^i = \pm H$ , can be evaluated by using the method of image charges and can be denoted as [8]

$$\begin{aligned} \mathcal{G}^i(\vec{r}^i, t; \vec{r}_{so}, t_{so}) &= \frac{\mathcal{N}_{st}^i}{[4\pi D^i \tau]^{3/2}} \exp(-\Gamma_{sp}^i \tau) \exp\left[-\frac{(x^i - x_{so})^2 + (y^i - y_{so})^2}{4D^i \tau}\right] \\ &\quad \times \sum_{n=-\infty}^{n=+\infty} (-1)^n \exp\left[-\frac{(z^i - z'_n)^2}{4D^i \tau}\right], \end{aligned} \quad (5.3)$$

where,  $z'_n = (-1)^n z_{so} + 2nH$  are related to the  $z$  coordinates of the image sources and  $n$

being the number of image sources.

## 5.2. Estimation of flux of galactic strangelets

For our case, we have considered that all sources of strangelets, ie., SSs in the binary stellar systems, are located over the galactic disc (ie.,  $z_{so} = 0$ ) [3]. Due to lack of observational evidence and experimental data, it is very difficult to predict the actual distribution of the sources of strangelets. For the sake of simplicity, we have taken the homogeneous model ie., we have considered that sources of strangelets are distributed uniformly over the galactic disc. Along with, we ignore the spallation of strangelets. As we are going to consider only stable strangelets and interactions of strangelets with normal nuclei are still very poorly known, we can ignore spallation for the first calculation. The differential flux (ie., the number of strangelets per unit area, time, kinetic energy and solid angle) (at the center of the disc) of (stable) strangelets of  $i^{\text{th}}$  species obtained from the merger of binary SSs with a merger rate  $\mathcal{R}_m$  is the following (using Eq. (5.3) and Refs. [3, 8])

$$\Phi_{st}^i = \frac{\beta^i c}{4\pi} \int_0^\infty d\tau \int_0^{R_d} dr^i \frac{2\pi r^i}{\pi R_d^2} \frac{\mathcal{N}_{st}^i \mathcal{R}_m}{[4\pi D^i \tau]^{3/2}} \exp\left[-\frac{(r^i)^2}{4D^i \tau}\right] \sum_{n=-\infty}^{n=+\infty} (-1)^n \exp\left[-\frac{(2nH)^2}{4D^i \tau}\right]. \quad (5.4)$$

In Eq. (5.4),  $\tau$  is the confinement time for the strangelets in the Milky Way Galaxy which is quite large such as  $10^6$  to  $10^7$  years if taken as the same to that of GCR. So, the upper (integration) limit of  $\tau$  may be taken as infinity without causing any significant error as  $\mathcal{G}^i(\vec{r}^i, t; \vec{r}_{so}, t_{so})$  decreases sharply with  $\tau$ . After carrying out the integration on  $\tau$  first and then on  $r^i$ , Eq. (5.4) becomes [8]

$$\Phi_{st}^i = \frac{\beta^i c}{4\pi} \frac{\mathcal{N}_{st}^i \mathcal{R}_m}{[2\pi D^i R_d]} \sum_{n=-\infty}^{n=+\infty} (-1)^n \left[ \sqrt{1 + \left(\frac{2nH}{R_d}\right)^2} - \sqrt{\left(\frac{2nH}{R_d}\right)^2} \right]. \quad (5.5)$$

For  $H \ll R_d$ , the sum over  $n$  gives  $\sim H/R_d$  [8] and Eq. (5.5) becomes

$$\Phi_{st}^i = \frac{\beta^i c}{4\pi} \frac{\mathcal{N}_{st}^i \mathcal{R}_m}{2\pi R_d^2} \frac{H}{D^i}. \quad (5.6)$$

## 5. Estimation of flux of galactic strangelets in the solar neighborhood

---

As  $\int \Phi_{st}^i d\mathcal{E}^i$  denotes the integral flux (ie., the number of strangelets per unit area, time, and solid angle but above some threshold kinetic energy or rigidity), therefore, integral flux of  $i^{\text{th}}$  species can be written as

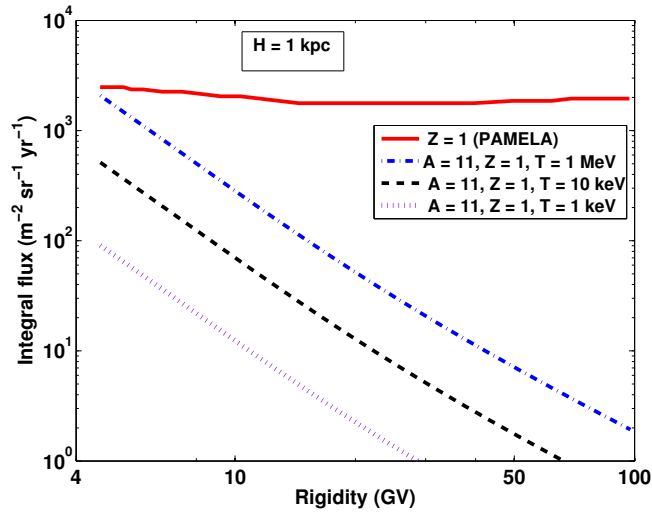
$$\mathcal{I}^i = 2.85 \frac{\omega^i}{\sum_i \epsilon_{\min}^i \omega^i} (Z^i)^{1.5} \left( \frac{H}{R_d} \right) \times \int_{\mathcal{R}_{\min}^i}^{\mathcal{R}_{\max}^i} (\beta^i)^2 (\Lambda^i)^{-2.7} d\mathcal{R}^i \text{ cm}^{-2} \text{sr}^{-1} \text{yr}^{-1} \quad (5.7)$$

$$= 2.85 \times 10^4 \frac{\omega^i}{\sum_i \epsilon_{\min}^i \omega^i} (Z^i)^{1.5} \left( \frac{H}{R_d} \right) \times \int_{\mathcal{R}_{\min}^i}^{\mathcal{R}_{\max}^i} (\beta^i)^2 (\Lambda^i)^{-2.7} d\mathcal{R}^i \text{ m}^{-2} \text{sr}^{-1} \text{yr}^{-1}, \quad (5.8)$$

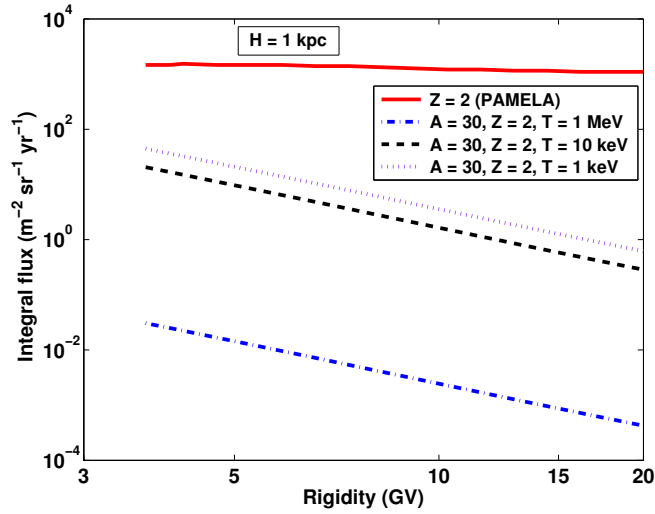
where,  $c$ , in Eq. (5.7), is in unit of cm/s and  $\mathcal{R}_m \approx 10^{-6} \text{yr}^{-1}$  [13]. The half height can be considered to be  $H \sim 0.3 - 1$  kpc [14] (ie.,  $H \ll R_d$  limit is valid) and  $\Lambda^i = \left( \frac{\mathcal{R}^i Z^i e}{\beta^i} - m_0^i \right)$ . The minimum rigidity for any  $Z^i$  can be represented as  $\mathcal{R}_{\min}^i = \frac{1}{Z^i e} \sqrt{\left( \mathcal{E}_{\min}^i \right)^2 + 2m_0^i \mathcal{E}_{\min}^i}$ , where,  $\mathcal{E}_{\min}^i$  is the minimum kinetic energy of  $i^{\text{th}}$  strangelet and for any species of strangelet  $\mathcal{R}_{\max}^i = \mathcal{R}_{\max} = 10^3$  GV [15]. The initial value of the  $\mathcal{R}_{\min}^i$ , for a particular  $Z^i$  and  $A^i$ , can be calculated by setting  $\mathcal{E}_{\min}^i = 1$  GeV.  $\mathcal{R}_{\min}^i$  is then varied and  $\mathcal{I}^i$  is calculated for particular value of  $Z^i$  and  $A^i$ . Although the strangelet flux, given in Eqs. (5.7) and (5.8), is evaluated at the centre of the galactic disc, it is to be expected that the diffusive system would ultimately attain a steady state at which the time averaged strangelet fluxes from all the sources on the galactic plane would be equal at all the points on that plane.

In Figs. 5.2(a,b) and 5.3(a,b), we have compared the estimated integral fluxes ( $\mathcal{I}^i$ ) of strangelets (formed at three different temperatures at freeze-out, namely,  $T = 1$  MeV,  $T = 10$  keV and  $T = 1$  keV) with the possible upper limits of the integral fluxes (with 95% confidence level [15]) obtained from the PAMELA [15] experiment for two different values of  $H$ , the baryon numbers ( $A^i$ ) and the corresponding values of  $Z^i$ . The  $A^i$  for each  $Z^i$  is chosen such that it is stable for the temperature range we have considered here and has maximum multiplicity ( $\omega^i$ ) for the corresponding  $Z^i$  at each  $T$  so that we can obtain maximum integral flux for the corresponding  $Z^i$ . The multiplicities at different temperatures are calculated by using Eq. (4.4) (see Chap. 4) by considering  $B^{1/4} = 145$  MeV,  $m_s = 95$  MeV and average mass ejection  $\sim 10^{-4} M_{\odot}$ . Only at  $T = 1$  MeV, the maximum integral flux at lowest rigidity for  $A^i = 11$ ,  $Z^i = 1$  and  $H = 1$  kpc (as shown in Fig 5.2(a)) is very close to the upper limit of integral flux as reported by PAMELA. Otherwise for both

5. Estimation of flux of galactic strangelets in the solar neighborhood



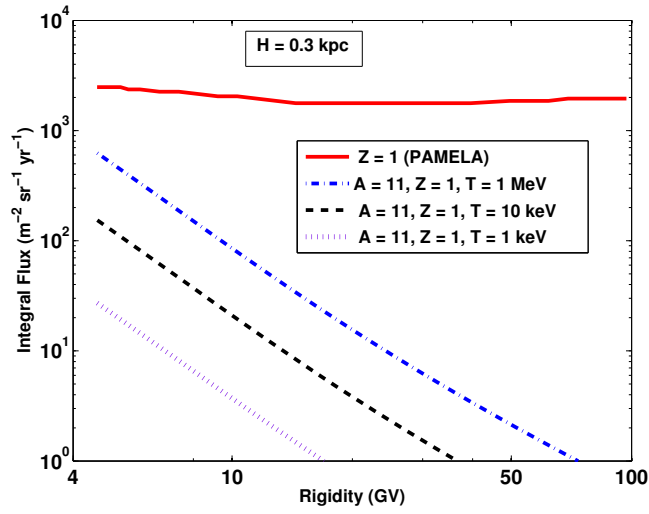
(a)



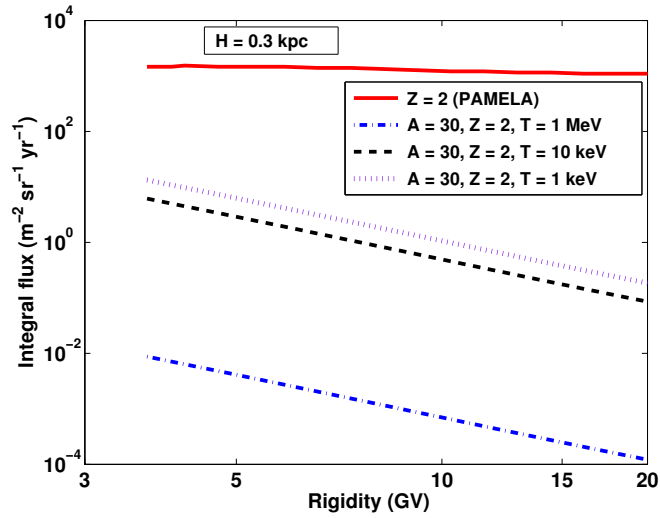
(b)

Figure 5.2.: Integral flux vs. rigidity of the strangelet-fragments with  $B^{1/4} = 145$  MeV and  $m_s = 95$  MeV that are formed at three different temperatures at freeze-out. Comparisons with PAMELA results [15] are displayed for (a)  $A = 11$ ,  $Z = 1$  and  $H = 1$  kpc, and for (b)  $A = 30$ ,  $Z = 2$  and  $H = 1$  kpc.

5. Estimation of flux of galactic strangelets in the solar neighborhood



(a)



(b)

Figure 5.3.: Integral flux vs. rigidity of the strangelet-fragments with  $B^{1/4} = 145$  MeV and  $m_s = 95$  MeV that are formed at three different temperatures at freeze-out. Comparisons with PAMELA results [15] are displayed for (a)  $A = 11$ ,  $Z = 1$  and  $H = 0.3$  kpc, and for (b)  $A = 30$ ,  $Z = 2$  and  $H = 0.3$  kpc.

the values of  $H$ , the theoretical integral fluxes for  $A^i = 11, Z^i = 1$  and  $A^i = 30, Z^i = 2$  are found to fall below the possible upper limit of the (integral) flux of the strangelet which is reported recently from the null observations of strangelets with the PAMELA detector system. We have also checked the integral fluxes for other  $Z^i (= 3 \text{ to } 8)$  values and we have obtained that such fluxes are also below the upper limits of (integral) fluxes of strangelets as given in Ref. [15]. Our results, presented in this section, seem, therefore, to justify the null results obtained from the PAMELA experiment [15]. The theoretical estimates of the integral flux also indicate that the integral fluxes for  $T = 1 \text{ MeV}, A^i = 30, Z^i = 2$  and for both the values of  $H$  are quite below the sensitivity limit (ie.,  $1 \text{ particle m}^{-2}\text{sr}^{-1}\text{yr}^{-1}$  [16]) of AMS-02. But for the other two temperatures and the same set of  $A^i$  and  $Z^i$  integral fluxes go below the sensitivity limit of AMS-02 at the higher rigidities (see Figs. 5.2(b) and 5.3(b)). On the other hand, integral fluxes, at various temperatures, for  $A^i = 11, Z^i = 1$  are within the sensitivity limit of AMS-02 for a broad range of rigidity as shown in the Figs. 5.2(a) and 5.3(a).

### 5.3. Discussion

Previously, J. Madsen estimated the (differential and integral) flux of strangelets considering the acceleration and propagation of strangelets [10]. But, he assumed that all the strangelets, produced in the merger of binary SSs, have the same size (or, baryon number) which is an oversimplified assumption [10]. In this chapter, we have estimated the flux of strangelets using the size (or, baryon number) distribution, as obtained in Chap. 4, at the site of merger along with the Fermi acceleration mechanism and the diffusive propagation model. In this present work, we have used the Green's function formalism to describe the propagation of strangelets from their sources. The sources, in the formalism, are modelled as discrete point-like sources in space and time with a spatial distribution [8]. However, in our final calculation, we have considered the homogeneous distribution of sources as the source distribution of SSs in the binary stellar systems is not well established. Our calculation, as presented in this chapter, is meant for the Milky Way Galaxy, but the same procedure is applicable for any other Galaxy if possibly having binary SS systems.

In Chap. 4, we have seen that the stability of strangelet decreases (see Fig. 4.4) with

## 5. Estimation of flux of galactic strangelets in the solar neighborhood

---

the increase in bag value. For  $B^{1/4} = 158$  MeV, the stable (at least stable than nucleon) strangelets have  $A^i \gtrsim 90$  and  $Z^i \gtrsim 4$ . Numerical simulations of coalescence of SSs predict that the mass ejection in binary SS merger for much higher bag value is quite small or nothing. Hence, we mainly presented the integral fluxes for  $B^{1/4} = 145$  MeV for which the estimated average mass ejection is  $10^{-4}M_{\odot}$  <sup>‡</sup>. The results, shown in this chapter, however, do not depend on the amount of the ejected mass as the ratio of the numerator and the denominator of  $\frac{\omega^i}{\sum_i \epsilon_{min}^i \omega^i}$  remains same for different mass ejection, and for a fixed value of bag and  $\beta_{min}$ .

In our calculation, we, however, do not take into account spallation, solar modulation, <sup>§</sup> and geomagnetic rigidity cut-off <sup>¶</sup>. Normally, spallation and solar modulation will suppress the flux of strangelets at lower kinetic energies or rigidities. As the effect of solar modulation dominates highly in the kinetic energy range of  $\sim 1$  GeV or below, we have considered  $\mathcal{E}_{min}^i \gtrsim 1$  GeV. From the point of view of diffusive propagation model, the calculation in this chapter may be close to GALPROP [17] or similar galactic propagation codes if we include spallation model for strangelets and a boundary condition such that free escape may happen at some finite radius along the lateral sides of the cylinder [8]. Hence, the diffusive propagation model, presented here, may be further improved by using more sophisticated galactic propagation models incorporating the spallation, solar modulation and geomagnetic rigidity cut-off. However, considering the fact that the PAMELA observations were mostly conducted during the period of minimum solar activity time cycle (ie., solar modulation is not significant), the Eqs. (5.7) and (5.8) give a reasonable approximation of the integral flux of strangelets. Hence, our results are consistent with the null result as obtained by PAMELA collaboration. The integral flux which we have estimated in this chapter can be treated as the flux at the top of the atmosphere (TOA). We would further consider the propagation of strangelets, using the flux at the TOA, through the Earth's

---

<sup>‡</sup>We have checked the integral fluxes for  $A^i = 90$ ,  $Z^i = 4$ ,  $B^{1/4} = 158$  MeV and ejected mass of  $10^{-4}M_{\odot}$ , keeping the other parameters same as denoted in this chapter. Such integral fluxes are well below the upper limit of integral fluxes as reported in Ref. [15].

<sup>§</sup>GCR flux, at the outskirts of the solar system, is modulated due to interaction with solar wind (ie., GCR are scattered by the magnetic field frozen in the solar wind plasma) which is originated from the corona of the Sun. This phenomenon is known as solar modulation. This type of modulation would also happen for strangelets.

<sup>¶</sup>This is a quantitative measure of the shielding against charged particles which is provided by the Earth's magnetic field.

## *5. Estimation of flux of galactic strangelets in the solar neighborhood*

---

atmosphere which would provide an estimate of the flux of strangelets at the mountain altitude or at the sea level (see also the discussion in Chap. 6). Such estimated values of flux would also be useful for ground-based detectors which are searching strangelets in the atmospheric CR. It is, therefore, expected that present results would serve as a benchmark for further theoretical calculations and will be useful for AMS-02 and other future experiments with more sensitive and sophisticated detectors which may detect strangelets and ultimately vindicate the SMH.

## Bibliography

- [1] E. Fermi, *Phys. Rev.* **75**, 1169 (1949).
- [2] T. K. Gaisser, *Cosmic Rays and Particle Physics*, Cambridge University Press, Cambridge, England (1990).
- [3] S. Biswas, A. Bhadra, J.N. De, P. S. Joarder, S. Raha, and D. Syam, *Proc. Sci. ICRC 2015*, 504 (2016).
- [4] D.A. Frail *et al.*, *Nature* **389**, 261 (1997); J. Goodman, *New Astron.* **2**, 449 (1997).
- [5] [http://missionscience.nasa.gov/ems/12\\_gammarays.html](http://missionscience.nasa.gov/ems/12_gammarays.html).
- [6] B. Gendre *et al.*, *Astrophys. Jour.* **766**, 30 (2013); J.F. Graham and A. S. Fruchter, *Astrophys. Jour.* **774** (2), 119 (2013).
- [7] W.I. Axford *et al.*, in *Proc. 15th International Cosmic Ray Conference*, Plovdiv, Bulgaria, **11**, 132 (1977); E. A. Helder *et al.*, *Astrophys. Jour.* **719**, L140 (2010), erratum *Astrophys. Jour.* **737**, L46 (2011).
- [8] P. Blasi and E. Amato, *Jour. Cosm. Astropart. Phys.* **1201**, 010 (2012).
- [9] K. Hotokezaka *et al.*, *Phys. Rev. D* **87**, 024001 (2013).
- [10] J. Madsen, *Phys. Rev. D* **71**, 014026-(1-9) (2005).
- [11] V.S. Berezhinsky, in R.J. Protheroe (Ed.), *Proc. 21st International Cosmic Ray Conference*, Adelaide, Australia, **11**, 115 (1990).
- [12] [http://fermi.gsfc.nasa.gov/science/mtgs/summerschool/2012/week1/CR3\\_Blasi.pdf](http://fermi.gsfc.nasa.gov/science/mtgs/summerschool/2012/week1/CR3_Blasi.pdf).
- [13] V. Kalogera *et al.*, *Phys. Rep.* **442**, 75 (2007); K. Belczynski *et al.*, *Astrophys. Jour.* **680**, L129 (2008).
- [14] H.W.R.J. Bovy, *Astron. Astrophys. Rev.* **21**, 61 (2013).
- [15] O. Adriani *et al.* (PAMELA collaboration), *Phys. Rev. Lett.* **115**, 111101 (2015).

- [16] A. Kounine (AMS-02 Collaboration), in *XVI International Symposium on Very High Energy Cosmic Ray Interactions* (ISVHECRI 2010), Batavia, IL, USA. [arXiv:1009.5349v1.pdf (astro-ph.HE)].
- [17] R. Trotta *et al.*, *Astrophys. Jour.* **729**, 106 (2011) [arXiv: 1011.0037].

## Chapter 6

### Summary and future outlook

The existence of SQM, a theorized ground state of strongly interacting matter, is still a mystery. For more than three decades, after E. Witten put forward the conjecture about SQM, experimentalists are searching for the signature of SQM, but apart from a few unusual events, no conclusive evidence has been found yet. Still, SQM, a novel form of matter, is a fascinating and intriguing subject for research as the stable SQM has several important consequences in astrophysics. Moreover, ongoing experiments such as PAMELA and AMS-02 with sophisticated detectors have been searching for strangelets, small lumps of SQM, in GCR. Hence, in the present context, it is important to investigate the possible production scenario of galactic strangelets and estimate the flux of such galactic strangelets in the solar neighborhood that would be useful for the ongoing as well as for the upcoming experiments which are the key motivations behind this thesis.

The entire work of this thesis is based on the SMH which would support the possible existence of SSs in compact binary stellar systems. A brief overview on compact stars has been outlined at the beginning of the thesis. Most of the events which support the (possible) existence of strangelets were obtained in the experiments related to CR. Hence, a preliminary idea about CR and the possible connection between CR and strangelets has also been discussed in the introductory chapter. Basic properties of bulk SQM and strangelets (both unpaired and CFL) are also discussed within the framework of MIT bag

model. In the present work, our main focus is on the astrophysical production of unpaired and CFL strangelets which may arise due to subsequent fragmentation of ejected matter in binary SS and CFLS-NS mergers, respectively. Various experiments involved in the search for these exotic particles (ie., strangelets) and the events with unusual  $Z/A$  (ie., charge to baryon number ratio), a distinguishable signature for strangelets, are also discussed here. In that chapter, we have introduced the SMM that has been adopted by us to study the fragmentation of SQM. Actually, we have used the SMM to obtain the plausible mass spectrum of strangelets originated at the different sites of the binary SS mergers.

In Chap. 2, we have implemented SMM in SQM system to derive the mass spectrum (or, size distribution) of astrophysical strangelets with the simplified assumption that all quark flavors are massless. Numerical simulations of coalescence of SSs predict a fraction of SQM, a self-bound matter, would possibly be ejected from the tip of the spiral arms originated in such merger events. Subsequent fragmentation of such gravitationally unbound ejecta (ie., ejected SQM) has been studied by invoking the SMM. In that chapter, we have considered a standard bag value, ie.,  $B^{1/4} = 145$  MeV, and shown the variation of multiplicities of strangelets with the baryon numbers for the plausible available volumes and for a wide range of temperatures which would possibly be attained by strangelet-fragments at the freeze-out. We have inferred that lighter (or, lower baryon number) fragments are increased in number with the increase in temperature which is a very common scenario in cases when SMM is applied to explain the experimental data of nuclear collision experiments. The results for the variation of multiplicities with the baryon numbers for different available volumes are also consistent with the results obtained in cases of nuclear fragmentation. The plot of energy per baryon vs. baryon number shows the stability of strangelets which originate from the fragmentation of ejected SQM in binary SS mergers. Along with this, we have also estimated an order of magnitude of the integrated intensity of stable galactic strangelets near the vicinity of the Sun using the simple diffusion approximation and the results are consistent with the previous prediction.

Chap. 3 is related to the fragmentation of CFL SQM (with the assumption of massless quarks) which possibly originates from the merger of CFLS and NS in a binary system. CFL SQM is more stable than normal SQM due to the Cooper-like pairing between quarks of different flavors and colors and for that reason the upper stability limit of bag value

for CFL SQM would be higher than the predicted value of normal (or, unpaired) SQM. In that chapter, we have studied the fragmentation patterns using the quantum statistical expressions of SMM rather than classical one which was used in Chap. 2. In that chapter, we have also discussed the production scenario of CFL SQM and shown the variation of multiplicity with baryon number for different parameters such as temperatures at freeze-out, different bag values, and gap parameters (pairing energy gaps). In a recent work, L. Paulucci *et al.* [1] showed the fragmentation patterns of CFL SQM which were dissimilar to those obtained in Chap. 2 and they suggested that the incorporation of color flavor locking in the calculations might be the cause of different behavior of the fragmentation patterns. But, we did not find any drastic change in the nature of the mass spectrum of CFL strangelets. The fragmentation patterns related to the variation of fragment size distributions with temperatures are similar to the patterns obtained in Chap. 2. We have also compared the fragment size distributions coming from quantum statistical expressions and approximate classical (or, Maxwell-Boltzmann) expression, and we have seen that the results do not differ very much, and we can apply expression of classical approximation for the temperature range we have considered in this work. However, a point should be noted that the coalescence between a CFLS and its companion NS is quite uncertain as the possibility of NS turning into a CFLS may not be ruled out. In that case, both CFLS may collapse to BH without spewing any CFL SQM in the ISM which indicates a very little or no mixture of CFL strangelets in GCR. Considering such uncertainty regarding the production of CFL strangelets, we did not further discuss the formation of CFL strangelets or estimate the tentative flux of CFL strangelets in this thesis.

In Chap. 4, we have tried to obtain a more realistic mass spectrum of strangelets. Unlike the previous two chapters, in that chapter we have taken the finite mass of strange quarks (ie.,  $m_s$ ) into account whereas the up and down quarks are still considered to be massless. Finite mass of  $s$  quarks introduces the surface tension, finite charge and Coulomb energy terms in the system. Surface tension and Coulomb energy terms try to destabilize the system by increasing the energy per baryon of the system. Hence, stability analysis of strangelets is quite important for estimation of the possible flux of strangelets in the solar neighborhood as only stable strangelets are considered to contribute in the estimation of flux. In that chapter, we have considered the same scenario, as discussed in Chap. 2, for the

production of astrophysical strangelets and fragmentation of SQM is obtained by invoking the SMM. We have also discussed the necessary modifications, due to finite  $m_s$ , needed for the adoption of SMM in our system. In that chapter, available volume is not taken as a free parameter; rather it has been calculated self-consistently by satisfying the global charge-neutrality and baryon number conservation in the strangelet-complex. The mass spectra of strangelets for different temperatures at freeze-out are displayed in that chapter. Mass spectra for different bag values are also shown there. The patterns of the mass spectra for the variation of temperatures are similar to the patterns obtained in Chap. 2 and Chap. 3. Hence, we can substantially conclude that the patterns of the fragment size distributions for the variation of temperatures do not substantially depend on  $m_s$  and type (ie., CFL or unpaired) of the strangelets. The stability of the strangelet fragments is then discussed, and integrated intensity of the stable strangelets, using the diffusion approximation, is also estimated in that chapter.

In Chap. 5, we have tried to obtain a more realistic estimate of the flux of galactic strangelets. In that chapter, we have also compared our results with the upper bounds of fluxes of strangelets as reported by PAMELA collaboration. For our calculations, we have compared the strangelets with CR. We have obtained the integral flux of galactic strangelets by using the first order Fermi acceleration mechanism and the standard diffusive propagation model. In that standard diffusive propagation model, we have used a diffusion coefficient that depends on the kinetic energy of the strangelet. We have also considered that strangelets, produced due to fragmentation of SQM (we have used the mass spectra of strangelets which we have obtained in Chap. 4), are accelerated by the shock waves generated in binary SS mergers and they attain a power-law spectrum. Those accelerated strangelets will further propagate through the ISM of the Milky Way, and we have estimated the integral flux of stable galactic strangelets in the solar neighborhood by solving the diffusive transport equation. For the estimates, we do not take spallation, solar modulation, and geomagnetic rigidity cut-off into account. The theoretical estimates are then compared with the upper limits of integral fluxes of strangelets reported by PAMELA collaboration. The comparisons show that our estimated fluxes for different  $Z$  (ie., charge) values are consistent with the recent findings of the PAMELA experiment. Moreover, the results would also be useful for the ongoing AMS-02 and other future experiments.

In a nutshell, we can say that in this work we have provided a possible production scenario of astrophysical strangelets and tried to obtain a more realistic mass spectrum (or, baryon number distribution) at the site of the binary SS mergers. With the help of that mass spectrum, and using Fermi first order acceleration mechanism and the standard diffusive propagation model, we have estimated the integral flux of stable galactic strangelets. Such estimated integral flux is then compared with the upper limit of the integral flux of strangelets as obtained by PAMELA which is based on the null detection of strangelets. The comparisons of our theoretical estimates with the results of PAMELA indicate that our theoretical estimates are consistent with the results reported by PAMELA and hopefully these would also be useful for the prediction of the flux of strangelets in AMS-02.

The possible modifications and the future extensions of our work are stated below.

- We have used the standard MIT bag model for the present work which is based on the asymptotic freedom and confinement of quarks in the hadrons. However, it does not incorporate the effects of dynamical (or, explicit) chiral symmetry breakdown in QCD vacuum (see the discussion in Sec. 4.2 of Chap. 4). One of the possible extensions of our work is to study the bulk properties of unpaired and CFL SQM and also the strangelets by using more sophisticated theoretical models of hadrons such as chirally invariant bag models [2]. Moreover, the mass spectrum of strangelets would also be studied by invoking SMM in these more advanced models.
- In the standard diffusive propagation model (as discussed in Chap. 5) we did not take into account the spallation, solar modulation, and geomagnetic cut-off. For spallation, we need to study the plausible interaction processes of strangelets with ordinary nuclei which are still not well known. The authors in Ref. [3] have outlined some plausible interaction processes of strangelets with ordinary nuclei. Hence, Ref. [3] would be the starting point to obtain useful interaction processes during the propagation of strangelets through ISM. Solar modulation and geomagnetic cut-off are studied in Ref. [4]. A possible spallation model for strangelets, solar modulation, and geomagnetic cut-off would, therefore, improve the present propagation (through ISM) model (see Chap. 5) of strangelets and more refined flux of strangelets would then be achieved.

- We have already calculated the integral fluxes of strangelets at the TOA. Hence, our present work can be extended further by considering the propagation of those strangelets (ie., the strangelets those reached at the TOA after being accelerated from the site of the SS merger and propagated through ISM) in the Earth's atmosphere. For such purpose, a model for the propagation of strangelets through the Earth's atmosphere has to be constructed by incorporating a model of possible interactions of strangelets [3] with the Earth's atmosphere and considering all the previous propagation (through the Earth's atmosphere) models [5, 6]. Using this improved propagation model the flux of strangelets would then be estimated that would be useful for ground-based detectors such as the PET detector used by the researchers at Bose Institute in their project (see Sec. 1.7.1.2 of Chap. 1) to search strangelets in atmospheric CR.
- Numerical simulations [7] of coalescence of SSs in a compact binary stellar system indicate that the characteristic frequency of gravitational wave emitted by SS mergers may be considered as a signal that may distinguish SS merger events from NS mergers. Numerical simulations also show that the maximum frequency during the inspiral phase and the frequency of the ringdown of the postmerging remnant are higher [7] for coalescence of SSs in comparison to NSs. The current gravitational wave detectors such as Laser Interferometer Gravitational-Wave Observatory (LIGO) [8] and VIRGO [9] and the upcoming detectors like Einstein telescope [10] and DUAL detector [11] are sensitive enough to detect the characteristic frequency of the gravitational wave that has been predicted in the simulation results. Hence, these highly sophisticated detectors may find out the actual source of the gravitational wave ie., whether it is originated due to SS merger or NS merger.

Finally, we can conclude that the results presented by us in this thesis could be taken as a guide for future theoretical calculations. These results would also be useful for ongoing experiments such as PAMELA, AMS-02 and for future experiments, involved in search of strangelets in GCR, which would ultimately vindicate the SMH.

## Bibliography

- [1] L. Paulucci and J.E. Horvath, Phys. Lett. B **733**, 164 (2014).
- [2] Yu.E. Pokrovsky, Sov. Jour. Nucl. Phys. **50**, 565 (1989); Yad. Fiz. **50**, 907 (1989); R. Friedberg and T.D. Lee, Phys. Rev. D **18**, 2623 (1978); R. Bhaduri, *Models of the Nucleon. From Quarks to Solitons*, Levant Books, Kolkata, India (reprinted in 2002).
- [3] L. Paulucci and J.E. Horvath, Jour. Phys. G: Nucl. Part. Phys. **36**, 095202 (2009).
- [4] J. Madsen, Phys. Rev. D **71**, 014026 (1-9) (2005).
- [5] S. Banerjee, S.K. Ghosh, S. Raha, and D. Syam, Jour. Phys. G **25**, L15 (1999).
- [6] S. Banerjee, *Some Aspects of Strange Matter In Astrophysics*, Ph.D. Thesis, Jadavpur University, India, 2003 [arXiv: 1408.6389 (astro-ph.HE)]; F. Wu, R.X. Xu, and B.Q. Ma, Jour. Phys. G: Nucl. Part. Phys. **34**, 597 (2007).
- [7] A. Bauswein, R. Oechslin, and H.-T. Janka, Phys. Rev. D **81**, 024012 (2010).
- [8] B. Abbott *et al.* (LIGO Scientific), Rep. Prog. Phys. **72**, 076901 (2009).
- [9] F. Acernese *et al.*, Class. Quant. Grav. **23**, S635 (2006).
- [10] <http://www.et-gw.eu/>.
- [11] <http://www.dual.lnl.infn.it/>.

## Appendix A

### Calculations of thermodynamic quantities ( $m_s = 0$ )

The content of this appendix is based on the Ref. J. Madsen, in: J. Cleymens (Ed.), *Lecture Notes in Physics: Physics and Astrophysics of Strange Quark Matter*, vol. **516**, Springer Verlag, Heidelberg, 1999, p. 162, arXiv: 9809032v1(astro-ph), (1998).

#### A.1. Standard thermodynamic quantities of strangelets ( $m_s = 0$ )

In Chap. 2, we have assumed that all quark flavors are massless and the chemical potential of each quark flavor is same, ie.,  $\mu_q$ . Along with we have also considered that the number of quarks of each flavor is same in a strangelet. With these assumptions, we can write down the following thermodynamic quantities of the strangelets.

The thermodynamic potential of  $i^{\text{th}}$  species is given by

$$\begin{aligned} \Omega^i = & -[(19\pi^2/36)T^4 + (3/2)\mu_q^2 T^2 + (3/4\pi^2)\mu_q^4]V^i \\ & + [(41/72)T^2 + (3/8\pi^2)\mu_q^2]C^i + BV^i. \end{aligned} \tag{A.1}$$

---

**A. Calculations of thermodynamic quantities ( $m_s = 0$ )**

---

Total number of quarks in  $i^{\text{th}}$  species is

$$\sum_f N_f^i = 3A^i = [3\mu_q T^2 + (3/\pi^2)\mu_q^3]V^i - (3/4\pi^2)\mu_q C^i, \quad (\text{A.2})$$

where,  $N_f^i$  denotes the number of quarks of  $f^{\text{th}}$  flavor in  $i^{\text{th}}$  species and  $A^i$  is the baryon number of  $i^{\text{th}}$  species. Here,  $\sum_f N_f^i = -\left(\frac{\partial\Omega^i}{\partial\mu_q}\right)_{T,V^i}$ . The expressions for Helmholtz free energy and total energy of  $i^{\text{th}}$  species are

$$F^i = \Omega^i + \sum_f N_f^i \mu_q, \quad (\text{A.3})$$

and

$$E^i = F^i + T\mathcal{S}^i = \Omega^i + \sum_f N_f^i \mu_q + T\mathcal{S}^i, \quad (\text{A.4})$$

where,  $\mathcal{S}^i = -\left(\frac{\partial\Omega^i}{\partial T}\right)_{\mu_q,V^i}$  is the entropy of the  $i^{\text{th}}$  species. The condition for mechanical equilibrium is  $P_{\text{ext}} = 0 = -\left(\frac{\partial\Omega^i}{\partial V^i}\right)_{T,\mu_q}$ , where,  $P_{\text{ext}}$  is the external pressure. The condition for mechanical equilibrium gives

$$\begin{aligned} BV^i &= [(19\pi^2/36)T^4 + (3/2)\mu_q^2 T^2 + (3/4\pi^2)\mu_q^4]V^i \\ &\quad - [(41/216)T^2 + (1/8\pi^2)\mu_q^2]C^i. \end{aligned} \quad (\text{A.5})$$

Using Eq. (A.5), Eq. (A.1) can be written as

$$\Omega^i = [(41/108)T^2 + (1/4\pi^2)\mu_q^2]C^i. \quad (\text{A.6})$$

## A.2. Analytical approach to estimate the range of $\mu_q$

At  $T = 0$ , Eq. (A.5) becomes

$$\begin{aligned}
 BV^i &= (3/4\pi^2)\mu_q^4 V^i - (1/8\pi^2)\mu_q^2 C^i \\
 \Rightarrow \left[(1/8\pi^2)\mu_q^2\right] 8\pi R^i &= \left[(3/4\pi^2)\mu_q^4 - B\right] \frac{4\pi}{3} (R^i)^3 \\
 \Rightarrow R^i &= \sqrt{\frac{3\mu_q^2}{4\pi^2} \frac{1}{\left(\frac{3\mu_q^4}{4\pi^2} - B\right)}}, \tag{A.7}
 \end{aligned}$$

where,  $R^i$  is the radius of the strangelet of  $i^{\text{th}}$  species. Using Eq. (A.7), Eq. (A.6) (at  $T = 0$ ) can be written as

$$\Omega^i = \frac{2\mu_q^2}{\pi} \frac{1}{\sqrt{\mu_q^2 - \frac{4\pi^2 B}{3\mu_q^2}}}. \tag{A.8}$$

Now, the total number of quarks in a strangelet must be positive which implies (from Eq. A.8)

$$\begin{aligned}
 &-\frac{\partial \Omega^i}{\partial \mu_q} > 0 \\
 \Rightarrow -\frac{1}{\pi \left(\mu_q^2 - \frac{4\pi^2 B}{3\mu_q^2}\right)^{3/2}} 2 \left[\mu_q^3 - \frac{4\pi^2 B}{\mu_q}\right] &> 0. \tag{A.9}
 \end{aligned}$$

The condition in Eq. (A.9) holds for

$$\begin{aligned}
 -\left[\mu_q^3 - \frac{4\pi^2 B}{\mu_q}\right] &> 0 \\
 \Rightarrow \mu_q &< \left(4\pi^2\right)^{1/4} B^{1/4}, \tag{A.10}
 \end{aligned}$$

*A. Calculations of thermodynamic quantities ( $m_s = 0$ )*

---

and

$$\begin{aligned} \left(\mu_q^2 - \frac{4\pi^2 B}{3\mu_q^2}\right)^{3/2} &> 0 \\ \Rightarrow \mu_q &> \left(\frac{4\pi^2}{3}\right)^{1/4} B^{1/4}. \end{aligned} \tag{A.11}$$

From Eqs. (A.10) and (A.11), we obtain

$$1.9B^{1/4} \text{ MeV} < \mu_q < 2.5B^{1/4} \text{ MeV}. \tag{A.12}$$

## Appendix B

### Calculation of Fermi & Bose integrals

#### B.1. Expressions of Fermi and Bose integrals used in the expression of multiplicity

From Eqs. (1.4) and (1.5) (Sec. 1.9, Chap. 1), we can write

$$\sum_{j=0}^{\infty} g_j^i J_{1/2}^{\pm}(\eta_j^i) = \sum_{j=0}^{\infty} g_j^i \int_0^{\infty} \frac{(x^i)^{1/2}}{e^{(x^i - \eta_j^i)} \pm 1} dx^i. \quad (\text{B.1})$$

---

*B. Calculation of Fermi & Bose integrals*

For low  $T$  and  $\eta_j^i < 0$ ,  $(x^i - \eta_j^i) \gg 1$ . Eq. (B.1) can be written as

$$\begin{aligned}
\sum_{j=0}^{\infty} g_j^i J_{1/2}^{\pm}(\eta_j^i) &\approx \sum_{j=0}^{\infty} g_j^i \int_0^{\infty} (x^i)^{1/2} e^{-(x^i - \eta_j^i)} dx^i \\
&= \sum_{j=0}^{\infty} g_j^i \int_0^{\infty} (x^i)^{1/2} e^{-\left(x^i - \frac{(\mu^i - E_j^i)}{T}\right)} dx^i \\
&= \sum_{j=0}^{\infty} g_j^i \int_0^{\infty} (x^i)^{1/2} e^{-\left(x^i - \frac{[\mu^i - (E_0^i + E_j^{*i})]}{T}\right)} dx^i \\
&= \sum_{j=0}^{\infty} g_j^i e^{-\frac{E_j^{*i}}{T}} \int_0^{\infty} (x^i)^{1/2} e^{-\left(x^i - \frac{(\mu^i - E_0^i)}{T}\right)} dx^i \\
&= \sum_{j=0}^{\infty} g_j^i e^{-\frac{E_j^{*i}}{T}} \int_0^{\infty} (x^i)^{1/2} e^{-(x^i - \eta_0^i)} dx^i \\
&\approx J_{1/2}^{\pm}(\eta_0^i) \phi^i(T).
\end{aligned} \tag{B.2}$$

For low  $T$  and  $\eta^i < 0$ ,  $(x^i - \eta^i) \gg 1$ . Fermi and Bose integrals can be written as

$$\begin{aligned}
J_{1/2}^{\pm}(\eta^i) &\approx \int_0^{\infty} (x^i)^{1/2} e^{-(x^i - \eta^i)} dx^i \\
&= \int_0^{\infty} (x^i)^{1/2} e^{-\left(x^i - \frac{(\mu^i - F^i)}{T}\right)} dx^i \\
&= \sum_{j=0}^{\infty} g_j^i e^{-\frac{E_j^{*i}}{T}} \int_0^{\infty} (x^i)^{1/2} e^{-\left(x^i - \frac{(\mu^i - E_0^i)}{T}\right)} dx^i \\
&\approx J_{1/2}^{\pm}(\eta_0^i) \phi^i(T).
\end{aligned} \tag{B.3}$$

## B.2. Mathematical expressions of Bose & Fermi integrals

Reference: E. W. Ng, C. J. Devine and R. F. Tooper, *Math. Comp.* **23**, 639 (1969).

Integral representation of Bose-Einstein function (of order  $p$ ) can be written as

$$B_p(\psi, u') = \frac{1}{\Gamma(p+1)} \int_0^{u'} \frac{x^p}{e^{x-\psi} - 1} dx, \quad (\text{B.4})$$

where,  $\psi$  and  $u'$  may be complex. Now,

$$B_p(\psi) \equiv \lim_{u' \rightarrow \infty} B_p(\psi, u'). \quad (\text{B.5})$$

For  $\psi < 0$ ,

$$B_p(\psi) = \sum_{k'=1}^{\infty} \frac{e^{k'\psi}}{(k')^{p+1}}. \quad (\text{B.6})$$

Bose integral can be written as

$$J_p^-(\psi) = \Gamma(p+1)B_p(\psi). \quad (\text{B.7})$$

Relation between polylogarithm function  $Li_p(\psi)$  and  $B_p(\psi)$  is

$$Li_p(\psi) = B_{p-1}(\ln\psi). \quad (\text{B.8})$$

If  $p \rightarrow p+1$  and  $\psi \rightarrow e^\psi$ , Eq. (B.8) becomes

$$B_p(\psi) = Li_{p+1}(e^\psi). \quad (\text{B.9})$$

Hence, the Bose integral can be written as

$$J_p^-(\psi) = \Gamma(p+1)Li_{p+1}(e^\psi). \quad (\text{B.10})$$

Similarly, Fermi integral can be written as

$$J_p^+(\psi) = \Gamma(p+1) \left[ Li_{p+1}(e^\psi) - \frac{1}{2^p} Li_{p+1}(e^{2\psi}) \right]. \quad (\text{B.11})$$

For  $p = 1/2$ , Bose and Fermi integrals become

$$J_{1/2}^-(\psi) = \Gamma(3/2) Li_{3/2}(e^\psi) \quad (\text{B.12})$$

and

$$J_{1/2}^+(\psi) = \Gamma(3/2) \left[ Li_{3/2}(e^\psi) - \frac{1}{\sqrt{2}} Li_{3/2}(e^{2\psi}) \right] \quad (\text{B.13})$$

respectively.

### B.3. MATLAB codes for calculation of Bose & Fermi integrals

Listing of three MATLAB codes, namely `bose_int.m`, `fermi_int.m` and `polylog.m`, are provided. `bose_int.m` and `fermi_int.m` calculate the Fermi and Bose integrals with the help of `polylog.m` code.

#### ★ bose\_int.m

```
1 % The program is bose_int.m
2 % To calculates the Bose integral using polylog.m
3 clc
4 format long
5 nn = -200.0:0.04:-0.001;
6 b = 3/2;
7 n = exp(nn);
8 y = polylog(b,n);
9 g = gamma(b).*y
10 be = [nn;g];
11 fid = fopen('Bose_integral_table.txt','w');
12 fprintf(fid, '%10.8e %10.8e\n',be);
13 fclose(fid);
```

#### ★ fermi\_int.m

```
1 % The program is fermi_int.m
```

```
2 % To calculates the Fermi integral using polylog.m
3 clc
4 format long
5 nn=-200.0:0.04:-0.001;
6 b=3/2;
7 n1=exp(nn);
8 y = polylog(b,n1);
9 r1= y;
10 n2=exp(2.0.*nn);
11 y = polylog(b,n2);
12 r2=y;
13 g = gamma(b)*(r1 - (r2/2^(1/2)))
14 fe=[nn;g];
15 fid = fopen('Fermi_integral_table.txt','w');
16 fprintf(fid,'%10.8e %13.11e\n',fe);
17 fclose(fid);
```

### ★ polylog.m

Ref.: <https://in.mathworks.com/matlabcentral/fileexchange/37229-enhanced-computation-of-polylogarithm-aka-de-jonquieres-function/content/polylog.m>

```
1 % Function file polylog.m
2 function [y errors] = polylog(n,z)
3 %% polylog - Computes the n-based polylogarithm of z: Li_n(z)
4 % Approximate closed form expressions for the Polylogarithm aka
   de
5 % Jonquiere's function are used. Computes reasonably faster than
   direct
6 % calculation given by  $\text{SUM}_{\{k=1 \text{ to } \text{Inf}\}}[z^k / k^n] = z + z^2/2^n$ 
   + ...
7 %
8 % Usage: [y errors] = PolyLog(n,z)
9 %
```

## B. Calculation of Fermi & Bose integrals

---

```
10 % Input:  z < 1    : real/complex number or array
11 %          n > -4  : base of polylogarithm
12 %
13 % Output: y          ... value of polylogarithm
14 %          errors   ... number of errors
15 %
16 % Approximation should be correct up to at least 5 digits for |z|
    > 0.55
17 % and on the order of 10 digits for |z| <= 0.55!
18 %
19 % Please Note: z vector input is possible but not recommended as
    precision
20 % might drop for big ranged z inputs (unresolved Matlab issue
    unknown to
21 % the author).
22 %
23 % following V. Bhagat, et al., On the evaluation of generalized
24 % Bose Einstein and Fermi Dirac integrals , Computer Physics
    Communications ,
25 % Vol. 155, p.7, 2003
26 %
27 % v3 20120616
28 %


---


29 % Copyright (c) 2012, Maximilian Kuhnert
30 % All rights reserved.
31 %
32 % Redistribution and use in source and binary forms, with or
    without
```

## *B. Calculation of Fermi & Bose integrals*

---

33 % modification , are permitted provided that the following  
conditions are  
34 % met:  
35 %  
36 %     Redistributions of source code must retain the above  
copyright  
37 %     notice , this list of conditions and the following  
disclaimer .  
38 %     Redistributions in binary form must reproduce the above  
copyright  
39 %     notice , this list of conditions and the following  
disclaimer in the  
40 %     documentation and/or other materials provided with the  
distribution .  
41 %  
42 % THIS SOFTWARE IS PROVIDED BY THE COPYRIGHT HOLDERS AND  
CONTRIBUTORS "AS  
43 % IS" AND ANY EXPRESS OR IMPLIED WARRANTIES, INCLUDING, BUT NOT  
LIMITED TO,  
44 % THE IMPLIED WARRANTIES OF MERCHANTABILITY AND FITNESS FOR A  
PARTICULAR  
45 % PURPOSE ARE DISCLAIMED. IN NO EVENT SHALL THE COPYRIGHT HOLDER  
OR  
46 % CONTRIBUTORS BE LIABLE FOR ANY DIRECT, INDIRECT, INCIDENTAL,  
SPECIAL,  
47 % EXEMPLARY, OR CONSEQUENTIAL DAMAGES (INCLUDING, BUT NOT LIMITED  
TO,  
48 % PROCUREMENT OF SUBSTITUTE GOODS OR SERVICES; LOSS OF USE, DATA,  
OR  
49 % PROFITS; OR BUSINESS INTERRUPTION) HOWEVER CAUSED AND ON ANY  
THEORY OF

## B. Calculation of Fermi & Bose integrals

---

```
50 % LIABILITY, WHETHER IN CONTRACT, STRICT LIABILITY, OR TORT (
    INCLUDING
51 % NEGLIGENCE OR OTHERWISE) ARISING IN ANY WAY OUT OF THE USE OF
    THIS
52 % SOFTWARE, EVEN IF ADVISED OF THE POSSIBILITY OF SUCH DAMAGE.
53 %


---


54
55 if nargin~=2
56     errors=1;
57     error(' [Error in: polylog function] Inappropriate number of
        input arguments! ')
58 end
59
60 if (isreal(z) && sum(z(:)>=1)>0) % check that real z is not
    bigger than 1
61     errors=1;
62     error(' [Error in: polylog function] |z| > 1 is not allowed')
63 elseif isreal(z)~=1 && sum(abs(z(:))>1)>0 % check that imaginary
    z is defined on unit circle
64     errors=1;
65     error(' [Error in: polylog function] |z| > 1 is not allowed')
66 elseif n<=-4 % check that n is not too largely negative (see paper
    )
67     errors=1;
68     error(' [Error in: polylog function] n < -4 might be
        inaccurate')
69 end
70
71 % display more digits in Matlab terminal:
```

## B. Calculation of Fermi & Bose integrals

---

```

72 %format long
73
74 alpha = -log(z); % see page 12
75
76 % if |z| > 0.55 use Eq. (27) else use Eq. (21):
77 if abs(z) > 0.55
78     preterm = gamma(1-n) ./ alpha.^(1-n);
79     nominator = b(0) + ...
80         - alpha.*( b(1) - 4*b(0)*b(4)/7/b(3) ) + ...
81         + alpha.^2.*( b(2)/2 + b(0)*b(4)/7/b(2) - 4*b(1)*b(4)/7/b
            (3) ) + ...
82         - alpha.^3.*( b(3)/6 - 2*b(0)*b(4)/105/b(1) + b(1)*b(4)
            /7/b(2) - 2*b(2)*b(4)/7/b(3) );
83     denominator = 1 + alpha.*4*b(4)/7/b(3) +...
84         + alpha.^2.*b(4)/7/b(2) +...
85         + alpha.^3.*2*b(4)/105/b(1) +...
86         + alpha.^4.*b(4)/840/b(0);
87     y = preterm + nominator ./ denominator;
88 else
89     nominator = 6435*9^n.*S(n,z,8) - 27456*8^n*z.*S(n,z,7) + ...
90         + 48048*7^n*z.^2.*S(n,z,6) - 44352*6^n*z.^3.*S(n,z,5) +
            ...
91         + 23100*5^n*z.^4.*S(n,z,4) - 6720*4^n*z.^5.*S(n,z,3) +
            ...
92         + 1008*3^n*z.^6.*S(n,z,2) - 64*2^n*z.^7.*S(n,z,1);
93     denominator = 6435*9^n - 27456*8^n*z + ...
94         + 48048*7^n*z.^2 - 44352*6^n*z.^3 + ...
95         + 23100*5^n*z.^4 - 6720*4^n*z.^5 + ...
96         + 1008*3^n*z.^6 - 64*2^n*z.^7 + ...
97         + z.^8;
98     y = nominator ./ denominator;

```

```

99 end
100
101 % define b:
102     function out = b(i)
103         out = zeta(n-i);
104     end
105 % define S as partial sums of Eq. 12:
106     function out = S(n,z,j)
107         out =0;
108         for i=1:j
109             out = out + z.^i./i^n;
110         end
111     end
112     function [out] = zeta(x)
113         %% Zeta Function
114         % Eq. 18
115         % following V. Bhagat, et al., On the evaluation of
116             generalized
117             % Bose Einstein and Fermi Dirac integrals , Computer
118             Physics Communications,
119             % Vol. 155, p.7, 2003
120             %
121             % Usage: [out] = zeta(x)
122             % with argument x and summation from 1 to j
123             %
124             % MK 20120615
125
126     prefactor = 2^(x-1) / ( 2^(x-1)-1 );
127     numerator = 1 + 36*2^x*eta(x,2) + 315*3^x*eta(x,3) +
128         1120*4^x*eta(x,4) +...

```

## B. Calculation of Fermi & Bose integrals

---

```
126         + 1890*5^x*eta(x,5) + 1512*6^x*eta(x,6) + 462*7^x*eta
           (x,7);
127 denominator = 1 + 36*2^x + 315*3^x + 1120*4^x + 1890*5^x
           + 1512*6^x + ...
128         + 462*7^x;
129 out = prefactor * numerator / denominator;
130
131 function [out] = eta(x,j)
132     %% Eta Function
133     % Eq. 17 (partial sums)
134     % following V. Bhagat, et al., On the evaluation of
           generalized
135     % Bose Einstein and Fermi Dirac integrals, Computer
           Physics Communications,
136     % Vol. 155, p.7, 2003
137     %
138     % Usage: [out] = eta(x,j)
139     % with argument x and summation from 1 to j
140     %
141     % MK 20120615
142
143     out=0;
144     for k=1:j
145         out = out + (-1)^(k+1) ./ k.^x;
146     end
147 end
148 end
149 end
```

## Appendix C

# Debye screening and thermodynamic potential

### C.1. Debye screening in strangelet

This section is based on the Refs. R. Jensen, *Searches for Strange Quark Matter*: Masters Thesis, University of Aarhus, Denmark, 2006. <https://dcwww.fysik.dtu.dk/robertj/speciale.pdf>; H. Heiselberg, Phys. Rev. D **48**, 1418 (1993). Here, we would try to give a most simple description of Debye screening in strangelet.

In most of the cases, strangelet is considered to be uniformly charged ie., charge is uniformly distributed throughout the body of the strangelet. But such scenario is not consistent as a smooth distribution of charge would provide an electric field along the radial direction of the strangelet and that electric field would exert an electric force on each of the quark inside the strangelet. If the quarks are free to move inside the strangelet (ie., quarks behave like electrons in conductor), the quarks will move along the direction of the electric field. This motion of the quarks will continue until there is no net force on any of the quark. Generally, the final charge distribution inside the strangelet varies on a length scale which is termed as Debye screening length ( $\lambda_D$ ) of the strangelet. Hence, in this scenario strangelet behaves like a conductor with a charged skin (near the surface of the strangelet) of length  $\lambda_D$  and a neutral interior. The expression of Debye screening

length of the  $i^{\text{th}}$  species is the following

$$\lambda_D^{-2} = 4\pi \sum_f q_f^2 \left( \frac{\partial n_f^i}{\partial \mu_f^i} \right)_{n_{j,j \neq f}^i}, \quad (\text{C.1})$$

where,  $f$  indicates particular flavor (ie.,  $u$ ,  $d$  and  $s$ ) of the quark and  $j$  is a dummy index for flavor.  $n_f^i$  is the number density of quarks of  $f^{\text{th}}$  flavor in  $i^{\text{th}}$  species and  $q_f$  is the charge (in unit of  $e$ ) of the quark of  $f^{\text{th}}$  flavor. For the calculation, we consider  $\mu_f^i = \mu_q$ ,  $\frac{\partial n_u^i}{\partial \mu_q} = \frac{\partial n_d^i}{\partial \mu_q} = \frac{\partial n_s^i}{\partial \mu_q}$ ,  $T = 0$ , and ignore the surface and curvature contributions of strangelets. Now, we can write

$$\lambda_D^{-2} = \left( \frac{8\alpha}{\pi} \right) \mu_q^2. \quad (\text{C.2})$$

## C.2. An approach to calculate thermodynamic potential for

$$m_s \neq 0$$

The discussion in this section is based on the Refs. P.B. Pal , *An introductory course of statistical mechanics*, Narosa, India (2008); J. Madsen, in: J. Cleymens (Ed.), *Lecture Notes in Physics: Physics and Astrophysics of Strange Quark Matter*, vol. **516**, Springer Verlag, Heidelberg, 1999, p. 162, arXiv: 9809032v1(astro-ph), (1998).

In Chap. 4 we have used the expression of the thermodynamic potential of  $s$  flavor ( $m_s \neq 0$ ). The outline of the calculation is given here.

Thermodynamic potential of  $s$  flavor in  $i^{\text{th}}$  species can be written as

$$\Omega^i \Big|_{s \text{ flavor}} = -gT \int_0^\infty dk \frac{dN_s^i}{dk} \ln \left[ 1 + \exp \left( - (\varepsilon(k) - \mu_s) / T \right) \right], \quad (\text{C.3})$$

where,  $g$  is the degeneracy,  $k$  is the momentum, ie.,  $k = \sqrt{\varepsilon^2 - m_s^2}$ ,  $\varepsilon$  is the energy of  $s$

---

### C. Debye screening and thermodynamic potential

quarks.  $\frac{dN_s^i}{dk}$  is the density of states of  $s$  quarks in  $i^{\text{th}}$  species and it can be written as

$$\begin{aligned} \frac{dN_s^i}{dk} = & \frac{k^2}{2\pi^2} \mathcal{V}^i + \left[ -\frac{1}{8\pi} \left\{ 1 - \frac{2}{\pi} \tan^{-1} \left( \frac{k}{m_s} \right) \right\} \right] k \mathcal{S}^i \\ & + \frac{1}{12\pi^2} \left[ 1 - \frac{3k}{2m_s} \left\{ \frac{\pi}{2} - \tan^{-1} \left( \frac{k}{m_s} \right) \right\} \right] \mathcal{C}^i. \end{aligned} \quad (\text{C.4})$$

At low temperature limit, ie.,  $\frac{\mu_s - m_s}{T} \gg 1$ , thermodynamic quantities can be expressed as power series in temperature and only leading order temperature dependent terms can be kept.

Now, if the thermodynamic quantities (for  $s$  flavor) have the generic form like the following

$$I_0 = \int_{m_s}^{\infty} d\varepsilon \nu(\varepsilon) Q(\varepsilon), \quad (\text{C.5})$$

for some function  $Q$ , then after integration by parts we have

$$I_0 = \nu(\varepsilon) G(\varepsilon) \Big|_{m_s}^{\infty} - \int_{m_s}^{\infty} d\varepsilon \frac{d\nu}{d\varepsilon} G(\varepsilon), \quad (\text{C.6})$$

where,

$$G(\varepsilon) = \int_{m_s}^{\varepsilon} d\varepsilon' Q(\varepsilon'). \quad (\text{C.7})$$

In Eq. (C.6), the first term goes to zero as  $\nu(\varepsilon) = 0$  when  $\varepsilon \rightarrow \infty$  ( $\nu(\varepsilon)$  has the form of Fermi distribution function) and  $G = 0$  when  $\varepsilon = m_s$ . At low temperature limit,  $\frac{d\nu}{d\varepsilon}$  is non-zero only in a small region near  $\mu_s$ . Taylor series expansion of  $G(\varepsilon)$  can be written as

$$I_0 = - \int_{m_s}^{\infty} d\varepsilon \frac{d\nu}{d\varepsilon} \sum_{r'=0}^{\infty} \frac{1}{r'!} G^{(r')}(\mu_s) (\varepsilon - \mu_s)^{r'}, \quad (\text{C.8})$$

where,  $G^{(r')}(\mu_s) = \frac{d^{(r')}G(\varepsilon)}{d\varepsilon^{(r')}} \Big|_{\varepsilon=\mu_s}$ . Eq. (C.8) can be rewritten as

$$I_0 = \sum_{r'=0}^{\infty} \frac{1}{r'!} G^{(r')}(\mu_s) J_{r'}, \quad (\text{C.9})$$

### *C. Debye screening and thermodynamic potential*

---

where,

$$J_{r'} = - \int_{m_s}^{\infty} d\varepsilon \frac{d\nu}{d\varepsilon} (\varepsilon - \mu_s)^{r'}. \quad (\text{C.10})$$

Now,  $J_{r'}$  vanishes if  $r'$  is odd. For  $r' = 0$ ,  $J_0 = 1$ . For even  $r'$  Eq. (C.10) becomes

$$J_{r'} = 2T^{r'} \times \Gamma(r' + 1) \left(1 - \frac{1}{2^{r'-1}}\right) \sum_{\zeta=1}^{\infty} \frac{1}{\zeta^{r'}}, \quad (\text{C.11})$$

where,  $T$  is the temperature. We have calculated the volume, surface and curvature parts of thermodynamic potential for  $m_s \neq 0$  using the procedure given in Eqs. (C.5 - C.11).

## Appendix D

### Calculations related to estimation of flux of strangelets

We can consider that accelerated CR follow a power-law distribution,  $\frac{d\mathcal{N}}{d\mathcal{E}} = \mathcal{N}_0 \mathcal{E}^{-2.2}$ . If the effective kinetic energy is  $\mathcal{E}_0$  which is used to accelerate the CR, then

$$\begin{aligned} \mathcal{E}_0 &= \int_{\epsilon_{\min}}^{\epsilon_{\max}} \mathcal{E} \frac{d\mathcal{N}}{d\mathcal{E}} d\mathcal{E} \\ &\approx \mathcal{N}_0 \frac{\epsilon_{\min}^{-0.2}}{0.2}. \end{aligned} \quad (\text{D.1})$$

In the above equation, we have assumed  $\epsilon_{\max} \gg \epsilon_{\min}$ , where  $\epsilon_{\max}$  and  $\epsilon_{\min}$  are the possible maximum and minimum kinetic energies of CR respectively. Now, we can write,

$$\mathcal{N}_0 = \frac{\mathcal{E}_0}{5} \epsilon_{\min}^{0.2}. \quad (\text{D.2})$$

The total number of particles which can be accelerated by the shock wave and with

---

*D. Calculations related to estimation of flux of strangelets*

---

kinetic energy above  $\epsilon_{\min}$  is

$$\begin{aligned}
 \mathcal{N}_{\text{tot}} &= \int_{\epsilon_{\min}}^{\epsilon_{\max}} \frac{d\mathcal{N}}{d\mathcal{E}} d\mathcal{E} \\
 &\approx \frac{\mathcal{N}_0}{1.2} \epsilon_{\min}^{-1.2} \\
 &= \frac{\mathcal{E}_0}{6\epsilon_{\min}}.
 \end{aligned} \tag{D.3}$$

In our case, shock wave, generated by the merger of SSs in the binary system, can accelerate different species of strangelet. Hence, we have modified the Eq. (D.3) by the following form

$$\mathcal{N}_{\text{tot}} = \frac{\mathcal{E}_0}{6 \langle \epsilon_{\min} \rangle}, \tag{D.4}$$

where,  $\langle \epsilon_{\min} \rangle$  is the average of minimum kinetic energy of all the species and it can be represented as

$$\langle \epsilon_{\min} \rangle = \frac{\sum_i \epsilon_{\min}^i \omega^i}{\sum_i \omega^i}. \tag{D.5}$$

$\epsilon_{\min}^i$  is the minimum kinetic energy of  $i^{\text{th}}$  species for a particular  $\beta_{\min} = v_{\min}/c$  ( $c$  is the speed of light) with  $v_{\min}$  being the minimum initial speed at which the strangelets are injected in the Galaxy. For a particular species, the power law distribution of strangelets can be written in a form

$$\frac{d\mathcal{N}^i}{d\mathcal{E}^i} = \mathcal{N}_0^i (\mathcal{E}^i)^{-2.2}. \tag{D.6}$$

---

*D. Calculations related to estimation of flux of strangelets*

We can write,

$$\begin{aligned}
 \mathcal{N}_0^i &\propto \omega^i \\
 \Rightarrow \mathcal{N}_0^i &= k\omega^i \\
 \Rightarrow \sum_i \mathcal{N}_0^i &= k \sum_i \omega^i \\
 \Rightarrow \mathcal{N}_{\text{tot}} &= k \sum_i \omega^i \\
 \Rightarrow k &= \frac{\mathcal{N}_{\text{tot}}}{\sum_i \omega^i} \\
 \Rightarrow k &= \frac{\mathcal{E}_0}{6 \langle \epsilon_{\text{min}} \rangle \sum_i \omega^i}.
 \end{aligned} \tag{D.7}$$

Eq. (D.6) can be rewritten as

$$\begin{aligned}
 \frac{d\mathcal{N}^i}{d\mathcal{E}^i} &= \frac{\mathcal{E}_0}{6 \langle \epsilon_{\text{min}} \rangle \sum_i \omega^i} \omega^i (\mathcal{E}^i)^{-2.2} \\
 &= \frac{\mathcal{E}_0 \omega^i}{6 \sum_i \epsilon_{\text{min}}^i \omega^i} (\mathcal{E}^i)^{-2.2}.
 \end{aligned} \tag{D.8}$$